Faculteit Bio-ingenieurswetenschappen

Academiejaar 2011 – 2012

Combined effects of heat and cadmium toxicity on *Populus canadensis* 'Robusta'

Marlies Christiaens

Promotoren: Prof. dr. ir. Kathy Steppe
Prof. dr. ir. Gijs Du Laing

Tutor: ir. Jochen Hanssens

Masterproef voorgedragen tot het behalen van de graad van
Master in de bio-ingenieurswetenschappen: milieutechnologie

Faculteit Bio-ingenieurswetenschappen

Academiejaar 2011 – 2012

Combined effects of heat and cadmium toxicity on *Populus canadensis* 'Robusta'

Marlies Christiaens

Promotoren: Prof. dr. ir. Kathy Steppe
Prof. dr. ir. Gijs Du Laing

Tutor: ir. Jochen Hanssens

Masterproef voorgedragen tot het behalen van de graad van
Master in de bio-ingenieurswetenschappen: milieutechnologie

ACKNOWLEDGEMENTS

Now this master thesis reaches its final form and the many hours of work finally pay off, the moment has come to thank some people who buoyed me during this final year of study.

The first person I would definitely like to thank is my promotor, Kathy, because every time we met, she gave me the motivation to go deeper into the data until I poured out everything. Thank you!

Also my other promotor, prof. Du Laing, deserves a well-meaned thank you for his assistance during this master thesis.

My tutor, Jochen… I promised him to put his name in capitals here, but, I will tell him my gratefulness by saying that I really appreciated his help during the experiments, the writing, and that I could not have wished a more supportive tutor! Thank you very much!

The research staff of the Laboratory of Plant Ecology, the Laboratory of Analytical Chemistry and Applied Ecochemistry and also Nancy gain my thankfulness for the support during the experiments and the tips.

Furthermore, I would like to thank Sofie for the pleasant talks and smooth collaboration during our experiments! It was nice to share this experience with you.

My gratefulness also goes to my parents who supported me throughout the years and also my brothers, Jochen and Jurgen, for giving their little sister advice every time I needed it.

A last person that definitely should be mentioned here is Jonathan. Thank you for the understanding and patience, especially the last weeks…

Marlies Christiaens, July 8, 2012

ABSTRACT

In the context of global change, heat waves will appear more frequently and more intensely, influencing tree photosynthesis. In addition, an enlarged and widespread soil contamination with heavy metals subjects plants to supplementary toxic stress. Although many studies can be found concerning heat stress or heavy metal stress (in particular cadmium (Cd)) on plants, few deal with the combination of both. With the aim of filling this knowledge gap, experiments were set up with *Populus canadensis* 'Robusta' over a period of 155 days in growth chambers. Cuttings were planted in potting compost and half of them were exposed to a bioavailable Cd concentration of approximately 0.5 mg Cd^{2+} l^{-1}. After two months of growth at a day/night temperature regime of 23/18°C, gas exchange and chlorophyll *a* fluorescence measurements started on August 9. The first measurement period (the spring phenological growth stage) was followed by a period of less intense measurements and on September 27, the summer growth stage started. Each growth stage comprised a control period, a heat wave of 7 days (40°C) and a recovery period. In total, six treatments of poplar plants, each containing five replicates, could be differentiated: control (C), Cd stress (S), control plants exposed to a spring (C.Sp) or summer (C.Sum) heat wave and Cd stressed plants exposed to a spring (S.Sp) or summer (S.Sum) heat wave.

Cd caused a net and gross photosynthesis (A_{net}, A_{gross}) decline resulting in lower biomass production, although no particular changes in dark respiration (R_d), stomatal conductance (g_s) or transpiration (E) could be observed due to acclimation to Cd. The degradation of chlorophyll in photosystem II light harvesting complexes (LHCII) together with oxidative damage to thylakoid membranes and thus photosystem II (PSII) were responsible for the reduced A_{net}. This could be observed by a decrease in the operating efficiency of the electron transport chain (Φ_{PSII}), the maximum efficiency in light-adapted leaves (F_V'/F_M') and an increase of minimal fluorescence both in light- and dark-adapted leaves (F_0 and F_0'). Photorespiration (Jo) of the Calvin cycle during the summer growth stage contributed to a further decline in A_{net} to even negative values (net respiration).

Heat stress resulted in decreased A_{net} and A_{gross}, a rise in R_d, E and a decline in g_s. Although F_V'/F_M' decreased, indicating a reversible light-induced injury of PSII reaction centres (RC), an increased Φ_{PSII} could be explained by a rise in non-photochemical quenching (NPQ). This kept PSII RCs open, even in recovery periods, pointing out irreversible damage. In the Calvin cycle, photorespiration rose consuming the excess energy produced by the stimulated electron transport chain and explaining low A_{gross}. Probably due to a heat-shock protein (HSP)-induced enhanced carboxylation activity of rubisco upon spring recovery, A_{net} became higher.

The combination of both Cd and heat stress caused A_{gross} to rise accompanied by a boosted R_d (resulting in net respiration), E and a decline in g_s. Even a further rise in Φ_{PSII} compared to C.Sp and C.Sum was observed, despite LHCII-degradation, oxidative thylakoid injury and reversible heat- and light-induced damage to PSII RCs. However, it was found that heat lessened thylakoid damage, probably due to extra HSPs. The extra energy produced could be consumed in the Calvin cycle by photorespiration, but also by a stimulated carboxylation pathway, probably because of Cd-induced HSPs which continued in the spring recovery.

SAMENVATTING

Als een gevolg van klimaatsverandering zal de frequentie en intensiteit van hittegolven toenemen met een effect op fotosynthese van bomen. Ook een verhoogde en wijdverspreide bodemverontreiniging met zware metalen onderwerpt planten aan toxische stress. Hoewel er veel onderzoek is uitgevoerd naar hittestress of stress door zware metalen (specifiek cadmium (Cd)) op planten, kunnen er weinig studies gevonden worden over het gecombineerde effect. Om deze kennis aan te vullen, werden experimenten uitgevoerd met *Populus canadensis* 'Robusta' in groeikamers over een periode van 155 dagen. Stekken werden uitgeplant in potgrond en de helft werd blootgesteld aan een biobeschikbare Cd concentratie van ongeveer 0.5 mg l^{-1}. Na twee maanden groei bij een dag/nacht temperatuur van 23/18°C, werden gasuitwisselings- en chlorofyl *a* fluorescentie metingen gestart op 9 augustus. De eerste meetperiode (lente fenologisch stadium) werd opgevolgd door een periode met minder intensieve metingen en op 27 september werd het zomer stadium gestart. Elk stadium omvatte een controleperiode, een 7 dagen-durende hittegolf (40°C) en een herstelperiode. In totaal konden zes verschillende behandelingen onderscheiden worden, elk bestaande uit vijf herhalingen: controle (C), Cd stress (S), controleplanten blootgesteld aan een hittegolf tijdens de lente (C.Sp) of zomer (C.Sum) en Cd stress planten blootgesteld aan een hittegolf tijdens de lente (S.Sp) of zomer (S.Sum).

Cd veroorzaakte een daling in netto en bruto fotosynthese (A_{net}, A_{gross}) met een lagere biomassa productie als resultaat, hoewel geen specifieke veranderingen in donkerrespiratie (R_d), stomatale geleidbaarheid (g_s) of transpiratie (E) konden geobserveerd worden, waarschijnlijk door Cd acclimatisatie. Chlorofyldegradatie in het fotosysteem II lichtcaptatiecomplex (LHCII) was samen met oxidatieve schade aan thylakoïdmembranen en dus aan fotosysteem II (PSII) verantwoordelijk voor een gereduceerde A_{net}. Dit kon waargenomen worden in een daling van de werkingsefficiëntie van de elektrontransportketen (Φ_{PSII}), de maximale efficiëntie in licht-geadapteerde bladeren (F_V'/F_M') en een toename van minimale fluorescentie in zowel licht- als donker-geadapteerde bladeren (F_0 en F_0'). Fotorespiratie (Jo) in de Calvin cyclus tijdens het zomerstadium droeg bij tot een verdere daling in A_{net} met zelfs negatieve waarden als gevolg (netto respiratie).

Hittestress resulteerde in een daling van A_{net}, A_{gross}, g_s en een stijging van R_d en E. Ondanks de daling van F_V'/F_M' die omkeerbare licht-geïnduceerde schade aan PSII RCs aanduidt, kon de toename van Φ_{PSII} verklaard worden door een stijging in niet-fotochemische quenching (NPQ). Dit hield PSII RCs open, zelfs in herstelperiodes wat wijst op onomkeerbare schade. Een lage A_{gross} is te wijten aan stijgende fotorespiratie in de Calvin cyclus die het teveel aan energie, dat door de gestimuleerde elektrontransportketen werd geproduceerd, consumeerde. Waarschijnlijk werd de carboxylatie acitivteit van rubisco verhoogd door heat-shock proteinen (HSP) tijdens de herstelperiode van het lentestadium waardoor A_{net} hoger werd.

De combinatie van Cd-en hittestress zorgde voor een toename van A_{gross} gepaarde gaande met een sterk verhoogde R_d (resulterend in netto respiratie), E en een daling in g_s. In vergelijking met C.Sp en C.Sum werd zelfs een verder stijging van Φ_{PSII} vastgesteld, ondanks LHCII-degradatie, oxidatieve thylakoïdschade en omkeerbare hitte- en light-geïnduceerde schade aan de PSII RCs. Verder werd geobserveerd dat hitte thylakoïdschade verminderde, waarschijnlijk door extra HSPs. De extra geproduceerde energie kon via fotorespiratie in de Calvin cyclus worden opgebruikt, maar ook via een gestimuleerde carboxylatie, hoogstwaarschijnlijk ook doordat Cd HSP-productie initieerde, zodat deze konden verder werken tijdens de herstelperiode in de lente.

LIST OF VARIABLES AND ABBREVIATIONS

RH	relative humidity	(%)
VPD	vapour pressure deficit	(kPa)
A_{net}	net photosynthesis rate	(μmol CO_2 m^{-2} s^{-1})
R_d	dark respiration rate	(μmol CO_2 m^{-2} s^{-1})
g_s	stomatal conductance	(mol H_2O m^{-2} s^{-1})
E	transpiration rate	(mol H_2O m^{-2} s^{-1})
F_0	minimal fluorescence level of dark-adapted leaves	(μmol photons m^{-2} s^{-1})
F_0'	minimal fluorescence level of light-adapted leaves measured on a moment of darkness	(μmol photons m^{-2} s^{-1})
F_M	maximum dark fluorescence level	(μmol photons m^{-2} s^{-1})
F_M'	maximum light fluorescence level	(μmol photons m^{-2} s^{-1})
F_s	steady-state fluorescence level	(μmol photons m^{-2} s^{-1})
F_V	variable fluorescence in the dark	(μmol photons m^{-2} s^{-1})
F_V'	actual variable fluorescence	(μmol photons m^{-2} s^{-1})
F_V/F_M	maximum quantum efficiency of PSII photochemistry	(-)
F_V'/F_M'	maximum efficiency of PSII photochemistry at a given photon flux density	(-)
Φ_{PSII}	operating quantum efficiency of PSII photochemistry	(-)
ETR	electron transport rate (linear)	(μmol photons m^{-2} s^{-1})
Φ_{CO2}	quantum efficiency of CO_2 assimilation	(μmol CO_2 μmol photons^{-1})
q_P	photochemical quenching	(-)
NPQ	non-photochemical quenching	(-)
Φ_{CO2}/Φ_{PSII}	Calvin cycle efficiency	(-)
S_R	specificity factor for rubisco	(-)
FW	fresh weight	(g)
DW	dry weight	(g)
$\%H_2O$	relative water content	(%)
IC	inorganic carbon	(mg l^{-1})
NPOC	non-purgeable organic carbon	(mg l^{-1})

PAR	photosynthetic active radiation
PSII	photosystem II
PSI	photosystem I
LHC	light harvesting complex
OEC	oxygen evolving complex
q_E	energy-dependent quenching
q_T	quenching related to phosphorylation of the pheripheral LHCII
q_I	quenching related to photoinhibition
HSP	heat-shock protein

CONTENTS

CHAPTER 1: INTRODUCTION

In recent years, an upsurge in research related to global change took place. This is necessary to gain an idea of the impact on daily life, the food supply, all kinds of currently used techniques, and how adaptation should be implemented. One of the elements of global change would be a more frequently occurrence of heat waves, which can already be noticed today (IPCC, 2007). Therefore, it would be interesting to study if and how forests or specific tree species will adapt to these heat waves.

Because poplars are fast growing trees, recently, they tend to get more attention in green energy production, but also in the context of phytoremediation (Brooks *et al*., 1998). The latter met wide general support as a low-cost natural technique to clean-up contaminated sites (Prasad & Freitas, 2003). Especially on industrial sites, but also naturally occurring, soils with an excess amount of heavy metals can form a danger to human health and ecosystem stability (Nriagu & Pacyna, 1988; Waalkes, 2000; Satarug *et al*., 2003).

As a consequence of these elements, the interaction of global change with environmental pollution will be studied in this master thesis. Therefore, poplar trees (*Populus canadensis* 'Robusta') will be exposed to heat and cadmium stress with reference to preceded research (Hanssens, 2010). In parallel to this study, which mainly focuses on the interaction of heat and cadmium, another master thesis will stress the acclimatization to several successive heat exposures (Goormachtigh, 2012).

First, an overview of current knowledge will be given (Chapter 2) followed by the specific research hypotheses of this master thesis (Chapter 3). In Chapter 4, the experimental set-up will be explained of which the results can be found in Chapter 5. A thorough discussion of these results (Chapter 6) will lead to the conclusions (Chapter 7).

CHAPTER 2: LITERATURE REVIEW

2.1 GLOBAL CHANGE

As this master thesis fits in with global change, it is relevant to give a general state of affairs. Based on the latest Intergovernmental Panel on Climate Change (IPCC) report (2007), human activities such as fossil fuel burning and land-use change increased greenhouse gases and aerosol concentrations in the atmosphere. According to Le Quéré et al. (2009), average atmospheric CO_2 concentrations in 2008 reached 385 ppm compared to a pre-industrial level of about 278 ppm and 379 ppm in 2005 (IPCC, 2007). More recent observations at Mauna Loa Observatory, Hawaii, indicate a monthly mean CO_2-level of 396.18 ppm for April 2012[1]. In addition, changes in solar radiation and in land surface properties contribute to the global warming which is about 0.2°C per decade (Figure 2.1) (IPCC, 2007). Especially over land and northern latitudes, the greatest rises in temperature are expected (IPCC, 2007). As a result, mountain glaciers, permafrost and ice sheets of Greenland and Antarctica are melting leading to a rise in the global average sea level with an average rate of 3.1 ± 0.7 mm per year for the period 1993 - 2003 (IPCC, 2007). In addition, changes in precipitation, ocean salinity, wind patterns and extreme weather such as the occurrence of droughts, heavy precipitation, intense tropical cyclones and heat waves, are reported to occur more frequently and intensely in the future but can already be noticed today (IPCC, 2007; Meehl & Tebaldi, 2004). In 2003 for example, Europe experienced a very hot and dry summer due to a severe and long-lasting heat wave causing an increased number of wildfires, rivers reaching their lowest levels, extreme glacier melt in the Alps, increased human mortality and a reduction in primary productivity (Alcamo *et al*., 2007; De Boeck *et al*., 2010).

According to De Boeck et al. (2010), a heat wave is determined as a consecutive period of seven days with temperatures above average. However, a single day with lower temperature can occur. Based on weather station data of western Europe, a heat wave is also characterized by 69% more sunshine hours, 78% less precipitation, 17% less relative humidity (RH) and a 111% increase in average vapour pressure deficit (VPD) compared to normal averages (De Boeck *et al*., 2010). In the seven days before a heat wave, precipitation drops with 45%. The probability that heat waves will occur more often in the future is increased due to a shift of mean temperatures and a rise in the variance in temperature probability functions (Figure 2.2) (Schär *et al*., 2004). Climate models predict that in the second half of the 21st century, a summer like 2003 can occur one another year (Schär *et al*., 2004) and heat waves will be longer-lasting and more intense, especially in western Europe, the Mediterranean and western USA (Meehl & Tebaldi, 2004).

[1] Earth System Research Laboratory (NOAA Research), Global Monitoring Division, Mauna Loa Observatory, Hawaii, USA (www.esrl.noaa.gov/gmd/ccgg/trends/)

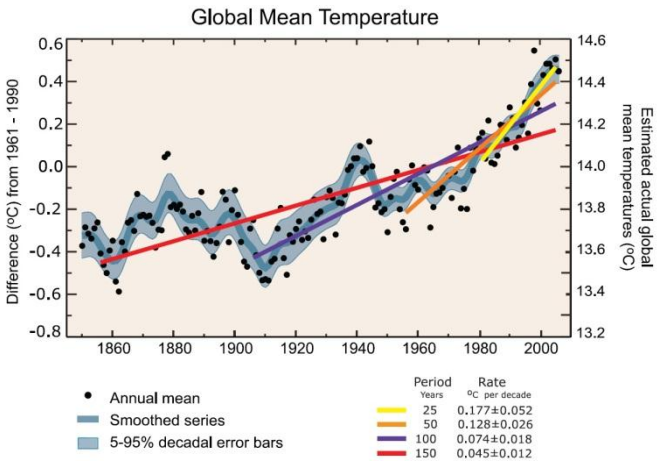

Figure 2.1: Development of global mean temperature over the past centuries. Black dots, which indicate the annual global mean observed temperatures, are connected by a thin blue curve representing decadal fluctuations accompanied by the 5 and 95% error ranges (light blue bands). Depending on the size of the past period, different linear regression lines are drawn with increasing slopes as periods become shorter. This indicates an accelerated global warming. The 150 year period corresponds to 1856-2005, the 100 year period to 1906-2005, the 50 year period to 1956-2005 and the 25 year period to 1981-2005 (from Trenberth, 2007).

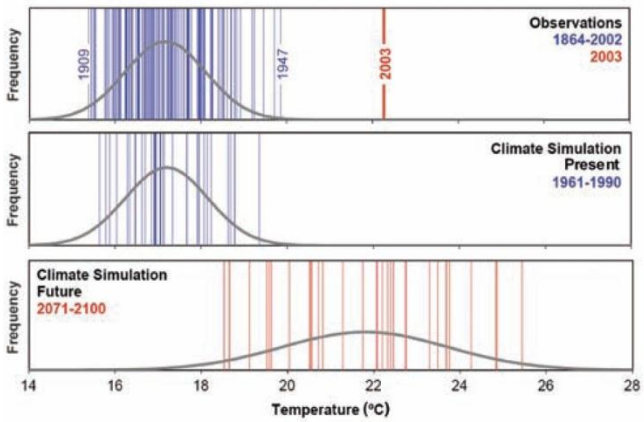

Figure 2.2: Above: Observed distribution of summer monthly temperatures (June, July and August) during the period 1864-2003 obtained from a Swiss weather station. Middle: Simulation of these temperatures with a regional climate model for the period 1961-1990. Below: Simulation of these temperatures for the future period 2071-2100. The curves represent the theoretical Gaussian frequency distributions of mean summer temperatures while the vertical bars indicate the annual mean summer temperatures (from Schär *et al*., 2004).

2.2 PHOTOSYNTHESIS AND CHLOROPHYLL *A* FLUORESCENCE: GENERAL INTRODUCTION

In the context of heat waves, cadmium pollution and their effects on plants, this master thesis focuses mainly on photosynthesis and chlorophyll *a* fluorescence of the C3 plant poplar (*Populus*). Concerning photosynthesis, a distinction can be made between light reactions and dark reactions. Chlorophyll *a* fluorescence deals with light reactions. When a plant suffers from stress, the electron transport chain can be affected causing an increase in emitted fluorescence radiation (Bolhàr-

Nordenkampf & Öquist, 1993). As such, chlorophyll *a* fluorescence is a measure of photosynthesis capacity. Light reactions are driven by light intensity and wavelength whereas dark reactions are mainly dependent on temperature because of the enzymes and biochemistry involved (Raven, 2005). Note that the described processes and mechanisms below are only applicable to C3 plants because C4 and CAM photosynthetic pathways are different.

2.2.1 Photosynthesis

Photosynthesis is the process of making sugars for growth and maintenance of the plant cells by taking up CO_2 and water while absorbing light energy (photons). This requires close interaction between the light photosynthetic reactions in the thylakoid membranes of chloroplasts and the dark photosynthetic reactions in the stroma, the liquid filling of chloroplasts (Figure 2.3). The grana thylakoids are grouped in piles of flat cylinders, grana, creating inner spaces, lumen, while stroma thylakoids connect the grana (Raven, 2005).

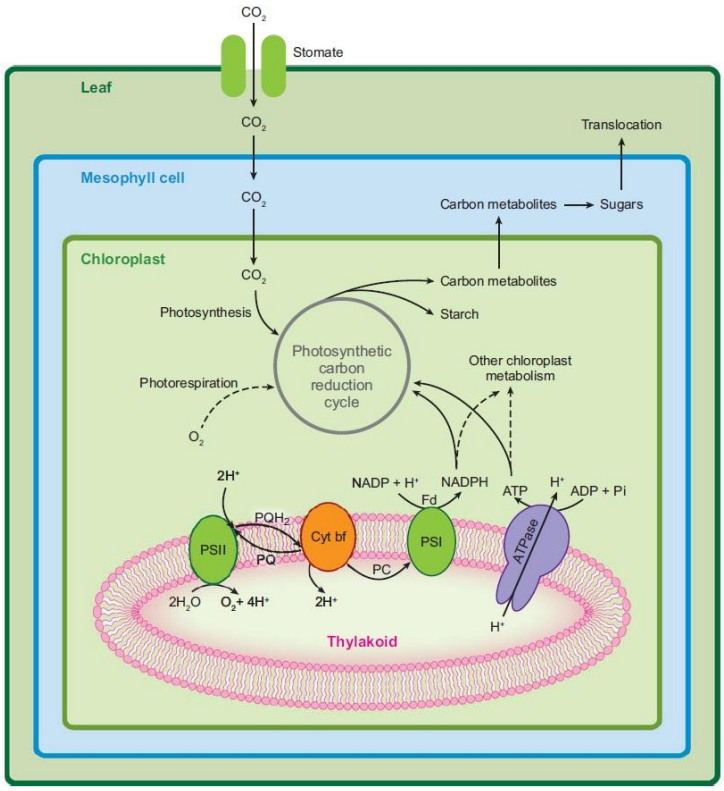

Figure 2.3: Schematic representation of light reactions (in the thylakoid membranes; H_2O and O_2 are the input respectively output) and dark reactions (in the stroma; CO_2 and carbon metabolites/starch are the input respectively output) of photosynthesis in a C3 plant (from Baker, 2008). A more detailed representation of the electron transport chain can be found in Figure 2.4.

In the light reactions, light energy is converted into chemical energy by absorbing photons in the light harvesting complexes and transferring electrons through the electron transport chain (Figure

2.4). Proteins necessary for this reaction are imbedded in the thylakoid membranes. The main protein complexes are photosystems II (PSII) and I (PSI) and a cytochrome b_6/f complex which are connected by electron carriers such as plastoquinone (PQ) and plastocyanin (PC). Each photosystem contains a light harvesting complex (LHC) which consists of an assembly of pigment molecules, called antenna complex, and a reaction centre chlorophyll *a* molecule. The optimal radiation wavelength at which this chlorophyll *a* molecule in PSII is excited is 680 nm whereas PSI absorbs photons at 700 nm. Following the absorption of photons by the pigment molecules (chlorophyll *a*, *b* and carotenoids) of the LHCs and thus their excitation, a resonance energy transfer will occur between neighboring pigment molecules towards the reaction centre chlorophyll *a* molecule, which is P680 or P700 depending on the photosystem to which it belongs. The energy excites the chlorophyll *a* molecule which causes the loss of a high energy electron. The velocity at which electrons are lost can be increased by reducing the wavelength while the quantity of electrons is influenced by light intensity. If two electrons are lost, the first electron acceptor, pheophytin, will be reduced. The electron deficit of P680 will be repleted by photolysis of water in the oxygen evolving complex or water splitting complex, whereas P700 receives new electrons from the reduced plastocyanin (Raven, 2005; Steppe, 2011).

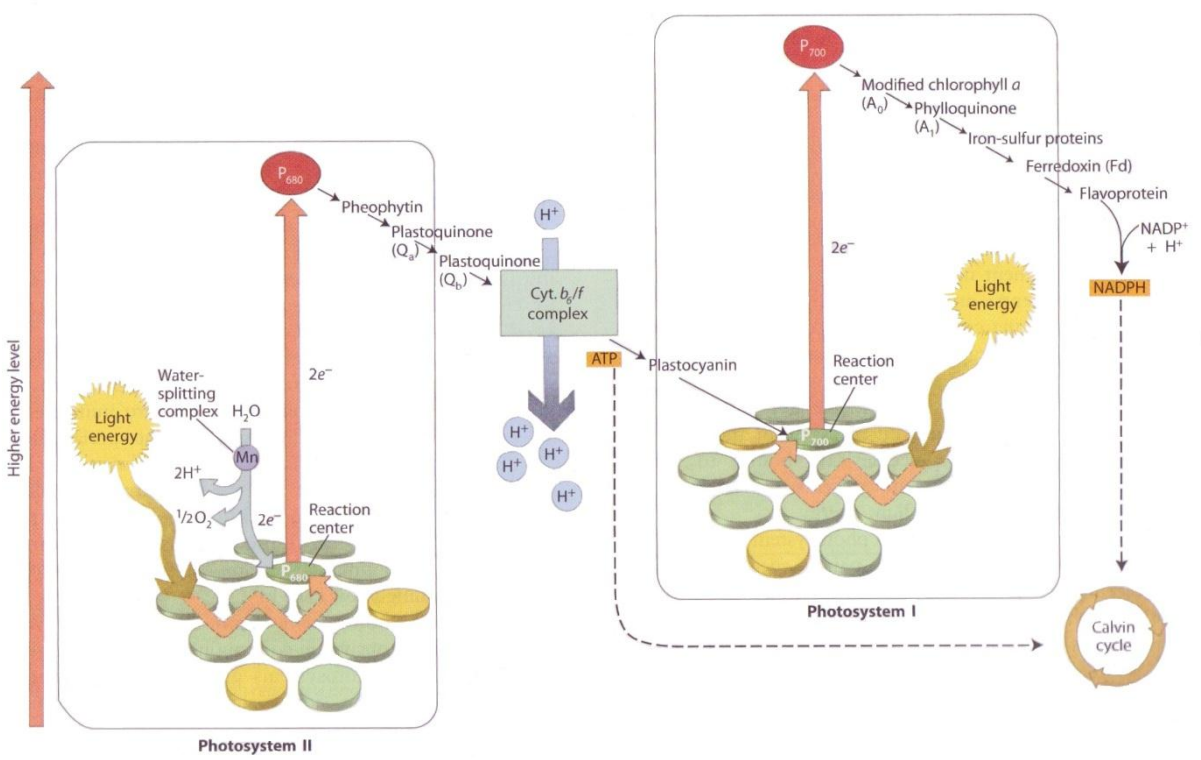

Figure 2.4: Overview of the electron transport chain with photosystem II, cytochrome b_6/f complex and photosystem I as the main components (from Raven, 2005).

The electron transport chain, especially the cytochrome b_6/f complex, creates an acidification of the lumen causing an electrochemical gradient across the thylakoid membrane. An adenosine

triphosphate (ATP) synthase complex will pump protons out of the lumen while reducing adenosine diphosphate (ADP) to ATP (phosphorylation). At the end of the chain, nicotinamide adenine dinucleotide phosphate ($NADP^+$) is also reduced yielding the chemical energy molecule NADPH. Both are consumed in the dark reactions or Calvin cycle (Raven, 2005; Steppe, 2011).
Since the Calvin cycle consumes ATP and NADPH at a ratio of 3:2 and the production is evenly distributed in the Calvin cycle, there is need for more ATP generated by cyclic electron transport. High energy electrons from P700 follow the same path as before to ferredoxin but instead of reducing $NADP^+$, the electrons are transported to cytochrome b_6/f complex. Consequently, the electrochemical gradient rises with the production of ATP as a result (Raven, 2005).

In the stroma of chloroplasts, CO_2 is assimilated in the dark reaction which can be divided in three main parts. In the first part, carboxylation, CO_2 is fixed on ribulose-1,5-bisphosphate (RuBP) by RuBP carboxylase/oxygenase (rubisco) yielding two molecules of 3-phosphoglycerate (PGA) for each CO_2. Subsequently, the reduction of PGA to glyceraldehyde-3-phosphate (G3P) oxidizing two moles ATP and NADPH per mole CO_2 is the second part. Finally, RuBP is regenerated by the oxidation of one mole ATP per mole CO_2 fixed. The glyceraldehyde-3-phosphate is used to create sugars, amino acids, starch etc. (Raven, 2005).

2.2.2 Chlorophyll *a* fluorescence and quenching

When a leaf is illuminated, a certain amount of the light energy absorbed by chlorophyll *a* molecules will be dissipated as fluorescence radiation (Bolhàr-Nordenkampf & Öquist, 1993). Chlorophyll *a* molecules absorb red photons (660 nm) and blue photons (420 nm) which both excite an electron of chlorophyll *a* from the ground state (S_0) to a higher energy level. The red photons lift an electron to the excited singlet 1 state (S_1) as shown in Figure 2.5 whereas the more energetic blue photons will excite the electron to the singlet 3 or 4 state (S_3 or S_4). However, an electron at S_3 or S_4 will quickly return to S_2 or S_1 by thermal de-excitation. (Roháček & Barták, 1999) Fluorescence radiation is emitted if an electron falls back from S_1 to the ground state (Schmidt, 1988). Due to the Stokes shift – that is, a rapid cascade of the excited electrons to the lowest levels of S_1 – fluorescence is dark red radiation and thus the emission peak is slightly shifted towards a higher wavelength compared to the red absorption peak (Schmidt, 1988). When the plant is not stressed, the quantity of fluorescence is about 0.6 to 5% at room temperature (Walker, 1987) and mainly (about 90%) emitted by LHCII chlorophyll *a* molecules (Govindjee, 1995). Only a small part of fluorescence originates in LHCI if wavelengths are below 700 nm which is always the case in this master thesis except for far-red radiation measurements (see below) (Schreiber, 2004). Another pathway for an electron to return to S_0 is the emission of phosphorescence radiation (Figure 2.5) on condition that intersystem crossing from S_1 to the triplet state T_1 has happened (Schmidt, 1988). In addition, an excited chlorophyll *a* molecule can return to the ground state by photochemical reactions (electron transport chain) or thermal deactivation (radiationless decay) (Baker, 2008; Baker & Oxborough, 2004; Maxwell &

Johnson, 2000; Roháček & Barták, 1999). Both of these de-excitation pathways can be seen as forms of quenching – that is, minimizing fluorescence: photochemical (q_P) and non-photochemical quenching (NPQ) respectively. Thus, fluorescence, photochemical reactions and thermal deactivation are in competition for the absorbed energy (Roháček & Barták, 1999). In fact, Kautsky and Hirsch (1931) observed that changes in fluorescence radiation arising upon illumination of dark-adapted leaves are correlated with photosynthesis rates. Such changes also correlate with CO_2 assimilation based on the assumption that produced ATP and NADPH molecules are consumed in the Calvin cycle and not in other processes such as photorespiration (see below) (Genty *et al.*, 1989). Therefore, measurements of emitted fluorescence radiation enable to calculate fluorescence parameters related to PSII photochemistry on condition that the contribution of q_P and NPQ to a decrease of the maximum fluorescence level can be distinguished (Baker, 2008). Although the electron flow through PSII indicates photosynthesis rates, care must be taken while interpreting data as in C3 plants photorespiration is often present (Baker & Oxborough, 2004). If CO_2 concentrations in the plant are quite low (perhaps because the stomata are closed due to excessive, dry heat), rubisco will bind O_2 yielding only one molecule of 3-phosphoglycerate and one of phosphoglycolate. To extract carbon atoms from the latter, energy will be consumed and CO_2 will be released (Raven, 2005). In conclusion, fluorescence parameters can reveal important information such as PSII efficiency and thus the impact of environmental stresses on photosynthesis (Maxwell & Johnson, 2000).

Photochemical and non-photochemical quenching

Photochemical quenching passes electrons through the photosynthetic light reactions, however, if the electron acceptors that have to oxidize the reaction centre molecules P680 and P700 are reduced, high energy electrons from these centres cannot pass. Consequently, the absorbed energy will be dissipated by the LHCs as fluorescence radiation (Schulze *et al*., 2005). Thus, emission of fluorescence radiation depends on the oxidation state of the reaction centre and more fluorescence radiation will be emitted if the centre is reduced or 'closed' (Baker, 2008). This is the case when the electron transport chain is saturated or the electron transport is diminished due to environmental stress (Baker, 2008). It should be noted that excited P700 is more stable than excited P680 (Miersch *et al.,* 2000). This explains why LHCI does not emit a large amount of fluorescence radiation.

Non-photochemical quenching includes energy-dependent quenching (q_E), quenching related to photoinhibition (q_I) and quenching related to phosphorylation of the peripheral LHCII (q_T) (Baker, 2008). Energy-dependent quenching is the consequence of a strong acidification of the thylakoid lumen due to high light intensity (photoinhibition) or malfunction of the Calvin cycle, resulting in an accumulation of ATP and NADPH (Baker, 2008). To reduce this energy build-up, protons bind to LHC molecules accompanied by heat dissipation. In the case of q_I, an easily repaired link between a D1 protein and the reaction centre of PSII is broken to protect the photosystem (Baker, 2008; Schulze *et al*., 2005).

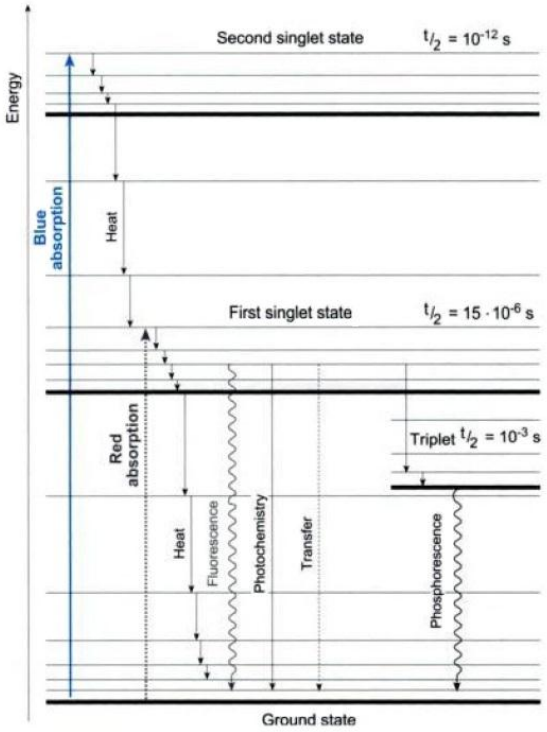

Figure 2.5: Overview of the excitation states of chlorophyll *a* upon absorption of light energy (blue or red photon) and the transfer to lower energy levels. Note that the third and fourth singlet state, which are reached if a blue photon is absorbed, are not represented because the excited electron will quickly fall back to the second singlet state by thermal de-excitation. Half-life times of each state are given as $t_{/2}$ (from Schulze *et al.*, 2005).

If photons are unequally absorbed by PSII and I leading to an energy imbalance, excess fluorescence can be avoided by phosphorylation of LHCII which causes a part of LHCII to loosen and move towards PSI (Maxwell & Johnson, 2000). Probably, this mechanism regulates the balance between cyclic and linear electron transport (Sharkey, 2005).

Chlorophyll a fluorescence measurements

Chlorophyll *a* fluorescence can be quantified in function of time by a fluorometer working on the principle of pulse-amplitude modulation (PAM) of chlorophyll fluorescence emission (Schreiber, 2004). By applying pulses of different light sources, fluorescence parameters are measured (Figure 2.6). Moreover, the saturation pulse method (Schreiber *et al*., 1986) originally introduced as a 'light-doubling' technique (Quick & Horton, 1984), is able to quantify the contribution of both photochemical and non-photochemical quenching. Especially when plants are stressed, the ratio of both forms of quenching can be drastically altered because of the rise in NPQ. This rise can be due to damage to the photosynthetic apparatus because of which the excess energy is dissipated as heat. However, the rise in NPQ can also serve as a protection mechanism against damage. Then, excess energy is removed to prevent that the photosynthetic apparatus is affected (Maxwell & Johnson,

2000). At any time equilibrium is assumed between photochemical and non-photochemical pathways (Roháček and Barták, 1999). Hence, measuring chlorophyll *a* fluorescence parameters is a non-destructive method to assess photosynthesis quantitatively and qualitatively in vivo (van Kooten & Snel, 1990; Roháček, 2002; Maxwell & Johnson, 2000; Baker & Oxborough, 2004).

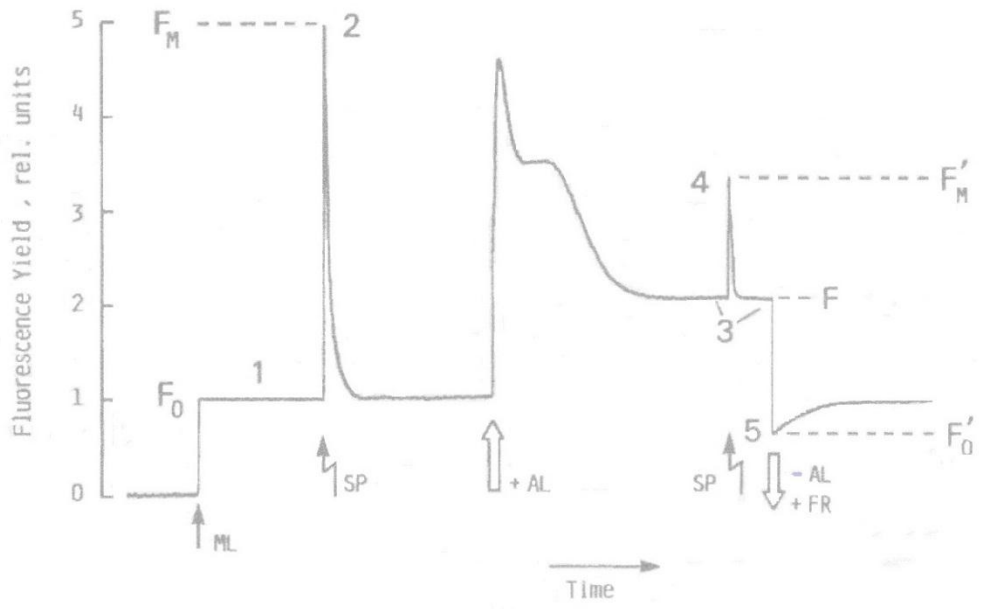

Figure 2.6: Chlorophyll *a* fluorescence (relative to F_0) in function of time measured on a dark-adapted leaf with a PAM fluorometer. Switching on the weak measuring light (ML) (< 0.2 µmol m^{-2} s^{-1}) allows quantifying F_0 (part 1). A saturation pulse (SP) (> 7000 µmol m^{-2} s^{-1}) in this dark period measures F_M (point 2). Next, the actinic light (AL) (hundreds of µmol m^{-2} s^{-1}) is switch on causing the fluorescence induction curve to arise. As fluorescence yield levels off towards steady state (F) (part 3) another SP is applied to measure F_M' (point 4). Darkness is introduced by switching off AL accompanied by a pulse of far-red radiation (FR) (tens of µmol m^{-2} s^{-1}) to quantify F_0'. If darkness lasts long enough, the F_0 level is obtained again. In literature, the part of the curve till the rising part of the peak arising on illumination is assigned to the fast fluorescence kinetics whereas the rest of the curve is described as the slow fluorescence kinetics (adapted from: van Kooten & Snel, 1990).

To quantify all parameters of the saturation pulse method, the PAM-fluorometer uses four different light sources: measuring light, actinic light, saturation pulses and far-red radiation (Schreiber, 2004). However, prior to the measurements, leaves have to be dark-adapted – that is, a photosynthetic inactive state or all reaction centres and electron carriers are oxidised – to maximise energy absorption by LHCII in the electron transport chain (Roháček, 2002). To generate the beginning of the curve (Figure 2.6, part 1), a dark-adapted leaf will be exposed to the measuring light (ML). This light is a modulated red radiation beam with very low photon flux density (PPFD, <0.2 µmol m^{-2} s^{-1}) (Baker, 2008; LI-COR, 2008; Roháček and Barták, 1999; van Kooten & Snel, 1990) to prevent initiation of photosynthesis and to measure F_0, the minimal fluorescence level of a dark-adapted leaf, which is characterised by electron absorption by LHCII but not by the reaction centres of the photosystems. Hence, photochemical quenching is maximal (q_P = 1). This state lasts for a few

picoseconds (Bolhàr-Nordenkampf & Öquist, 1993). During darkness, a first peak (point 2 on Figure 2.6) originating from a pulse of saturated light (SP) (> 7000 µmol m^{-2} s^{-1}) (Baker, 2008; LI-COR, 2008; van Kooten & Snel, 1990) quantifies the maximum fluorescence level F_M. Such a saturation pulse consists of red and blue photons to completely reduce the plastoquinone pool Q_A and thus turning reaction centres of PSII in the 'closed' state resulting in elimination of photochemistry (q_P = 0) (Baker, 2008; Licor manual; Roháček, 2002). Non-photochemical quenching and photosynthesis efficiency are not changed in large amounts by this saturation pulse (Maxwell & Johnson, 2000; LI-COR, 2008; van Kooten & Snel, 1990). Nevertheless, a quick return to F_0 levels occurs.

If an actinic light source (AL) (hundreds of µmol m^{-2} s^{-1}) (Baker, 2008; Roháček and Barták, 1999), which drives photosynthesis, illuminates a dark-adapted leaf, the emitted fluorescence radiation follows a typical pattern (Kautsky *et al.*, 1960). This fluorescence induction curve results from the above-mentioned processes, which compete for the absorbed light energy. The rising part of the first peak, which appears upon illumination with actinic light, comprises the fast kinetics of electron transport (2 s) as it involves PSII processes. Literature states that also the preceding dark period is assigned to the fast kinetics. The other part is rather slow (in the order of minutes) due to the additional dependence on non-photochemical processes. The exact duration is determined by the plant on which measurements are conducted (Maxwell & Johnson, 2000). If the operation rate of the Calvin cycle equilibrates with the electron transport rate, fluorescence stabilises at F_S, the steady state fluorescence level (part 3 on Figure 2.6; F is F_s) (Roháček, 2002).

At this fluorescence level, a new saturation pulse is induced to measure F_M', the maximum fluorescence level of a light-adapted leaf (point 4). Next, fluorescence radiation quickly falls back to F_S followed by another drop in fluorescence caused by switching off the actinic light and introducing a pulse of far-red radiation (FR) (tens of µmol m^{-2} s^{-1}) (Baker, 2008; Roháček and Barták, 1999; van Kooten & Snel, 1990). This 'dark' pulse aims at activating PSI resulting in a rapid reoxidation of the electron carrier plastoquinone and thus opens reaction centres at PSII. This pulse can be used to measure F_0', the minimal fluorescence level of a light-adapted leaf measured in a moment of darkness (point 5) (Maxwell & Johnson, 2000; Roháček, 2002; van Kooten & Snel, 1990).

Fluorescence parameters

Based on the measured fluorescence variables F_0, F_M, F_S, F_M', and F_0', other important fluorescence parameters can be calculated. Literature offers a broad and diverse range of parameters with sometimes different meanings for the same symbols. In the list below, an overview can be found of the calculated chlorophyll *a* fluorescence parameters relevant for this master thesis with their most commonly used meaning and remarks. Parameters indicated with an apostrophe (') are calculated from variables measured on a light-adapted leaf, whereas parameters without are derived from variables quantified on dark-adapted leaves. Derivation of parameters from fast and slow fluorescence kinetics parallels with parameters derived from the dark respectively light period in Figure 2.6. The unit of fluorescence variables F measured is µmol photons m^{-2} s^{-1}. As all calculated

variables are expressions of these fluorescence variables, they have the same unit or are dimensionless. (Baker, 2008; Baker & Oxborough, 2004; Maxwell & Johnson, 2000; Roháček, 2002; Roháček and Barták, 1999; LI-COR, 2008; Schreiber *et al*., 1986)

- Variable fluorescence: the ability of PSII to perform photochemistry in the dark

$$F_V = F_M - F_0 \tag{2.1}$$

- Maximum quantum efficiency of PSII photochemistry:

$$\Phi_{PSII,\max} = \frac{F_V}{F_M} = \frac{P_{\max}}{I_a} \tag{2.2}$$

  This parameter quantifies the maximum proportion of absorbed energy used in photosynthesis in a dark-adapted leaf (LI-COR, 2008). Typical values for healthy plants at room temperature range from 0.75 to 0.85 (Björkman & Demmig, 1987; LI-COR, 2008). As PSII is sensitive to stress, stress diminishes $\Phi_{PSII,max}$. Therefore, it is very often used as a stress indicator. Roháček (2002) attributes this decrease to the contribution of PSI fluorescence to F_0. In the equation, I_a is the total absorbed energy and P_{max} quantifies the maximum energy used in photosynthesis, both in µmol photons m^{-2} s^{-1}.

- Actual variable fluorescence: the ability of PSII to perform photochemistry in the light

$$F_V' = F_M' - F_0' \tag{2.3}$$

- Maximum efficiency of PSII photochemistry at a given PPFD:

$$\frac{F_V'}{F_M'} = \frac{F_M' - F_0'}{F_M'} \tag{2.4}$$

- Photochemical quenching coefficient:

$$q_P = \frac{F_M' - F_s}{F_M' - F_0'} \tag{2.5}$$

  The fraction of open reaction centres of PSII is quantified by this parameter. It reaches his highest value at low light intensities as leaves then use light more efficiently (LI-COR, 2008).

- Operating quantum efficiency of PSII photochemistry:

$$\Phi_{PSII} = \frac{F_V'}{F_M'} \cdot q_P = \frac{F_M' - F_s}{F_M'} \tag{2.6}$$

  This quantifies the proportion of absorbed energy used for photochemical reactions at a given PPFD (Baker & Oxborough, 2004). According to Baker (2008), the F_V'/F_M' can be used to estimate the contribution of non-photochemical quenching processes in the light. Furthermore, due to environmental stresses decreases in the PSII operating efficiency can occur. Both q_P and NPQ contribute in a complex and not fully understood pattern to this decrease resulting in a malfunction of the photosynthetic apparatus.

- Non-photochemical quenching:

$$NPQ = \frac{F_M - F_M'}{F_M'} \tag{2.7}$$

NPQ is shown to be linearly related to excess radiation (Roháček and Barták, 1999). An increase can be the result of damage or as a protection reaction (Maxwell & Johnson, 2000).

- Electron transport rate (linear):

$$ETR = \Phi_{PSII} \cdot 0.87 \cdot I \cdot 0.5 \quad (2.8)$$

The ETR (µmol photons m^{-2} s^{-1}) is the amount of electrons passing through the electron transport chain per unit of surface and time. (Steppe, 2011) It is sometimes explained as the actual flux of photons driving PSII (LI-COR, 2008). In this equation, 0.87 is the photon leaf absorptance (α_{leaf}, -) and I the incident photon flux density (µmol photons m^{-2} s^{-1}). The product of α_{leaf} and I equals I_a, which was mentioned before. The factor 0.5 reflects the fact that transporting one electron requires the absorption of two photons. This is an approximation and therefore not always correct.

In addition, the parameter Φ_{CO2} (µmol CO_2 µmol photons^{-1}), calculated based on gas exchange measurements, indicates the quantum efficiency of CO_2 assimilation and can be used to determine the energy allocation to q_P or NPQ processes (LI-COR, 2008).

$$\Phi_{CO2} = \frac{A_{net} - R_d}{I \cdot \alpha_{leaf}} \quad (2.9)$$

The measured variable A_{net} is the net CO_2 assimilation rate (µmol CO_2 m^{-2} s^{-1}), R_d is the dark respiration rate (µmol CO_2 m^{-2} s^{-1}), I is the incident photon flux density (µmol photons m^{-2} s^{-1}) and α_{leaf} (-) is the photon leaf absorptance.

2.3 CADMIUM AND EFFECTS ON PLANTS

As cadmium (Cd) happens to be a widely spread and highly toxic pollutant that has been accumulating in soils over the past decades, the impact of this heavy metal on poplar was studied in this master thesis.

Cd is a heavy metal which means it has a density greater than 5 g cm^{-3} (Schulze *et al*., 2005). In contrast with some other heavy metals that are micronutrients (e.g. iron), Cd is a non-essential element or xenobiotic (Schulze *et al.,* 2005). All heavy metals are toxic if they accumulate in cells (even at low concentrations), which they tend to do if taken up, because of their low mobility and the fact that they cannot be degraded but only converted into another physical or chemical form (Tack, 2010). Moreover, Cd is relatively more mobile (Cottenie & Verloo, 1984; Hasan *et al*., 2009; see below) and has a higher soil to plant transfer rate resulting in an enhanced plant uptake and incorporation in plant tissues (Satarug *et al*., 2003). In this way, elevated levels of Cd can easily enter the food chain resulting in, among others, human renal dysfunction and bone decalcification (Itai-itai disease, Japan) (Nordberg, 2004). In addition, one of the reasons for lung cancer due to smoking is

the fact that the tobacco plant (*Nicotiana* spp.) tends to be a bioaccumulator of Cd (Satarug *et al*., 2003).

In Flanders, which is an area that is humanly polluted with heavy metals, a Cd background concentration of 0.8 mg kg^{-1} DW in a standard soil with 10% clay and 2% organic matter prevails (Bierkens *et al.*, 2010). Throughout western Europe, local severely polluted areas contain much higher Cd concentrations. Nearby a metal smelter in Auby in Northern France, for example, soil Cd levels ranging from <1 to >300 mg kg^{-1} DW were reported accompanied by Cd concentrations up to 209 mg kg^{-1} DW in leaves of poplar (*Populus tricocapa* x *Populus deltoides*) (Robinson *et al*., 2000).

2.3.1 Cd in the soil and bioavailability

Cd is a rather rare element in the earth's crust as its abundance lies between 0.08 and 0.5 ppm (Habashi, 1997). Despite the fact that only a few specific Cd minerals exist, it is frequently present in zinc minerals (Sadegh Safarzadeh *et al.*, 2007). As such, Cd is a by-product of zinc metallurgy (Sadegh Safarzadeh *et al.*, 2007) and used in batteries, pigments, coatings, stabilizers for plastics, non-ferrous alloys, photovoltaic devices, etc. (ATSDR, 2008; Nordic, 2003). The mining, smelting and refining of the ores leads to the discharge of Cd in the soil through atmospheric deposition (dry or wet) of Cd dust and contaminated process water (ATSDR, 2008). Although this is a main source of Cd pollution, other anthropogenic activities are contributing to the elevated occurrence of Cd in soils. Direct pollution sources are the use of phosphate fertilizers and sewage sludge on agricultural land and the disposal of industrial and municipal wastes. The release of Cd dust in the atmosphere occurs also due to burning coal, the incineration of household waste and process industries such as iron and steel processing, cement production and non-ferrous metals processing (ATSDR, 2008; Dokmeci *et al*., 2009; Nordic, 2003; Nriagu & Pacyna, 1988; Pacyna *et al*., 2007; Sadegh Safarzadeh *et al*., 2007; Satarug *et al.*, 2003). In addition, nature contributes to Cd dispersion due to volcanic eruptions, forest fires and the weathering of rocks. However, this will rarely cause elevated Cd levels in the environment (Nordic, 2003).

Upon entering the soil, Cd is distributed between the soil solution and the solid phase where Cd occurs in different chemical forms (speciation) (Figure 2.7). In the solution, Cd is dissolved as a hydrated divalent cation, as an organic (e.g. with $EDTA^{2-}$) or inorganic (e.g. with Cl^- or SO_4^{2-}) complex depending on the ligand (when an organic complex is formed with an internal ring structure, it is called a chelate) and suspended due to binding to colloids such as organic matter, which becomes more soluble at neutral to alkaline pH (Tack, 2010). The soil solid phase contains the largest pool of Cd as it is exchangeably bound to charged surfaces such as adsorption on organic matter, occluded in soil solids and incorporated in soil minerals (Tack, 2010). Only the organic matter pool is able to exchange Cd with the soil solution in a short time period and can therefore equilibrate with it. Within the normal pH range of soils (pH 4 – 8), organic matter is negatively charged resulting in its behaviour as cation exchanger (Tack, 2010). As in time Cd will also adsorb on inner surfaces of soil

particles due to diffusion, less Cd will be available in the soil solution (aging) (Kirkham, 2006; Seuntjens *et al*., 2001). This process results in a lower uptake of Cd by plants or other biota.

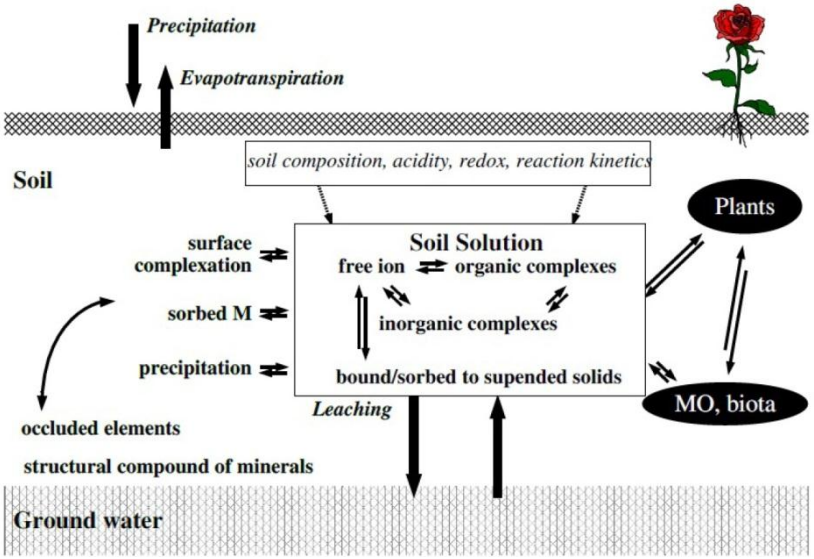

Figure 2.7: Overview of the presence of Cd as different chemical forms in soils, the factors determining speciation, the transfer and interaction processes between solid soil and soil solution on the one hand and soil solution, plants and biota on the other hand (from Tack, 2010).

Depending on pH, redox potential and organic matter content as the most important factors, the speciation will influence the bioavailability of Cd in soils (Tack, 2010). Although Cd concentrations in soils can reach stunning levels (up to 150 mg kg^{-1} soil dry weight in western Europe reported by Tack (2010)), the bioavailable fraction rather than the total Cd content of a soil must be taken into account when assessing the effects on plants (Kirkham, 2006). According to Tack (2010), the Cd in the soil solution is referred to as the bioavailable fraction. Moreover, Tudoreanu and Philips (2004) stated that Cd in the soil solution is mostly present as hydrated Cd^{2+} and Cd chelates. Both forms are important in the uptake of Cd by plants (Lux *et al*., 2011; Schulze *et al*., 2005; see below).

If the first factor, pH, decreases, the mobility of hydrated Cd ions and thus plant uptake will be enhanced (Tudoreanu & Philips, 2004; Lux *et al*., 2011) because of competition for sorption between other cations such as Ca^{2+} and Zn^{2+}, a decline in the total amount of negative sorption sites and an elevated solubility of iron and aluminium hydroxides (Bradl, 2004; Tack, 2010). If the pH drops below 6 and relative mobility of the metals is expressed as the fraction of total amounts dissolved, Cd is more mobile compared to other heavy metals (Cottenie & Verloo, 1984) resulting in an increased plant uptake (Nordic, 2003). At neutral to alkaline pH, it precipitates as a hydroxide (Evans, 1989). However, if the soil solution has a pH value above 6 or 7, Cd organic complexes dominate and their stability and thus plant uptake will be enhanced with pH as they are mostly negatively charged (Tack, 2010). The complexes will dissociate when pH falls below 6 (Tack, 2010). It must be noted that the effects of rises and decreases of pH, described here, only occur if the buffered pH range is left. Soils

containing a high amount of free $CaCO_3$, are strongly buffered (Du Laing *et al.,* 2007) and allow Cd^{2+} to sorb on $CaCO_3$ or precipitate as $CdCO_3$ (Martin & Kaplan, 1996). However, at high Cd concentrations, the precipitation occurs rather slowly. Also, if dissolved organic matter is present, precipitation can be avoided (Bradl, 2004; Tack, 2010).

The second factor determining bioavailability is the redox potential. Reducing conditions in the soil, e.g. due to flooding, cause the immobilization of Cd because in the presence of sulphates CdS will precipitate or large molecular humic material containing Cd will become insoluble (Du Laing et al., 2007; Tack, 2010). However, at the initial phase, a peak in mobile Cd will occur because of the dissolution of iron and manganese hydrated oxides in which occluded and adsorbed Cd was present (Du Laing *et al*., 2007). Likewise, Cd is released from organic matter under oxidising conditions because of the mineralization of the organic matter (Forstner, 1993).

Lastly, the organic matter content has also been shown to influence bioavailability. Sauvé et al. (2003) reported that organic forest soils in Canada had a sorption affinity of organic matter for Cd that was 30 times greater than for mineral soils. As organic material usually accumulates in the top soil (Kirkham, 2006), it can be concluded that Cd will be retained in the surface layers of a soil profile (Lux et al., 2011). Kirkham (2006) reported that Cd applied on acid Canadian forest soils occurred to a depth of 0.25 m after three years. Because organic matter is negatively charged and has a large surface area, it supports the fact that Cd^{2+} will be retained. In this way, organic matter becomes a large and important pool of Cd, but also of essential elements and nutrients for plant growth, which will become available in the soil solution at a slow but continuous rate during the organic matter's decay (Tack, 2010).

2.3.2 Uptake of Cd by plants

According to Lux et al. (2011) and Uraguchi et al. (2009a), Cd^{2+} is mainly transported towards the plant roots due to a transpiration-driven mass flow of the soil solution. In addition, molecular diffusion towards lower concentrations, which exist near roots as plants may take up Cd, occurs (Tack, 2010). The symplasmic entry of Cd^{2+} in root cells is established by non-selective calcium cation channels and zinc-regulated transporter/iron-regulated transporter-like proteins (ZIPs) (Verbruggen *et al*., 2009) resulting in a reduction of Ca^{2+} in plants in the presence of high Cd concentrations (Hasan *et al*., 2009). Cd chelates may enter root cells through yellow-stripe 1-like proteins (YSLs) which are root cell membrane transporters for the uptake of iron chelates (Curie *et al.,* 2009). The excretion of plant produced exudates (e.g. carboxylase) can acidify the rhizosphere or form chelates resulting in an increased uptake of Cd but in a limited influx in the cell cytosol as the Cd chelates are bound to the cell wall (Clemens *et al*., 2002; Schulze *et al*., 2005; Tack, 2010; 2 in Figure 2.8). The chelates are less toxic than Cd^{2+} (Hasan *et al*., 2009). In addition, the symbiosis of mycorrhizal fungi with plant roots can prevent or enhance Cd availability (Blaudez *et al*., 2000; Clemens *et al*., 2002; 1

in Figure 2.8). Sell et al. (2005) showed that the association of *Populus canadensis* with the ectomycorrhizal fungi *Paxillus involutus* increased Cd concentrations in poplar and enhanced the root-to-shoot translocation.

Once in the cytoplasm, Cd is sequestered within root vacuoles as Cd^{2+} and Cd chelates (5, 7 and 8 Figure 2.8), but can also continue its symplastic transport through plasmodesmata and enter the xylem as Cd^{2+} via heavy metal ATPases or via a yet unidentified transporter for Cd chelates (Clemens *et al*., 2002; Verbruggen *et al.,* 2009). Depending on the ligand, Cd will be transported into the xylem (histidine, nicotianamine and citrate) or sequestered in vacuoles (phytochelatins and metallothioneins, see below) (Clemens *et al*., 2002). However, in most plants, the Cd shoot concentration is far less than root concentrations (Lux *et al*., 2011). For example, Lunáčková et al. (2003) reported root concentrations of 5014.3 mg kg^{-1} DW for poplar plants exposed to 1.1 mg Cd^{2+} l^{-1} as $Cd(NO_3)_2$ compared to 29.2 mg kg^{-1} DW in shoots. If plants are exposed to higher concentrations of Cd, sequestration will be enhanced. Hyperaccumulators of Cd will have a greater amount of Cd moving into the xylem whether they experience low or high Cd concentrations (Verbruggen *et al.*, 2009).

Another pathway for Cd to enter plants is the apoplasmic route through cell walls. Generally, this is restricted to the root tip and the areas where lateral roots initiate (Clemens *et al*., 2002; Lux *et al*., 2011). Only if no Casparian bands are present in the endodermis – that is, a cell layer in the root that separates the cortex from the xylem and phloem – Cd can reach the stele. However, exposure to high Cd concentrations results in the accelerated maturation of the endodermis and in the production of suberin lamellae, Casparian bands and lignification of its cell walls, in particular close to the root apex where Cd is taken up (Lux *et al*., 2011). These responses can be seen as avoidance mechanisms of the plant to let Cd enter the xylem. Uraguchi et al. (2009b) reported that Cd can also be bound in the root cell wall to avoid translocation to the shoot (2 in Figure 2.8). It was found that the concentration of Cd granules in root cell walls and vacuoles of bioaccumulators was greater, respectively lower than in non-accumulators. Hasan et al. (2009) reported that an accumulation of Cd^{2+} in cell walls causes a sufficient electrochemical gradient between the cell wall and the cytoplasm to result in an influx into the cytoplasm, even at low Cd^{2+} concentrations.

Finally, Schulze et al. (2005) mentioned the uptake of Cd dust through leaves.

Upon entering the xylem, the Cd^{2+} and Cd chelates are transported towards the leaves. Via an apoplasmic or symplasmic route they will be distributed over the leaf cells, entering via various transport mechanisms (Clemens *et al*., 2002). According to Ernst (1980), a mesophyll cell accumulates on average 48% of its total Cd content in the cell wall, 39% in the cytoplasm and vacuole and 13% in chloroplasts and mitochondria.

2.3.3 An overview of potential detoxification mechanisms

The toxicity of Cd may result from its affinity for sulphydryl groups, amines and oxygen ligands in proteins causing the degradation of their structure and thus inhibiting their function (Hall, 2002; Hasan *et al.*, 2009). Cd ions may also replace essential elements such as Ca^{2+} or Zn^{2+} in molecules leading to a mineral deficiency (Hasan *et al*., 2009). Excess Cd concentrations can result in oxidative stress and lipid peroxidation (membrane damage) as reactive oxygen species (ROS) can be formed and antioxidant concentrations (e.g. glutathione) may decrease (Hall, 2002; Hasan *et a*l., 2009; Verbruggen *et al*., 2009). Moreover, the mitochondrial electron transfer chain is thought to be the primary production site of ROS (Heyno *et al*., 2008). Cd^{2+} is also toxic to the photosynthetic electron transport chain in chloroplasts (DalCorso *et al*., 2008).

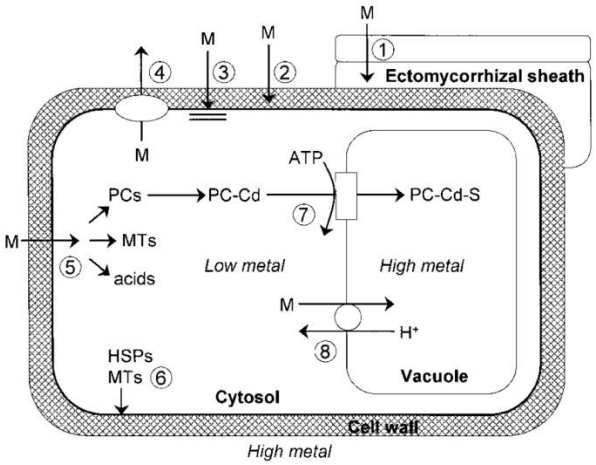

Figure 2.8: Overview of cellular detoxification mechanisms in plants. 1. Root symbiotic extracellular mycorrhizal fungi preventing metal uptake; 2. Cell wall and root exudates binding metals; 3. Plasma membrane reduced metal influx; 4. Active efflux; 5. Metal chelates consisting of different ligands; 6. Repair and protection of plasma membrane; 7. Sequestration of metal chelates in vacuole; 8. Sequestration of metal ions in vacuole. Abbreviations: M stands for metal, PCs for phytochelatins, MTs for metallothioneins and HSPs for heat shock proteins (from Hall, 2002).

In general, all detoxification mechanisms are focused on the avoidance of Cd toxicity rather than creating resistant proteins (Hall, 2002). The first two mechanisms are already discussed above. A third mechanism is the reduced influx of Cd in cells. Metal transporters such as cation diffusion facilitators (CDF) and ZIPs are involved in metal uptake and can therefore play a role in detoxification (Hall, 2002). In parallel with bacterial avoidance strategies, the plasma membrane may, as a fourth mechanism, actively export Cd ions by means of a P-type ATPase cation pumps (Silver, 1996).
The fifth mechanism binds Cd^{2+} to different chelates to prevent reaction with S, N or O groups of metabolically important proteins. In response of exposing plants to high Cd concentrations, cysteine-rich peptides are produced: the smaller phytochelatins and the larger metallothioneins (Clemens *et al*., 2002; Schulze *et al*., 2005). Phytochelatins (PCs; formula: $(\gamma\text{-Glu-Cys})_n$-Gly with n ranging from 2

to 11) are derived from glutathione (GSH) which is also a cellular antioxidant (Schulze *et al*., 2005; Verbruggen *et al*., 2009). The PC-Cd and oxidised glutathione (GS)-Cd complexes are transported by ABC transporters into the vacuole where they are stored as high-molecular-weight compounds that contain S^{2-} for stabilization (Cd aggregates) (Hall, 2002; Verbruggen *et al.,* 2009; 7 in Figure 2.8). This storage is rather short-term because PCs were found to play a major role in the intracellular Cd^{2+} transport (Schulze *et al*., 2005). Thus, the Cd induced PC synthesis results in an enhanced Cd binding capacity (Verbruggen *et al.,* 2009). The other group of ligands, the metallothioneins (MTs), contain about 60 amino acids with two cysteine-rich ends. According to the plant tissue, four types of MTs exist related to the cysteine arrangement (Schulze *et al*., 2005). Although their exact function remains unclear, possible functions have been ascribed to MTs: storage of Cd as MT-Cd complexes in the cytosol (Verbruggen *et al*., 2009), facilitating the transport into the vacuole (Schulze *et al*., 2005), and antioxidant or plasma membrane repair (Hall, 2002; 6 in Figure 2.8). On the contrary, Gaudet et al. (2011) reported no major role for MTs upon exposure of poplar to 5.6 mg Cd^{2+} l^{-1} as $CdSO_4$. Also, they seem not to be substrate-specific for Cd (Schulze *et al.,* 2005).

In addition to MTs' membrane repair, heat-shock proteins (HSPs) can fulfil the same function (Hall, 2002; 6 in Figure 2.8). There exist several families of these stress proteins according to their size: HSP70, HSP60, HSP90, HSP100 and small HSPs (smHSP) are best known (Wang *et al*., 2004). The smHSPs are of particular interest in plants (Vierling, 1991). Upon exposure of plants to elevated Cd levels, the gene expression for HSP70s and smHSPs will be particularly enhanced. However, also heat or cold stress, salt stress or anaerobic stress can trigger HSP production (Vierling, 1991). In non-stressed cells, HSP70, HSP60 and HSP90 are present as molecular chaperones which are involved in protein folding and transport across membranes (Vierling, 1991). In general, HSP functions in stressed cells include the protection, repair and degradation of in particular proteins (Schulze *et al*., 2005). Heckathorn et al. (2004) reported that smHSPs levels in chloroplasts were increased upon heavy metal exposure and were able to protect photosynthetic proteins such as rubisco (section 2.2.1).

As the last detoxification mechanism (8 in Figure 2.8), the sequestration of Cd^{2+} in the vacuole was established by Cd^{2+}/H^{+} antiporters in the tonoplast (Verbruggen *et al*., 2009). Together with chelate sequestration this process is called compartmentalization and attributes to the immobilization of Cd (Larcher, 2003).

2.3.4 Phytoremediation

Depending on the amount of Cd that can be tolerated in their shoots, plants can either be Cd sensitive or Cd hyperaccumulators such as *Thlaspi caerulescens* (Verbruggen *et al.,* 2009). Hyperaccumulators will also experience toxic effects but only at a higher threshold (Schulze *et al*., 2005). The toxicity of Cd is defined as the Cd concentration in plant leaves (mg kg^{-1} DW) which decreases the yield with 10% (White & Brown, 2010). For Cd intolerant plants, Cd leaf concentrations of 5 to 10 mg kg^{-1} DW are considered toxic (White & Brown, 2010).

Hyperaccumulators, on the other hand, can reach concentrations of 100 mg kg^{-1} DW (Brooks *et al*., 1998). As an advantage of their high metal content, they may be protected against fungal or viral infections. However, accumulating metals is physiologically expensive because of the enhanced synthesis of metallothioneins and phytochelatins, the sequestration in vacuoles or cell walls and the repair after damage (Schulze *et al.,* 2005). According to Schulze et al. (2005), plants that can extract large amounts of heavy metals from soils even in a short vegetation period or at relatively low but still toxic soil concentrations, can be useful to clean Cd polluted soils (phytoremediation) or even mine Cd from mineralized soils (phytomining) (Brooks *et al*., 1998). The ideal plant for those purposes is characterised by a large production of biomass in a short period, deep roots, an easy harvest and high metal accumulation in the harvestable plant parts which depends on its mobilization and uptake from the soil, the sequestration within the root, the efficiency of xylem loading and the storage in leaf cells (Clemens *et al.*, 2002).

2.3.5 Effects of Cd on plants

Although the toxic effects of Cd were already briefly described above (section 2.3.3), a more detailed overview is given here, particularly of the effects on photosynthesis and chlorophyll *a* fluorescence. According to Krupa (1999), the general cause of multiple Cd (indirect) effects can be attributed to photosynthetic damage and reduction, since many metabolic processes depend on it. Moreover, the enzymes of the Calvin cycle are among the primary targets of Cd (Kieffer *et al*., 2009a; Prasad, 1995). As a result, especially during longer exposure periods, the electron transport chain can be affected either by down-regulation – that is, increasing non-photochemical quenching – or by feedback inhibition due to insufficient oxidation of NADPH and ATP by the Calvin cycle (Krupa, 1999).

In general, several studies showed a decline in net photosynthesis and transpiration rates (Dong *et al*., 2005; Pietrini *et al*., 2010; Solti *et al*., 2008b, Sárvári *et al*., 2011). Gaudet et al. (2011) compared the Cd response of two genotypes of poplar and reported a 30 to 70% decrease in net photosynthesis and a decline of 50 to 75% in transpiration rates when poplars were exposed to 5.6 mg Cd^{2+} l^{-1} as $CdSO_4$. Moreover, Schulze et al. (2005) showed a linear relationship between the inhibition of net photosynthesis and transpiration rates in maize and sunflower plants treated with 505.85 to 2023.4 mg Cd^{2+} l^{-1} as $CdCl_2$ suggesting stomatal closure as a cause of photosynthesis inhibition because of a reduced CO_2 uptake (Krupa *et al*., 1993). Cd is indeed proven to increase stomatal resistance (Poschenrieder *et al.*, 1989) and simultaneously reduce plant water content (Kieffer *et al*., 2009a). Because Cd-induced root damage and thus diminished water uptake has often been reported (Larbi *et al*., 2002; Prasad, 1995; Seregin & Ivanov, 2001), a loss of plant water content can result in stomatal closure. In fact, if plants are exposed to Cd concentrations above 5.5 mg Cd^{2+} l^{-1} for more than three weeks, a hydropassive – that is, due to general leaf turgor loss – stomatal closure may occur with wilting as a result (Barceló *et al*., 1986; Poschenrieder *et al*., 1989; Prasad, 1995).

Nevertheless, disturbed photosynthesis is not only due to reduced CO_2 uptake because Cd also showed direct interference with the electron transport chain and Calvin cycle (Kieffer *et al.*, 2009a).

The electron transport chain affected by Cd

One of the most crucial elements of the electron transport chain that is affected by Cd is the LHCII (section 2.2.1) (Krupa, 1999). On the one hand, the oligomeric structure which is important in efficient light harvesting is indirectly altered due to a decrease in the fatty acid compounds (Krupa *et al*., 1993). As LHCII, on the other hand, comprises about 70% of the total leaf chlorophyll content (Krupa, 1999), the Cd-induced retardation of chlorophyll synthesis causes a decline in the amount of LHCII (Krupa, 1999; Solti *et al*., 2009). Therefore, leaf chlorosis is a major visible effect of Cd stress (Milone et al., 2003; Pandey *et al*., 2007; Prasad, 1995; Sárvári *et al*., 2011; Solti *et al*., 2008b). Also Solti et al. (2009), who exposed poplar to 1.1 mg Cd^{2+} l^{-1} as $Cd(NO_3)_2$ for two weeks, reported strong chlorosis. In addition, a Cd-induced iron deficiency attributed to leaf chlorosis and reduced chlorophyll content in a study of Sárvári et al. (2011), who reported a 32% decrease of iron content in chloroplasts upon exposure of poplar to 1.1 mg Cd^{2+} l^{-1} as $Cd(NO_3)_2$ for two weeks. This was due to a reduced activity of ferric-chelate reductase which decreased iron uptake of mesophyll cells (Fagioni *et al*., 2008; Larbi *et al*., 2002; Sárvári *et al.,* 2011).

Next, photosystem II is shown to be highly sensitive to Cd stress, both at its electron donor and acceptor side (Sigfridsson *et al*., 2004). At the donor side, the oxygen evolving complex (OEC) may be destructed or its interaction with functional ions such as Mn^{2+}, Ca^{2+} and Cl^- can be altered (Prasad, 1995; Krupa, 1999). For example, Cd^{2+} may bind competitively with the Ca^{2+} site in PSII inhibiting photoactivation – that is, the assembly of OEC which is the last step in activation of newly formed PSII (Faller *et al*., 2005). In addition, Solti et al. (2009) found that Cd led to photodamage at low light intensities (120 µmol m^{-2} s^{-1}) upon exposure to 1.1 mg Cd^{2+} l^{-1} ($Cd(NO_3)_2$) of poplar for two weeks. This can be explained by Cd-induced oxidative stress causing ROS, which primarily acted as inhibitors of PSII repair by suppressing the synthesis of D1 protein (Nishiyama *et al*., 2006). Moreover, inhibition by ROS is accelerated by the deceleration of the Calvin cycle that occurs if CO_2 is limited due to stomatal closure (Nishiyama *et al*., 2006). Thus, photoinhibition, which is an imbalance between photodamage and repair of PSII, is caused by Cd (Nishiyama *et al*., 2006). Gaudet et al. (2011), however, reported no photoinhibition because chloroplast structure was intact, F_V/F_M values did not change and a significant increase in NPQ prevented oxidative damage.
At the acceptor side of PSII, on the other hand, the plastoquinone pool is decreased (Krupa, 1999; Prasad, 1995). The reaction centre of PSII can also be affected by Cd due to its redox components, which are sensitive for oxidative stress (Krupa, 1999).

Solti et al. (2009) showed an elevated amount and stability of LHCII-PSII aggregates under a 1.1 mg Cd^{2+} l^{-1} ($Cd(NO_3)_2$) treatment of poplar for two weeks. However, their reaction centres were not

operational in electron transport but in thermal energy dissipation. It seemed that, although q_E and q_I are important mechanisms in the protection of photosystem reaction centres, for long-term Cd stress these LHCII-PSII aggregates are the major source of non-photochemical quenching (Sárvári *et al*., 2011; Solti *et al*., 2009). This is in agreement with a decreased turn-over rate of D1 protein (Franco *et al*., 2001) and was confirmed by a significant decrease in Φ_{PSII}, q_E and q_I. Cd^{2+} also interacts with cysteine residues in zeaxanthin-epoxidase, thereby disturbing and thus decreasing the q_E and q_I non-photochemical pathway (Latowski *et al*., 2005; Solti *et al*., 2008a). In addition, photoinhibited PSII centres contributed to a large extent to thermal energy dissipation (Solti *et al*., 2009). In the study of Gaudet et al. (2011) (see above) a decline in Φ_{PSII} was also reported, in addition with an unchanged F_V/F_M, a decrease in photochemical quenching (q_P) and increase in non-photochemical quenching (NPQ). Sárvári et al. (2011) exposed poplar to 1.1 mg Cd^{2+} l^{-1} as $Cd(NO_3)_2$ for two weeks and found that Φ_{PSII} and F_V/F_M decreased with 15% while thermal dissipation significantly increased. Therefore, there seems to be controversy about the effect of Cd on F_V/F_M. The loss of PSII efficiency correlated with a decreased chlorophyll content according to Kieffer et al. (2009a) who exposed poplar for two weeks to 2.2 mg Cd^{2+} l^{-1} as $CdSO_4$.

Additionally, PSI suffers from Cd stress as one of its electron acceptors, ferredoxin (Fd), may show decreased functionality due to Cd-induced iron deficiency (Siedlecka & Baszynski, 1993). Moreover, according to Sárvári et al. (2011), PSI becomes the most sensitive complex upon iron deficiency. Fagioni et al. (2009) reported a high sensitivity of PSI with a significant reduction in LHCI in the basal leaves during the first 15 days of Cd exposure of spinach to 11.2 mg Cd^{2+} l^{-1} for 30 days. Only after two weeks, PSII began to disintegrate. Antenna proteins appeared to be most sensitive while ATP-synthase and the cytochrome b_6/f complex were not affected. Cd damaged significantly the basal leaves' photosynthetic apparatus while apical leaves contained less or no Cd, so, they kept functioning and providing the plant's energy and assimilates.

Finally, as the electron transport chain is imbedded in thylakoid membranes, Cd-induced oxidative stress and thus lipid peroxidation causes thylakoid disintegration. In addition, chlorophyll-protein complexes tend to accumulate upon Cd exposure resulting in serious structural changes of thylakoids (Solti *et al*., 2009). However, the chloroplastic ATP synthase complex was not dramatically affected (Kieffer *et al*., 2009a).

The Calvin cycle affected by Cd

In the Calvin cycle, the carboxylation step appears to be the most sensitive as rubisco is inhibited by Cd (Krupa, 1999; Prasad, 1995). Depending on the concentrations of Cd and the plant's growth stage, rubisco's structure may be altered in different ways (Krupa, 1999): Cd may replace the essential cofactor Mg^{2+} or induce the oxygenase activity instead of its carboxylase function (photorespiration, section 2.2.2) (Krupa, 1999; Prasad, 1995). Fagioni et al. (2009) reported a decline in the activation

of rubisco during the first 10 days of treatment (see above), possibly by an interaction of Cd with the sulphydryl group of rubisco. Full inhibition can be caused by high Cd concentrations (in the order of 100 mg Cd^{2+} l^{-1}) disconnecting rubsico's subunits with a decrease in sugar production as a result (Malik *et al*., 1992). Kieffer et al. (2009a) exposed poplar for two weeks to 2.2 mg Cd^{2+} l^{-1} as $CdSO_4$ and found an excess of sugar production because both light and dark reactions were still operational, despite the lower rate, and plant growth was inhibited. A role as protector against Cd stress was suggested because a direct injection into mitochondrial respiration would be possible. Cd is indeed reported to elevate wound respiration because of oxidative stress which requires a high reducing power (ATP and NADPH) (Kieffer *et al*., 2009a; Schulze *et al*., 2005). Also other enzymes necessary in the Calvin cycle may be influenced by Cd (Kieffer *et al*., 2009a; Malik *et al*., 1992).

Other typical effects of Cd stress

As already mentioned, plant growth has been reported to be inhibited because of the reduced photosynthesis, especially in younger plants (Hasan *et al*., 2009; Krupa, 1999; Milone *et al*., 2003; Prasad, 1995; Sárvári *et al*., 2011; Schulze *et al*., 2005). Lunáčková et al. (2003) reported that roots of poplar were shorter and thicker when exposed to 1.1 mg Cd^{2+} l^{-1} as $Cd(NO_3)_2$. Gu et al. (2007) also indicated reduced root growth upon exposure of 11.2 mg Cd^{2+} l^{-1}. According to Poschenrieder et al. (1989), Cd rigidifies cell walls by cross-linking of the pectins, which leads to the inhibition of cell wall expansion (Prasad, 1995). However, reduced growth may also be caused by turgor loss in cells (Prasad, 1995). An increased lignification of cell walls could lead to breaking the leaves upon touching and leaf roll (Kieffer *et al*., 2009a; Milone *et al*., 2003). Other symptoms of phytotoxicity are yellow streaks and pinpoint necrosis on leaves, becoming large spots if Cd concentrations increase (Kieffer *et al*., 2009a; Pietrini *et al*., 2010; Schulze *et al*., 2005). However, older leaves showed minor necrosis compared to younger leaves but exhibited an accelerated senescence, probably due to permanent stomatal closure and an increased ethylene production (Kieffer *et al.*, 2009a; Prasad, 1995). Also other plant parts such as roots are reported to exhibit increased senescence (Krupa, 1999; Lux *et al.,* 2011). Furthermore, degradation of the chloroplast lamellar structure and photosynthetic apparatus can be seen as consequences of senescence (Krupa, 1999). As a last effect of high Cd concentrations, plasma membrane leakage due to lipid peroxidation has also been reported (Hall, 2002; Prasad, 1995).

2.4 HEAT WAVES AND THE EFFECTS OF MODERATE HEAT STRESS ON PLANTS

Heat waves are characterized by an increase in temperature, light intensity and drought, with the latter resulting from a decline in RH and precipitation and thus a rise in VPD (De Boeck *et al*., 2010). If heat waves are simulated in plant experiments these three factors should be taken into account (De Boeck *et al*., 2010). As in this master thesis plants were well watered and light intensities were kept constant (see below), this literature review is mainly focused on high temperature effects.

Moderate heat stress implies a temperature rise of about 10 to 15°C above ambient (Wahid *et al*., 2007). However, as poplar species occur globally, ambient temperatures cover a broad range. Salvucci and Crafts-Brandner (2004) defined temperatures of 30 to 42°C as moderate heat stress. The damaging effect of heat stress depends on the intensity, duration and rate of temperature increase, but also on the species, growth conditions (transpirational cooling, see below), phenological stage, activity of post-stress repair mechanisms, and the potential for heat tolerance (Allakhverdiev *et al*., 2008; Sage & Kubien, 2007; Wahid *et al*., 2007). In general, photosynthesis is determined as the most sensitive cell function because it manifests vital changes upon heat stress (Berry & Björkman, 1980). Several studies have tried to find evidence whether the electron transport chain or the Calvin cycle is most sensitive and thus which process is the primary cause for decreased photosynthesis rates (Sage & Kubien, 2007). As a small difference in research methodology (e.g. slightly higher temperature) can alter the outcome completely, more systematic studies are definitely necessary to tackle this research question. Nevertheless, numerous targets and potential mechanisms of heat stress have been identified. It should be noted that plants own fast and slow response mechanisms to heat stress. Some studies also concentrate on studying these mechanisms in vitro and do not incorporate a whole-plant response.

2.4.1 Effects on the electron transport chain

In general, literature reported a decrease in electron transport rate if moderate heat stress is applied to plants (Allakhverdiev *et al.*, 2008; Berry & Björkman, 1980; Schrader *et al*., 2004; Silim *et al*., 2010). The reduction of the plastoquinone pool in the dark resulting in a stimulation of the cyclic electron flow through PSI and cytochrome b_6/f complex (Figure 2.4) is suggested as the potential mechanism behind this diminished rate upon exposure to heat stress (Havaux, 1996; Sharkey, 2005). Normally, PQ is not in redox equilibrium with the stroma in the dark, but heat stress must have opened a path for electrons mediated by an unknown enzyme (Havaux, 1996). Yamane et al. (2000) confirmed this because exposure of tobacco to 36°C for several minutes induced this reduction of plastoquinone. Due to this blockage at the acceptor side of PSII, non-photochemical quenching, particularly q_I, will increase, because LHCII is phosphorylated resulting in its disconnection and movement towards PSI thereby stimulating cyclic electron flow (Schrader *et al*., 2004; Sharkey, 2005; Sage & Kubien, 2007). Because the turn-over rate of PSII wanes, a decline in the linear electron transport rate follows (Sage & Kubien, 2007; Yamasaki *et al*., 2002). Berry and Björkman (1980) also reported a decline in Φ_{PSII}. Further, a rise in F_0 was found due to energy that cannot pass PSII (Hüve et al., 2012) accompanied by a decrease in F_M, which indicated the separation of LHCII from PSII (Schreiber & Armond, 1978). Another consequence is a larger transthylakoid electrochemical gradient leading to an additional ATP, but no NADPH production (Sharkey, 2005). According to Mohanty et al. (2002), who exposed pea plants to 42°C for 14 to 15 hours, a two fold increase in phosphorylated LHCII was observed compared to control plants.

Beside the loss of LHCII, PSII suffers from other stresses induced by elevated temperatures. According to Allakhverdiev et al. (2008) and Sage and Kubien (2007), the OEC, reaction centre and D1 protein are other weak PSII elements. It should be noted that damage has to be interpreted as the net result of the balance between damage and repair (Allakhverdiev et al., 2008). Yamashita et al. (2008) reported the production of ROS in spinach thylakoids during a 30 minutes exposure to 40°C. Probably, ROS damages the D1 protein of PSII resulting in the release of two manganese atoms of the manganese-containing cluster in the OEC and the elimination of the extrinsic proteins which stabilize this cluster (Nash *et al*., 1985). Yamashita et al. (2008) demonstrated that under anaerobic conditions damage was suppressed, supporting this hypothesis. Reaction centres can also be cleaved by ROS and their aggregation results in non-active PSII (Allakhverdiev et al., 2008). The pathway of ROS production is not yet revealed, but one possibility is the water-water cycle around PSI (Heber, 2002). This cycle competes for electrons with the cyclic electron flow to reduce oxygen with the formation of water or potentially toxic active oxygen species (Heber, 2002). Asada (2006) reported the generation of ROS in both PSI and II. Furthermore, it can be assumed that photodamage of PSII follows the same potential pathway as heat damage (Yamashita *et al.,* 2008). It should also be noted that illumination of damaged PSII can cause photo-inhibition, even at low light intensities (Murata *et a*l., 2007; Yamashita *et al.,* 2008).

To put it briefly, most research pointed out that PSII is more damaged than PSI, certainly upon short heat exposure, but the reason remains unclear. Generally, it was assumed that PSII was simply more sensitive to heat stress (Allakhverdiev *et al*., 2008; Berry & Björkman, 1980; Wahid *et al*., 2007; Weis & Berry, 1988). However, Sharkey (2005) asserted that, because PSI is generally inhibited at lower temperatures (40°C) compared to PSII (45°C), PSII suffering from reversible heat stress (thus, at lower temperature than 45°C) can be a regulatory mechanism to spare PSI.

Another potential target of heat stress that is closely related to the electron transport chain is the thylakoid membrane. Sage and Kubien (2007) stated that thylakoid membranes become more fluid if they are less saturated. Since temperature favours unsaturation of lipids (Los & Murata, 2004), the fluidity of thylakoids is expected to increase upon temperature rise. However, the opposite (more saturation with higher temperatures and thus an augmented fluidity) has also been reported (Schulze *et al*., 2005). High temperatures also induce disintegration of the lipid bilayer (Allakhverdiev *et al*., 2008) and stimulate lipid peroxidation (Yamashita *et al*., 2008) resulting in leakage (Sage & Kubien, 2007). However, no direct link with a reduced photosynthesis rate is assumed because the cyclic electron flow keeps ATP levels stable although NADPH levels dropped considerably due to the disturbance of the linear electron flow (Sage & Kubien, 2007; Wahid *et al.,* 2007). This was also hypothesized by Schrader et al. (2004), who had grown Pima cotton under a 32/26°C day/night temperature regime and reported an increased membrane permeability starting at 36°C but no difference in ATP levels. Although it is controversial, membrane fluidity was proposed to be a cellular

thermometer because several other functional elements are dependent on membranes (Allakhverdiev *et al*., 2008; Wahid *et al*., 2007).

2.4.2 Effects on the Calvin cycle

The heat-induced decline of net photosynthesis can also be contributed to a diminished CO_2 assimilation rate. In this case, four distinct causes can be defined depending on a diverse range of factors such as species, temperature and CO_2 concentration: activity of rubisco enzyme, RuBP regeneration determined by the Calvin cycle and electron transport rate, phosphate (P_i) regeneration by starch and sucrose synthesis or rubisco activase which is the main regulatory protein for rubisco (Sage & Kubien, 2007). First, rubisco, is the enzyme that catalyses the Calvin cycle by binding CO_2 on RuBP (carboxylase function). However, rubisco also has affinity for O_2 (oxygenase function) which can lead to photorespiration (section 2.2.2), a widely appearing effect of heat stress in C3 plants (Berry & Björkman, 1980). Although this process has the advantage of CO_2 production, it will not be counterbalanced by the costs (energy consumption) (Sharkey, 2005). As temperature rises, both CO_2 carboxylation and photorespiration rates are stimulated but the latter dominates resulting in a decline in photosynthesis (Berry & Björkman, 1980). Augmented photorespiration rates can be partly explained by a higher need for CO_2 to cope with higher assimilation rates at elevated temperatures (Brooks & Farquhar, 1985), partly by a decline in CO_2/O_2 solubility and partly by a diminution in substrate specificity (CO_2 versus O_2) (Sage & Kubien, 2007). In addition, the production of ROS (H_2O_2) can be observed in rubisco that has a greater affinity for O_2. This was found by Kim & Portis (2004) upon exposure of spinach rubisco to 38°C.

Secondly, RuBP regeneration is largely dependent on the electron transport rate: a decline herein decreases RuBP regeneration and thus CO_2 assimilation (Berry & Björkman, 1980). However, Law and Crafts-Brandner (1999) found that CO_2 assimilation was affected at temperatures that had no influence on the electron transport chain (represented by F_V/F_M) for cotton and wheat. Values for NPQ rose starting from 35 and 30°C for cotton and wheat, respectively, indicating that ATP was not been utilized in the Calvin cycle because of its inhibition (Salvucci & Crafts-Brandner, 2004), whereas F_V/F_M declined from 40 and 35°C for cotton and wheat respectively, indicating that the Calvin cycle was inhibited earlier than the electron transport chain.

P_i regeneration by starch and sucrose synthesis is a potential third cause of decreased CO_2 assimilation because a quick rise in their capacity occurs as soon as temperatures are elevated (Sage & Kubien, 2007). This may lead to an excessive drain of Calvin cycle intermediates slowing the turn-over of CO_2 assimilation (Stitt & Grosse, 1988).

Lastly, rubisco activase is strongly related to the first potential cause because this enzyme regulates the (de)activation of rubisco (Portis, 2003) with a shift towards inactivation upon higher temperatures through several mechanisms (reviewed in Salvucci & Crafts-Brandner, 2004). The rate at which this happens is usually greater than the re-activation rate of rubisco activase (Salvucci & Crafts-Brandner, 2004) resulting in less CO_2 assimilation. Probably, the reason is the thermal lability

of this ATPase enzyme, leading to denaturation and aggregation into insoluble complexes (Feller *et al*., 1998), however, a scarcity of ATP can also lead to inhibition of rubisco activase (Sage & Kubien, 2007).

2.4.3 Effects on transpiration, dark respiration, stomatal and mesophyll conductance and organelle structure

Beside the negative effects on photosynthesis and the resulting decline in plant growth, heat has consequences for other plant mechanisms as well (Allakhverdiev *et al*., 2008; Wahid *et al*., 2007). An obvious one is stomatal closure because heat normally induces a rise in VPD resulting in drought stress (Berry & Björkman, 1980). However, as long as water is not limiting, plants will diminish their leaf temperature by transpirational cooling (Salvucci & Crafts-Brandner, 2004). Law and Crafts-Brandner (1999) observed a 70% increase in transpiration rates for cotton plants grown at 28°C upon exposure to 45°C. Stomatal control plays also a role in CO_2 availability for the Calvin cycle because diffusion of CO_2 through stomata is accelerated at elevated temperatures on condition stomata remain open (Law & Crafts-Brandner, 1999; Sage & Kubien, 2007). Silim et al. (2010) reported a decrease in stomatal conductance of *Populus balsamifera* (grown at 27/16°C) of about 350 mmol H_2O m^{-2} s^{-1} if temperatures increased from 17 to 37°C. In addition, the diffusion into chloroplasts (mesophyll conductance), which depends on proteins such as aquaporines and carbonic anhydrases, is shown to imply a major limitation of the Calvin cycle rate (Yamori *et al*., 2006). Bernacchi et al. (2002) reported an increase in mesophyll conductance of mature tobacco leaves to rising temperatures with a maximum at 37.5°C. Further, a decline was observed inhibiting CO_2 assimilation. Another heat-induced effect is an augmented dark respiration rate as found by Law and Crafts-Brandner (1999): increasing leaf temperatures of cotton from 25 to 40°C caused a nearly two-fold upsurge of R_d. Moreover, dark respiration is reported to be more intense influenced by heat than photosynthesis. *Populus balsamifera* grown at 27/16°C, for example, displayed a tripled R_d compared to a 40% decrease in CO_2 assimilation rate if temperatures rose from 17 to 37°C (Silim *et al*., 2010). Hüve et al. (2012) observed a 10-fold linear rise in R_d of *Populus tremula* at 46°C compared to 22°C. Mitochondrial respiration was also found to increase with rising temperatures depleting the plant from energy and stimulating ROS production (Sage & Kubien, 2007; Wahid *et al*., 2007).

Heat also causes structural changes such as destacking of thylakoid membranes, swelling of chloroplasts, destruction of chloroplasts accompanied by bleaching, antenna-depleted PSII and clump-forming vacuoles (Efeoğlu, 2009; Wahid *et al*., 2007). It is assumed that some of these changes that allow photosynthesis to acclimate cause damage when heat is no longer applied (Sharkey, 2005). Finally, enhanced membrane permeability and fluidity due to protein denaturation or a change in saturation of membrane fatty acids is reported (Los & Murata, 2004; Wahid *et al*., 2007).

2.4.4 Acclimation mechanisms

As mentioned before, these effects of high temperatures on plants are strongly subjected to numerous factors, including growth temperature. It is reported that maximal photosynthesis rates of plants grown at elevated temperatures exhibit a shift towards higher optimal growth temperatures developing an enhanced thermotolerance (Havaux, 1993; Yamasaki *et al*., 2002). This was confirmed by Silim et al. (2010) who grew *Populus balsamifera* both in a cool (19/10°C) and warm (27/16°C) environment, although the difference in net photosynthesis at the thermal optimum was rather small (1.5 µmol CO_2 m^{-2} s^{-1}). After a period of heat, the acclimation to a cooler environment takes usually more time (about five to six days) (Schulze *et al*., 2005).

According to Allakhverdiev et al. (2008), heat tolerance is governed by the production of heat shock proteins (HSP), antioxidants, membrane lipid rigidity, and the accumulation of solutes. It is also reported that a more heat stable form of rubisco activase can be produced (Salvucci & Crafts-Brandner, 2004). If plants are exposed to temperatures of more than 10°C above their optimal temperature, HSPs which are present in small amounts in cells will be the only proteins produced during the first hours of this heat shock (Schulze *et al*., 2005). As a first task, HSPs (especially HSP70 and 17) will conserve mRNA of normal proteins in heat shock granules to facilitate the return to non-stressed cell metabolism after heat exposure. Next, proteolysis of irreversibly denatured and aggregated proteins is catalysed by HSPs. A last function, the molecular chaperone function, is assisting protein (re)folding, transport across membranes and translocation into chloroplasts and mitochondria (Schulze *et al*., 2005; Wang *et al*., 2004). More concrete, smHSPs, for which a strong correlation between their accumulation and plant stress tolerance was reported (Wang *et al*., 2004), were shown to protect mitochondrial respiration chain and PSII electron transport (Efeoğlu, 2009). Moreover, a smHSP occurring in thylakoid membranes is able to protect the OEC from oxidative stress but fails to reactivate it after denaturation (Heckathorn *et al*., 1999). After heat stress, a gradual resumption of normal cell metabolism occurs. Perhaps HSPs play also a role in this recovery because of their long half-life times (30 to 50 hours) (Efeoğlu, 2009).
Another process that attributes to thermotolerance is the accumulation of compatible osmolytes such as glycinebetaine, choline, proline, and glycerol (Wahid *et al*., 2007). These are assumed to enhance the stability of photosystems, to keep rubisco activated, to accelerate de novo synthesis of D1 proteins, and to buffer the cellular redox state and thus protect against oxidative stress (Allakhverdiev *et al*., 2008; Schulze *et al*., 2005; Wahid *et al*., 2007).
In a short time period, the fluidity of membranes is stabilized by zeaxanthin and isoprene which protect the lipids against oxidative stress (Wahid *et al*., 2007). A rapid production of hydrophobic zeaxanthin is possible due to a maintained electrochemical gradient associated with cyclic electron flow induced by heat (Sharkey, 2005). Over a longer period (hours to days), membrane rigidity is enhanced by increasing the hydrophobic interactions between fatty acids due to saturation. Upon cooling, a loss of fluidity will however be the cost (Berry & Björkman, 1980; Sage & Kubien, 2007).

For an effective repair of heat-induced damage, energy is necessary for protein synthesis (Murata *et al*., 2007). An augmented cyclic electron flow observed in recovering plants provides cells with ATP while protecting PSII from photoinhibition at low light intensities. In addition, weak light energy attributes to the stimulation of repaired enzymes (Allakhverdiev *et al*., 2008).

2.5 COMBINED HEAT AND CADMIUM STRESS

In literature, only few studies were found that have examined the combined effects of heat and Cd on plants. For instance, Hermle et al. (2007) studied the impact of Cd (10 mg kg^{-1} topsoil) on *Populus tremula* for the three year-period 2001-2003. Photosynthesis rates, stomatal conductance and water use efficiency declined and the internal CO_2 concentration rose in 2001 and 2002 due to Cd. Dark respiration rates were not significantly affected by Cd, but declined upon leaf aging. However, in 2003, Europe experienced a very hot and dry summer resulting in a stabilisation of photosynthesis and transpiration rates and stomatal conductance, although control plants suffered from a continued lowering of these variables. The lower need for water in Cd stressed plants can be explained by a Cd-induced lower biomass production and reduced root water uptake. In addition, dark respiration rates tended to increase as triggered by heat stress. As no significant difference could be observed between dark respiration rates of control and Cd treated plants, any metal stress symptoms are assumed to be masked.

Another study specifically focused on the response of PSII of broad beans (*Vicia faba*) upon exposure to 112.41 mg Cd^{2+} l^{-1} as $CdCl_2$ and/or to 38 or 43°C (Franco *et al*., 1999). PSII activity, monitored as F_V/F_M, showed a 10% decrease for heat treatment and less than 5% decrease for Cd treatment. The combination of both stresses at 38°C for 24 hours kept PSII activity relatively stable at first, but caused a faster decline compared to heat stress later on. At 43°C no such trend was observed. In addition, the electron transport rate declined to about 66% of control after 24 hours of heat treatment (38°C) but rose slightly in Cd treatment. The combined treatment maintained high rates for 48 hours followed by a drastic decrease. Franco et al. (1999) concluded that Cd combined with heat stress resulted in protection of plants for a short period but afterwards a synergistic effect appeared.

CHAPTER 3: RESEARCH OBJECTIVES

In literature, there seems to be a knowledge gap about the combined effects of Cd and heat on poplar plants. This master thesis aims to clarify how Cd and heat can influence photosynthesis, which will be studied by means of chlorophyll *a* fluorescence parameters. Therefore, the effect of Cd and heat will be researched separately and in combination. Plant exposure to heat will take place during two successive growth stages which can be referred to as a spring and summer phenological stage, respectively. Each stage is divided in a preheat period, a heat period, a recovery period and a follow-up period. Concretely, these are the research hypotheses:

1. The exposure of poplar plants to Cd negatively influences photosynthesis.
    a. The main targets of Cd in the electron transport chain are LHCII, PSII and the thylakoid membranes. In the Calvin cycle, Cd induces the oxygenase activity of rubisco (photorespiration).
    b. Photosynthesis is more affected during the spring phenological stage because of a more intense growth.

2. Photosynthesis declines during a heat period.
    a. Heat induces injury to the electron transport chain, mainly LHCII, PSII, and thylakoid membranes. Furthermore, the Calvin cycle is slowed down due to rubisco oxygenase activity and denaturation of the rubisco activase enzyme.
    b. A heat wave during the spring phenological stage has more negative effects on photosynthesis than during the summer phenological stage for the same reason as mentioned above.

3. The combination of Cd and heat stabilizes photosynthesis, thus, plants which are already exposed to Cd do not experience as much extra stress upon heat compared to plants grown in potting compost without added Cd^{2+}.

CHAPTER 4: MATERIALS AND METHODS

4.1 PLANT MATERIAL

In this master thesis, measurements were conducted on cuttings of *Populus canadensis* 'Robusta' obtained at Sylva Van Hulle, Waarschoot, Belgium where they had been preserved in cold storage. Poplar was chosen for its potential use in phytoremediation or phytomining as it meets the needs necessary for those purposes (section 2.3.4). During the experiments, most plants were diseased, probably by the mosaic virus. However, it was still possible to continue the experiments because of the sufficient presence of healthy leaves.

4.2 POTTING COMPOST

Prior to planting, potting compost (DCM Potting Compost for Home & Garden, containing manure for about 100 days) was prepared for 30 pots of about three liters in the Laboratory of Analytical Chemistry and Applied Ecochemistry, Ghent University. First, the potting compost was homogenized by mixing. Next, an average fresh weight of one liter potting compost was determined based on six samples to simplify the distribution of potting compost over the pots. Fiftheen pots were filled with three times the average weight of one liter potting compost. Before filling the remaining 15 pots, potting compost was spiked with a $CdSO_4$ solution containing 1000 mg Cd^{2+} l^{-1}. For an optimal homogenization, one liter of potting compost was spread out in a tray and thoroughly mixed after sprinkling 50 ml of the Cd^{2+} solution by means of a pipette. This action was repeated 45 times to fill 15 pots with three times this quantity of Cd^{2+} containing potting compost. All filled pots were covered with cellophane to obtain equilibrium before planting the cuttings.

4.3 GROWTH CHAMBERS AND EXPERIMENTAL SETUP

On the first of June 2011, the cuttings were planted in the 30 pots, of which 15 with added Cd^{2+} and 15 without, and then placed in one growth chamber at the Laboratory of Plant Ecology, Ghent University. All experiments were conducted in growth chambers making it able to control the environmental conditions. Until the start of the experiments on August 9, the plants could grow under a light regime of about 140 µmol PAR m^{-2} s^{-1} during 15 hours a day from 6 a.m. till 9 p.m. and a day/night temperature regime of about 23/18°C. Plants were well watered during their growth and during the experiments to avoid effects of drought stress.

All 15 plants without added Cd^{2+} in the potting compost were randomly divided in groups of five plants resulting in three different treatments: control, C.Spring and C.Summer (Table 4.1). This was also done with the plants grown in Cd^{2+} containing potting compost. Stress, S.Spring and S.Summer

were the other three treatments. The terms ‘spring’ and ‘summer’ refer to the first and second phenological growth stages of the plants.

Table 4.1: Overview of the treatments of *Populus canadensis* ‘Robusta’

treatment	*Code*	*Cd^{2+}*	*Heat wave 1 (during spring)*	*Heat wave 2 (during summer)*
Control	C	-	-	-
C.Spring	C.Sp	-	+	-
C.Summer	C.Sum	-	-	+
Stress	S	+	-	-
S.Spring	S.Sp	+	+	-
S.Summer	S.Sum	+	-	+

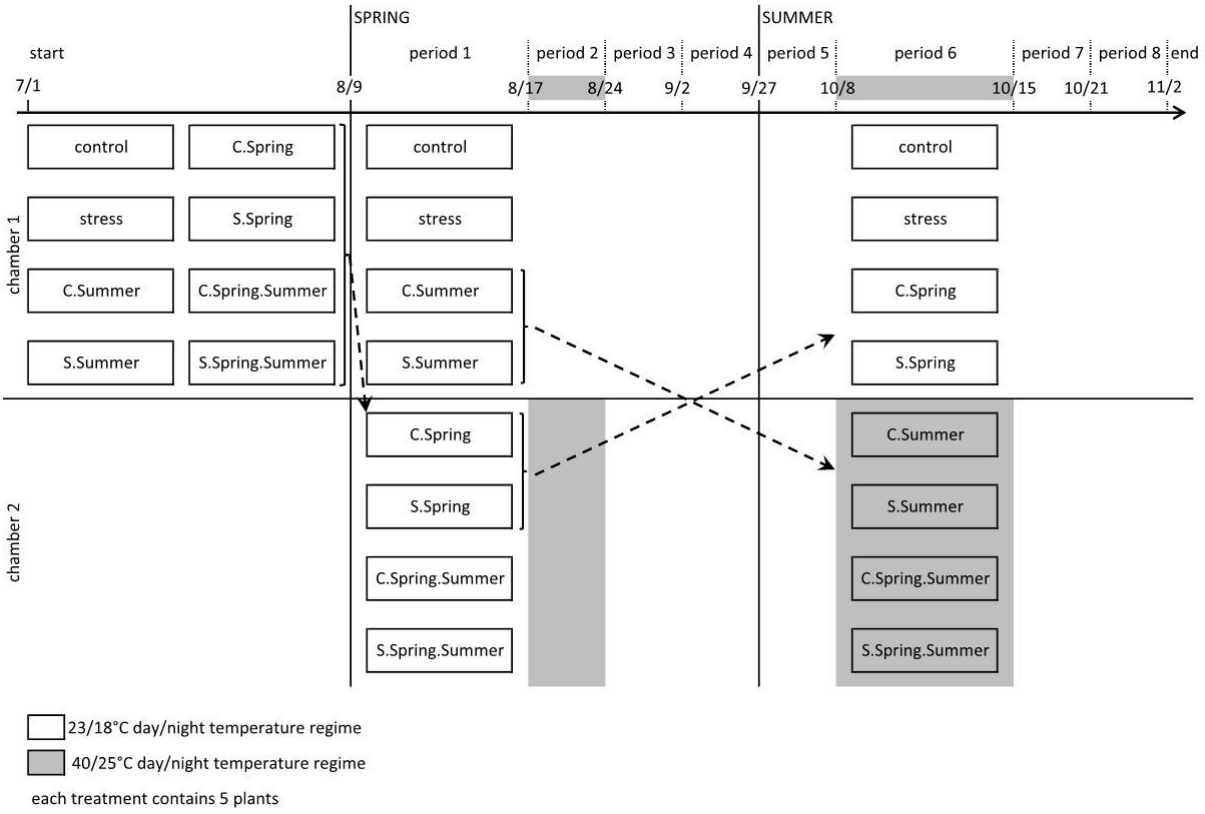

Figure 4.1: Schematic overview of the experiment. On top, a time axis indicates the timing of the experiments. ‘Spring’ and ‘summer’ refer to the first and second phenological growth stages of the plants. The corresponding periods 2 and 6 had a heat wave day/night temperature regime of 40/25°C whereas all other periods had a regime of 23/18°C. The time indication ‘period’ simplifies data processing and discussion further on. Periods 1 and 5 are preheat periods, 2 and 6 heat periods, 3 and 7 recovery periods and 4 and 8 follow-up periods. In boxes the different plant treatments are given according to the growth chamber in which they were placed. Treatments C.Spring.Summer and S.Spring.Summer will not be investigated in this master thesis (Goormachtigh, 2012). The arrows indicate the switching of plants between chambers.

On August 9, plants from treatments C.Sp and S.Sp were placed in chamber two (period 1). Environmental conditions were kept identically and constant at both chambers until the first heat wave was applied in chamber two (period 2). The heat wave started on August 17 during the spring phenological stage by changing the day/night temperature regime to 40/25°C and lasted for seven days. Afterwards, day/night temperatures changed back to 23/18°C (recovery period 3 and period 4). The same was done for the second heat wave in the summer phenological stage starting at October 8 after switching the plants from treatments C.Sum and S.Sum (chamber one) with those from C.Sp and S.Sp (chamber two) as indicated in Figure 4.1. Experiments were finished at November 2.

In order to maintain and control environmental growing conditions, growth chambers were equipped with 1) an air conditioning (M5WM, McQuay Inc., Minneapolis, MN, Minnesota) and a ventilation system to ensure a fixed temperature, 2) tubular lighting which radiates PAR light of about 140 µmol PAR m^{-2} s^{-1}, 3) a PAR sensor at plant height (Quantum, LI-COR Biosciences, Inc., Lincoln, NE, USA), 4) a relative humidity and temperature sensor at plant height (EE08, E+E Elektronik, Engerwitzdorf, Austria), 5) two thermocouples at plant height for extra temperature measurements (type T: copper-constantan), 6) a thermocouple (Pt-100) to regulate temperature automatically and in chamber two a fan heater (VH 206, AEG, EHT Haustechnik GmbH, Nürnberg, Germany) to warm the chamber during a heat wave. Data were collected by a data logging device (34970A, Agilent Technologies, Inc., Santa Clara, CA, USA). In Figure 4.2, the sensors that were used are shown.

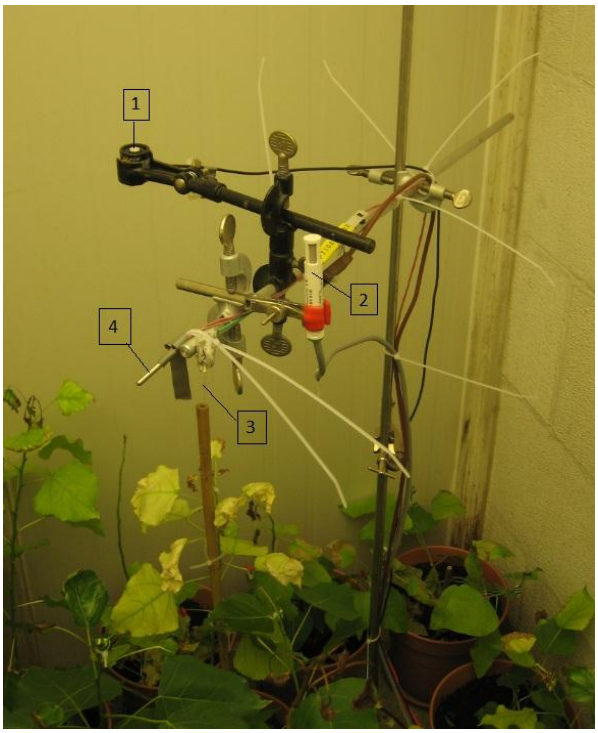

Figure 4.2: Sensors at plant height in the growth chambers: 1) a PAR sensor, 2) a RH and temperature sensor, 3) a type T thermocouple, and 4) a Pt-100 thermocouple.

4.4 MEASUREMENTS

In this master thesis, the main objective is to research the impact of cadmium and heat waves on *Populus canadensis.* As both cadmium and heat waves strongly affect carbon relations in plants, photosynthesis and chlorophyll *a* fluorescence, as a measure of photosynthetic capacity, have to be quantified. Heat waves also have an important influence on water relations, but this will only be examined in the context of photosynthesis.

4.4.1 Gas exchange and chlorophyll *a* fluorescence measurements

Photosynthesis and chlorophyll *a* fluorescence measurements were collected by means of the LI-6400XT portable photosynthesis system equipped with the sensor head LI-COR 6400-40 Leaf Chamber Fluorometer (LI-COR Biosciences, Inc., Lincoln, NE, USA) (Figure 4.3). This device is an open differential infrared gas analyser (IRGA). It is able to calculate photosynthesis and transpiration rates at different light intensities by comparing measured CO_2 and H_2O concentrations of the reference air stream with the air stream that passes through the leaf chamber as shown in Figure 4.4. Therefore, the incoming air first passes through the chemical tubes: the first contains soda lime to scrub all CO_2 and the second a desiccant to control humidity. Subsequently, CO_2 concentration is controlled at 400 ppm by injection of pure CO_2 whereas humidity control is achieved by regulating sample air flow rate by a flow diverter. In the outgoing reference and sample air, absolute CO_2 concentrations are quantified by two infrared gas exchange analysers incorporated in the sensor head. Based on the absorption of infrared radiation by CO_2 in the reference and sample air streams, CO_2 filled reference and sample analyser detectors are able to quantify the remaining infrared radiation and therefore the CO_2 concentration. The water content of the reference and sample air streams is additionally measured by these IRGAs (LI-COR, 2008).

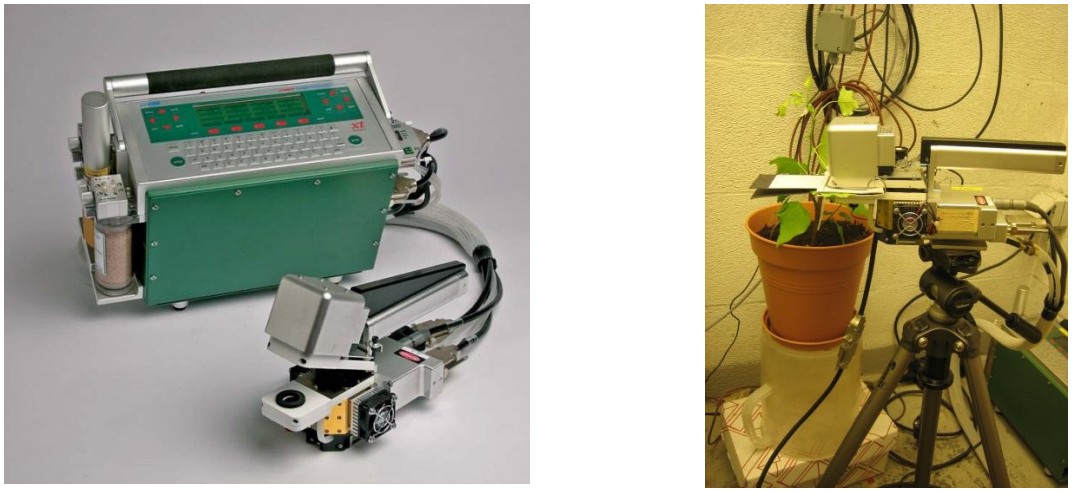

Figure 4.3: left: LI-COR LI-6400XT Portable Photosynthesis System with LI-COR 6400-40 Leaf Chamber Fluorometer as a sensor head (from LI-COR, 2008); right: experimental set-up during measurements.

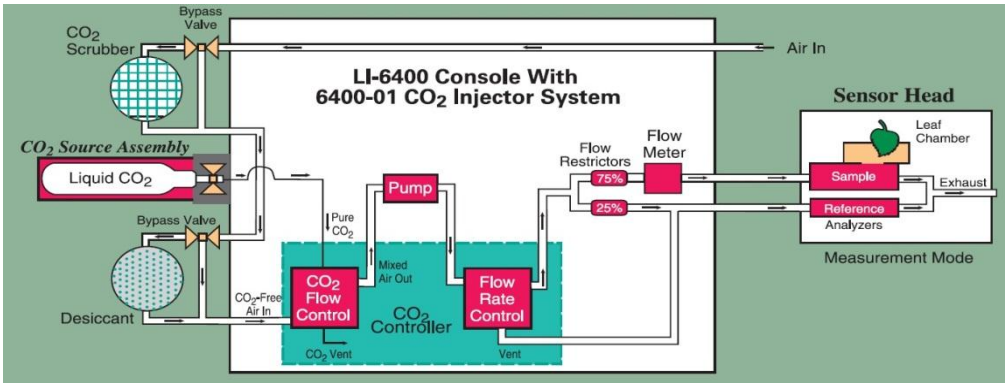

Figure 4.4: Schematic representation of the LI-COR LI-6400XT Portable Photosynthesis System: principle of operation (from LI-COR, 2012).

The calculation of photosynthesis and transpiration rates is based on equations 4.1 and 4.2, respectively.

$$A_{net} = \frac{\Delta CO_2 \cdot air\ \ flow\, rate}{leaf\ \ area} \tag{4.1}$$

$$E = \frac{\Delta H_2O \cdot air\ \ flow\, rate}{leaf\ \ area} \tag{4.2}$$

A_{net} is the net photosynthesis rate (µmol CO_2 m^{-2} s^{-1}); E is the transpiration rate (mol H_2O m^{-2} s^{-1}); ΔCO_2 and ΔH_2O are the differences in CO_2 and H_2O concentrations between sample and reference air (µmol CO_2 mol^{-1} and mol H_2O mol^{-1}). The air flow rate (µmol s^{-1}) and leaf area (cm^2) in the leaf chamber were adjusted at 300 µmol s^{-1} and 2 cm^2 respectively. A measurement of the exact sample air flow rate is necessary to calculate net photosynthesis rates more precisely.

As temperature influences photosynthesis and transpiration rates, it has to be controlled as well. In this master thesis, measurements were conducted at a chamber block temperature of 25°C or 40°C depending on whether a day/night temperature regime of 23/18°C or 40/25°C was applied.

By applying the Leaf Chamber Fluorometer (LCF) as a light source, simultaneous measurements of gas exchange and chlorophyll *a* fluorescence were possible over the same leaf area. Quantifying chlorophyll *a* fluorescence and quenching enabled to detect the allocation of absorbed energy to photosynthesis and heat. Moreover, studying photosynthesis at the level of the electron transport chain became possible (LI-COR, 2011b).
The LCF is a pulse-amplitude modulated (PAM) fluorometer which contains red, one far-red and blue LEDs to generate four different lights: measuring light, actinic light, saturation pulses and far-red radiation. Except for the actinic light, each of these light sources measures a fluorescence parameter according to the saturation pulse method: the minimal fluorescence level F_0 (after 20 minutes of

dark adaptation), the maximum fluorescence level F_M, the maximum light fluorescence level F_M', and F_0', the minimal fluorescence level of a light adapted leaf measured on a moment of darkness. Leaves were dark adapted by using dark adapting clips (LI-COR Biosciences, Inc., Lincoln, NE, USA) and lamp settings included 10% blue light. For more detailed information about this saturation pulse method, section 2.2.2. The LI6400XT device uses these measured parameters to calculate other chlorophyll *a* fluorescence parameters – such as F_V, F_V', F_V/F_M, F_V'/F_M', Φ_{PSII}, q_P, NPQ, ETR and Φ_{CO2} – that allow quenching analysis and thus a more detailed study of photosynthesis. A list of equations can be found in section 2.2.2.

In this master thesis, fluorescence light response curves were measured on a marked leaf of each plant. During periods 1, 3, 5 and 7, the 15 plants in each chamber were measured one another day. When a heat wave was applied, in periods 2 and 6, the plants in chamber two were measured every day during the whole heat wave except for one day on which plants in chamber one were measured. This was done to closely follow changes in the plants as a consequence of the heat. During recovery periods 4 and 8, all plants were measured once a week.
To make this time scheme possible, fluorescence light curves were only recorded at two light intensities: 0 and 1000 µmol PAR m^{-2} s^{-1}. The latter value was found by measuring light curves on randomly selected plants prior to the start of the experiments. It is the light intensity at which photosynthesis rates reached a saturation plateau in the light response curve. Further, a minimum and maximum waiting time of 5 respectively 7 minutes was applied before measurements on a leaf were recorded to allow stabilisation.

Simultaneous with the fluorescence light curve and thus photosynthesis and transpiration rates and chlorophyll *a* fluorescence parameters, other variables were measured or calculated such as stomatal conductance (g_s) and dark respiration rates (R_d).

4.4.2 Chlorophyll content

To gain an indication of the quantity of chlorophyll in the leaves, the "greenness" of the leaf, measurements with the Chlorophyll meter SPAD-502 (Konica Minolta Sensing, Inc., Osaka, Japan) were carried out. Simultaneously with the LI6400XT measurements, the chlorophyll content was determined on each leaf as a mean of three SPAD measurements on that leaf. This was necessary due to spatial variation in chlorophyll content.

To link the photosynthesis and fluorescence data to cadmium, keeping track of the cadmium concentrations in the soil-plant continuum was necessary. Therefore, leaf, potting compost and potting compost solution samples were analysed for their cadmium concentration and bioavailability by determining relevant characteristics of the matrix. Note that roots, stems and branches were not analysed.

4.4.3 Leaf samples

At the end of periods 1, 2, 5, and 6, both during the spring and summer phenological stage, randomly selected leaves were collected after measuring photosynthesis and chlorophyll *a* fluorescence parameters. At the end of periods 3 and 7, the marked leaves on which measurements were conducted during spring respectively summer, were also sampled. If a leaf was damaged before it could be harvested, a new leaf was marked and collected at the end of the experiment. Sometimes, leaves could not be measured anymore, but were still on the plant when the marked leaves were harvested or other times, there were no leaves left. Therefore, in periods 3 and 7 there were more or less than the 15 leaves that would be expected from 15 plants grown with and 15 plants grown without added Cd^{2+} in the potting compost. Reasons for the inability of measuring on leaves were the mosaic virus, too small leaves because of cadmium stress, shrivelled leaves due to heat stress, etc.

Immediately after harvesting, the fresh weight (FW, g) of the leaves was determined. Then, leaves were put through the leaf surface meter (LI-3000 Portable Area Meter, LI-COR Biosciences, Inc., Lincoln, NE, USA) to quantify leaf surface area (cm^2). Subsequently, leaves were stored in paper bags and dried in an oven at 60 - 70°C for about three days. After dry weight (DW, g) was obtained, the water content in terms of percentage ($\%H_2O$) could be calculated from FW and DW (4.3).

$$\%H_2O = \frac{FW - DW}{FW} \tag{4.3}$$

To assess cadmium concentrations in the leaves, first an open microwave destruction of the dried leaves was performed at the Laboratory of Analytical Chemistry and Applied Ecochemistry, Ghent University. This method was chosen because of its complete destruction of leaf particles resulting in a more accurate quantification.

First, dry leaves were grinded to a fine powder. Next, the powder was weighed, put into microwave resistant tubes and 3.5 ml 65% HNO_3 and 3.5 ml H_2O_2 was added. Caps were screwed on the tubes and left overnight. Before the tubes were placed in the microwave (Mars 5, CEM Corporation, Matthews, North Carolina, NC, USA), the caps were screwed one turn back to keep at atmosphere pressure and in one tube a temperature probe was added. The method OMNI/XP1500 was selected. This method generates a gradual temperature rise to 55, 75 and 100°C, each in ten minutes. The samples were left for ten minutes at 55 and 75°C and for 35 minutes at 100°C. After cooling down, the liquid in the tubes was filtered; the tubes, caps and the filter paper were rinsed twice with 1% HNO_3 and once with milli-Q water. Each 50 ml volumetric flask was diluted with milli-Q water. To homogenise, the volumetric flasks were well mixed and for each leaf sample a glass tube was filled.

The leaf samples of the Cd^{2+} containing treatments were analysed for cadmium in an inductively coupled plasma optical emission spectrometer (ICP-OES) (VARIAN Vista MPX CCD Simultaneous ICP-

OES, Agilent Technologies, Inc., Santa Clara, CA, USA). Cadmium was measured at a wavelength of 228.802 nm using external standards attained from a 1000 ppm accredited cadmium solution. The limit of detection (LOD) and the limit of quantification (LOQ) for the ICP-OES amount to 4 ppb and 10 ppb respectively.
The leaf samples without added Cd^{2+} were expected to contain too low cadmium concentrations to be detected with an ICP-OES. Therefore, these samples were analysed by ICP mass spectroscopy (ICP-MS) (ELAN DRC-e, PerkinElmer, Inc., Massachusetts, MA, USA) as the LOD is approximately 0.2 ppb and the LOQ 0.05 ppb. Internal indium standards were used.

4.4.4 Potting compost solution samples

Potting compost solution samples were collected from all pots once in periods 1 and 5 and in periods 2, 3, 6, and 7 at the start and the end of the period. Therefore, rhizon soil moisture samplers were placed in every pot at the beginning of the experiments. When samples had to be taken, vacuum tubes (Vacuette, Greiner Bio-One GmbH, Kremsmünster, Austria) that collected potting compost moisture during the night were pricked on the syringes.

To characterise the potting compost, 2 ml of the liquid samples was used to measure pH with a pH micro-electrode (Knick Portamess 911 (X) pH, Van London – pHoenix Company, Houston, Texas, TX, USA). A pH value was obtained being the average of all periods and pots. Inorganic carbon (IC) and non-purgeable organic carbon (NPOC) were determined by a carbon analyser (TOC-5000A, Shimadzu Benelux BV, Antwerp, Belgium) at the Laboratory for Environmental Toxicology, Ghent University. The remaining potting compost solution samples were acidified by adding a drop of 69.4% HNO_3 to store the samples awaiting the cadmium concentration analysis.
The liquid samples of pots containing Cd^{2+} were all analysed for cadmium by an ICP-OES (VARIAN Vista MPX CCD Simultaneous ICP-OES, Agilent Technologies, Inc., Santa Clara, CA, USA). However, cadmium concentrations of the samples from pots without added Cd^{2+} were quantified by an ICP-MS (ELAN DRC-e, PerkinElmer, Inc., Massachusetts, MA, USA). Moreover, only those samples that corresponded to a leaf sample were analysed because the samples without added Cd^{2+} were assumed to have about equal background concentrations making it unnecessary to analyse all samples. All analyses for cadmium concentration were conducted at the Laboratory of Analytical Chemistry and Applied Ecochemistry, Ghent University. Values for IC, NPOC and Cd concentrations in potting compost solutions are given in Tables 5.2, 5.3 and 5.4, respectively (section 5.2). Also the pH value can be found there.

4.4.5 Potting compost samples

At the start of the experiments, a sample of each pot containing potting compost with added Cd^{2+} and five samples randomly selected from pots without added Cd^{2+} were oven dried at 60 - 70°C for about three days. At the Laboratory of Analytical Chemistry and Applied Ecochemistry, Ghent University, 2.5 ml H_2O, 2.5 ml 65% HNO_3 and 7.5 ml 37% HCl were added to 1 g of potting compost and left overnight to determine cadmium concentrations. Before boiling the solutions for 2 hours at 150°C, an extra quantity of 1.5 ml H_2O, 1.5 ml 65% HNO_3 and 3.5 ml 37% HCl were added to avoid drying of the samples. After filtering, cadmium concentrations were measured using an ICP-OES for samples with Cd^{2+} and an ICP-MS for samples without added Cd^{2+}. Results are shown in Table 5.4, section 5.2.

In order to quantify the percentage of organic matter for potting compost characterization, five times 1 g of potting compost from a mixture of the five samples without added Cd^{2+} were gradually incinerated in a muffle oven: in 30 minutes 250°C was reached and kept there for 1 hour, 550°C was reached in 3 hours and temperature was maintained at 550°C for 2 hours. After cooling down, samples were once more weighed and the organic matter percentage could be calculated (section 5.2).

4.5 DATA ANALYSIS

Data were graphically analysed by means of the software SigmaPlot 12 (Systat Software, Inc., San Jose, CA, USA). Throughout the master thesis, all data represent a mean over the days per period and the plants of a treatment, accompanied by a standard error (SE).

A statistical analysis was conducted in SPSS Statistics 20 (IBM Corporation, Armonk, New York, USA). Therefore, a paired-samples T-test was applied to examine significant differences induced by heat stress between periods within the same treatment (C.Sp, C.Sum, S.Sp and S.Sum) whereas one-way ANOVA followed by a Bonferroni test as a post hoc multiple comparisons test was needed to locate significant differences between treatments per period. Generally, a significance level of 0.05 was used.

CHAPTER 5: RESULTS

In this master thesis, the effects of Cd, heat and a combination of both on photosynthetic processes of *Populus canadensis* 'Robusta' plants were investigated. Chlorophyll *a* fluorescence parameters were useful to discover which particular component of photosynthesis was targeted. After a description of the environmental conditions, the potting compost characterization and Cd concentrations, results concerning the effects of the different stressors on poplar will be presented in this chapter. This will be done according to a systematic approach to allow a thorough discussion in Chapter 6, with first the potential effect on A_{net} and R_d in relation to g_s, followed by the response of the water relations, and finally chlorophyll *a* fluorescence parameters. It should be noted that only data exhibiting a trend are presented.

5.1 GROWTH CHAMBERS: ENVIRONMENTAL CONDITIONS

Experiments were conducted in two growth chambers which both supplied a day light intensity of about 140 µmol PAR m^{-2} s^{-1}. Temperature and VPD (Table 5.1) differed only according to the spring and summer heat wave (period 2 respectively period 6) applied in chamber 2, as described in section 4.3. Although heat wave temperatures were aimed at 40°C, actual growth chamber temperatures were slightly lower.

Table 5.1: Mean values (± SE) for VPD (kPa) and temperature (°C) in growth chambers 1 and 2 during daytime for the days of the periods throughout the experiment. Heat wave values are marked grey.

	Chamber 1		*Chamber 2*	
	Temperature (°C)	VPD (kPa)	Temperature (°C)	VPD (kPa)
Period 1	22.54 ± 0.07	2.046 ± 0.012	21.93 ± 0.87	2.159 ± 0.011
Period 2	22.53 ± 0.05	1.995 ± 0.004	37.66 ± 0.10	5.610 ± 0.019
Period 3	22.16 ± 0.04	1.827 ± 0.009	22.60 ± 0.05	1.988 ± 0.008
Period 4	22.08 ± 0.02	2.030 ± 0.009	22.37 ± 0.01	2.064 ± 0.015
Period 5	22.28 ± 0.04	1.896 ± 0.006	22.57 ± 0.05	1.895 ± 0.013
Period 6	22.39 ± 0.05	2.079 ± 0.007	35.43 ± 0.06	5.614 ± 0.035
Period 7	22.20 ± 0.06	2.309 ± 0.006	22.36 ± 0.06	2.427 ± 0.019
Period 8	22.09 ± 0.04	2.211 ± 0.008	22.35 ± 0.04	2.212 ± 0.010

5.2 POTTING COMPOST CHARACTERIZATION AND CADMIUM CONCENTRATIONS IN POTTING COMPOST, POTTING COMPOST SOLUTION AND LEAVES

5.2.1 Potting compost characterization

The potting compost that was used had a global mean pH of 7.35 ± 0.02 and an organic matter percentage of 73.43 ± 0.70%. IC concentrations (Table 5.2) are noticeable smaller for potting compost solutions with added Cd^{2+} whereas NPOC concentrations (Table 5.3) increase during heat periods. In general throughout this master thesis, it should be noted that values per period and treatment are means for all the days of the period that measurements were conducted (section 4.4) and for all the plants belonging to that treatment (section 4.3). Note that periods 4 and 8 are omitted throughout the master thesis because they had no added value.

Table 5.2: Mean IC values (± SE) (mg l^{-1}) in potting compost solutions per period and treatment. Values preceded by '<' indicate the presence of data lower than the LOQ (5 mg l^{-1}) of the carbon analyser. Heat wave values are marked grey.

IC	*C*	*S*	*C.Sp*	*S.Sp*	*C.Sum*	*S.Sum*
period 1	-	-	-	-	-	-
period 2	36.9 ± 5.2	12.3 ± 0.7	30.6 ± 4.9	13.4 ± 0.6	27.2 ± 4.9	10.7 ± 0.6
period 3	34.9 ± 6.6	13.5 ± 0.7	27.1 ± 4.4	13.7 ± 0.4	21.6 ± 4.4	10.5 ± 0.7
period 5	36.2 ± 12.7	14.4 ± 2.8	17.8 ± 4.9	10.5 ± 1.6	25.2 ± 7.5	8.9 ± 1.1
period 6	24.1 ± 4.9	15.2 ± 2.2	14.9 ± 2.0	<8.5 ± 0.7	15.9 ± 3.0	11.7 ± 1.6
period 7	<13.9 ± 3.1	<12.8 ± 4.1	<11.7 ± 3.1	<6.9 ± 1.6	<12.1 ± 3.5	<7.3 ± 1.4

Table 5.3: Mean NPOC values (± SE) (mg l^{-1}) in potting compost solutions per period and treatment. Heat wave values are marked grey.

NPOC	*C*	*S*	*C.Sp*	*S.Sp*	*C.Sum*	*S.Sum*
period 1	-	-	-	-	-	-
period 2	184.0 ± 40.3	129.9 ± 8.7	187.7 ± 26.0	193.8 ± 17.6	114.9 ± 17.5	145.1 ± 13.7
period 3	194.0 ± 37.8	116.5 ± 8.6	157.1 ± 25.5	140.9 ± 21.1	103.9 ± 19.0	139.5 ± 13.2
period 5	137.0 ± 25.1	106.9 ± 12.4	130.3 ± 15.8	164.1 ± 26.8	119.7 ± 22.2	143.2 ± 5.9
period 6	133.4 ± 19.2	107.3 ± 13.9	118.8 ± 11.6	197.6 ± 28.6	156.1 ± 23.6	175.8 ± 9.6
period 7	132.0 ± 27.8	125.9 ± 23.8	109.8 ± 22.5	203.5 ± 35.0	116.7 ± 18.9	147.4 ± 13.1

5.2.2 Cadmium concentrations

Cadmium concentrations in potting compost solutions, potting compost and leaf dry weight reported in Table 5.4 will be discussed in section 6.1. For C, C.Sp and C.Sum treatments one mean value is reported because Cd levels correspond to background concentrations.

Table 5.4: Mean Cd concentrations (± SE) in potting compost (mg kg^{-1} DW), potting compost solution (µg l^{-1} for C, C.Sp and C.Sum; mg l^{-1} for S, S.Sp and S.Sum) and leaves (mg kg^{-1} DW) per period and treatment. No samples were analysed for C, C.Sp and C.Sum in periods 1, 2 and 5. Heat wave values are marked grey, except for C.Sp and C.Sum.

	C, C.Sp and C.Sum		*S*		*S.Sp*		*S.Sum*	
	Potting compost		Potting compost		Potting compost		Potting compost	
At the start	0.202 ± 0.011		521 ± 61		561 ± 71		499 ± 28	
	Solution	Leaf	Solution	Leaf	Solution	Leaf	Solution	Leaf
Period 1	-	0.553 ± 0.056		88.0 ± 18.2	0.616 ± 0.233	73.6 ± 10.6	0.673 ± 0.113	102 ± 3
Period 2	-	0.597 ± 0.051	0.456 ± 0.067	81.8 ± 17.2	0.636 ± 0.201	95.3 ± 11.6	0.602 ± 0.165	96.5 ± 12.4
Period 3	0.080 ± 0.008	0.693 ± 0.056	0.341 ± 0.045	90.0 ± 12.5	0.514 ± 0.226	98.6 ± 20.6	0.502 ± 0.187	79.4 ± 20.3
Period 5	-	0.843 ± 0.108	0.276 ± 0.051	76.3 ± 22.3	0.423 ± 0.116	101 ± 20	0.405 ± 0.065	111 ± 16
Period 6	0.089 ± 0.012	0.933 ± 0.097	0.281 ± 0.088	98.5 ± 7.3	0.523 ± 0.150	117 ± 22	0.439 ± 0.069	58.2 ± 25.3
Period 7	0.097 ± 0.014	0.995 ± 0.081	0.344 ± 0.078	89.1 ± 7.7	0.529 ± 0.127	107 ± 10	0.425 ± 0.054	79.3 ± 13.6

5.3 EFFECTS OF CADMIUM STRESS ON *Populus canadensis* 'Robusta'

Because this part focuses on Cd stress, the S treatment (added Cd^{2+}, no heat) will be compared with the C treatment (no Cd^{2+}, no heat).

5.3.1 Net photosynthesis, dark respiration and stomatal conductance

The effects of Cd on A_{net} as a major indicator for plant health are of utmost importance because of the consequences for the entire plant (Krupa, 1999; Pinto, 1980; Raven, 2005). Figure 5.1.A displays this variable per period for C and S treatments. Since A_{net} is the result of gross photosynthesis (A_{gross}) minus R_d, a bar chart of the latter reveals useful information (Figure 5.1.B). For instance, a rising trend in A_{net} and R_d for both treatments is noticeable during spring phenological stage (periods 1 to 3) followed by a decline during summer phenological stage (periods 5 to 7). Thereby, A_{net} values for C during spring have not yet reached mature levels whereas R_d is higher than during summer. The negative value for S in period 7 indicates a larger R_d compared to A_{gross} resulting in the net respiration of biomass. Furthermore, the large significant differences between C and S treatments for A_{net} cannot be elucidated by the rather limited decrease of R_d values for S compared to C, indicating a drop in A_{gross} for S. This can also be seen in mean leaf areas and fresh and dry weights of harvested leaves (Table 5.6).Table 5.5 reports for mean A_{net}, R_d and A_{gross} values per period and treatment, the increase or decrease in terms of percentage for the S treatment compared to C.

In order to locate the photosynthesis related targets of Cd, limitations on the necessary elements will be examined. These elements are CO_2, water, chlorophyll and light energy. The CO_2 supply through stomata is regulated by g_s (Mott, 1988). In Figure 5.1.C, a gradual incline of g_s for both C and S can be observed except for the last period. Mean percentages increase or decrease for S compared to C can be found in Table 5.5.

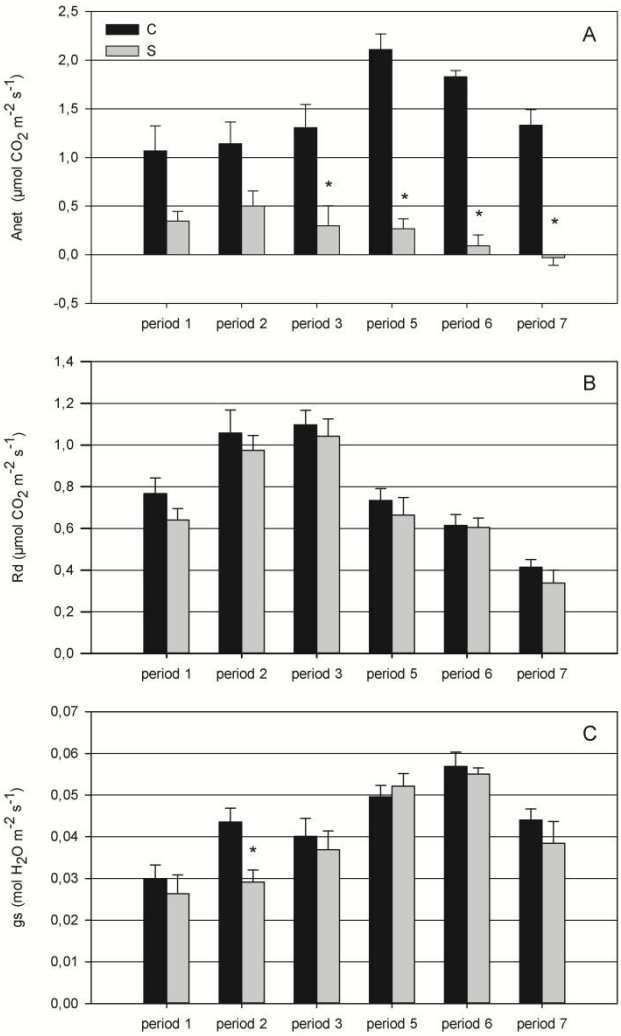

Figure 5.1: Net photosynthesis (A_{net}) (A), dark respiration (R_d) (B) and stomatal conductance (g_s) (C) for C and S treatments as a function of discrete time periods. A bar represents the mean (± SE) of the data per period and treatment. Significant differences within a period are indicated by '*' ($P < 0.05$). Driving forces temperature and VPD can be found in Table 5.1 (chamber 1).

Table 5.5: Relative difference (%) (increase, +; decrease, -) of S compared to C per period and for mean A_{net}, R_d, A_{gross}, g_s and E values per period and treatment reported in Figures 5.1 and 5.2, except for A_{gross}.

	A_{net}	R_d	A_{gross}	g_s	E
Period 1	-67.5	-16.5	-46.2	-11.5	-3.1
Period 2	-55.9	-7.8	-25.6	-33.1	-29.5
Period 3	-77.2	-5.0	-44.3	-8.0	-8.5
Period 5	-87.2	-14.8	-67.8	+5.7	+5.5
Period 6	-94.9	-1.5	-71.4	-3.3	+0.5
Period 7	-102.1	-18.4	-81.0	-12.7	-14.6

Table 5.6: Mean values (± SE) of fresh weight (FW, g), dry weight (DW, g), leaf area (cm^2) and relative water content (%H_2O,%) for all harvested leaves of C and S over all periods.

	FW	*DW*	*leaf area*	*%H_2O*
C	1.112 ± 0.119	0.353 ± 0.036	68.88 ± 5.49	66.8 ± 2.4
S	0.563 ± 0.061	0.161 ± 0.012	46.86 ± 4.41	68.3 ± 2.9

5.3.2 Water relations

In this section, the possibility of water limitation to photosynthesis is explored. Although plants were well watered throughout the experiment, possibly less water could be absorbed due to root damage by Cd (section 2.3.5). For all harvested C and S leaves relative mean water contents over all periods were calculated (section 4.4.3) and reported in Table 5.6.

For completeness, transpiration rates are provided in Figure 5.2. The evolution in time and the differences between C and S are parallel to g_s. In Table 5.5, the increase or decrease in terms of percentage of mean E values for the S treatment compared to C can be found.

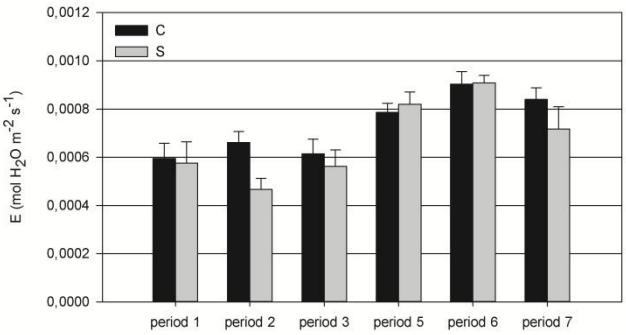

Figure 5.2: Transpiration (E) for C and S treatments as a function of discrete time periods. A bar represents the mean (± SE) of the data per period and treatment. No significant differences were observed ($P < 0.05$). Driving forces temperature and VPD can be found in Table 5.1 (chamber 1).

5.3.3 Chlorophyll content and chlorophyll *a* fluorescence parameters

A third potential limiting factor is chlorophyll content which is qualitatively obtained as "leaf greenness" (section 4.4.2). In Figure 5.3, this parameter is displayed in a bar chart of which the axis values are merely a measure of 'more' or 'less' greenness. Pictures of selected examples of both C and S treatments give an impression of the leaf chlorosis.
Other visual alterations due to Cd include the curling up of leaves, especially newly formed (Figure 5.3 right picture, leaves at the top), pinpoint necrosis spreading over the leaf in time, overall reduced plant growth, and faster abscission of older leaves.

Chlorophyll *a* fluorescence parameters allow a more in-depth study of Cd targets which would stay latent if only gas exchange measurements were examined.

Figure 5.3: Bar chart: leaf greenness for C and S treatments. A bar represents the mean (± SE) of the data per period and treatment. Significant difference is indicated by '*' ($P < 0.05$). Left picture: C plant (August 10, 2011). Note the symptoms of the virus on the top leaves. Right picture: S plant (August 12, 2011).

A diminished chlorophyll content could indicate damage to LHCII. To quantify to which extent the electron transport chain may be affected, the PSII operating efficiency, Φ_{PSII}, will be studied because in literature the assumption is made that it can be used as a measure for the whole electron transport chain efficiency (Baker & Oxborough, 2004). Figure 5.4.A presents Φ_{PSII} per period for C and S treatments and reveals rather constant values in time which are significantly different for S. In order to reveal more information, Φ_{PSII} is broken down in the factors q_p, the fraction of open PSII reaction centres, and F_V'/F_M', the maximum PSII efficiency in light-adapted leaves. Both can be found in function of time in Figures 5.4.B and C. F_V'/F_M' values nearly show no variation between periods and are significantly lower for S, thereby largely clarifying trends for Φ_{PSII}. The same parameter for dark-adapted leaves, F_V/F_M, varies in a similar way (data not shown): S values are close to 0.6 in contrast to C values reaching 0.77. The fraction of open PSII reaction centres exhibits more variation in time for the S treatment with only a significant difference for period 3. As a last parameter in this

context (Figure 5.4.D), non-photochemical quenching shows an interesting declining trend in time for the S treatment and rather constant values for C, which are, however, lower in summer phenological stage compared to spring. Globally, a higher NPQ for S is observed of which the connotation will be described in Chapter 6.

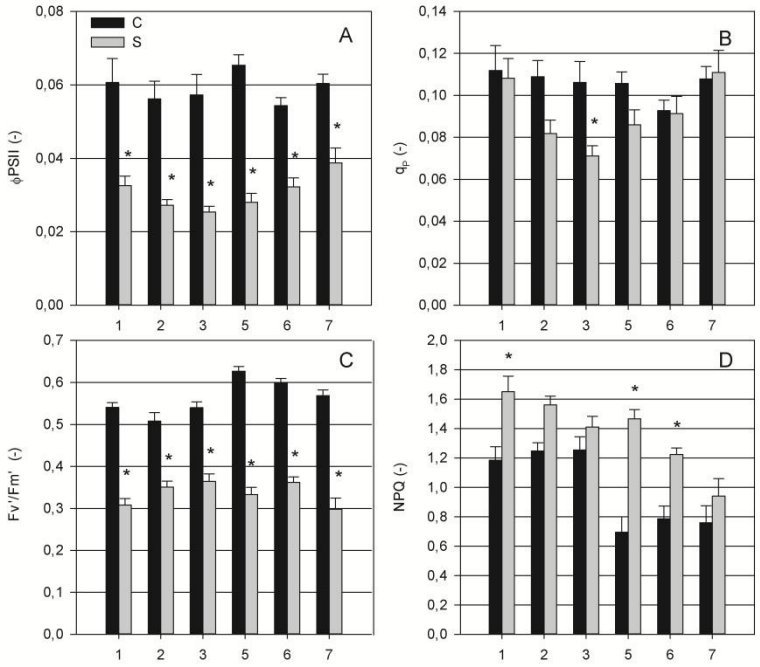

Figure 5.4: PSII operating efficiency (Φ_{PSII}) (A), fraction of open PSII reaction centres (q_p) (B), maximum PSII efficiency in light-adapted leaves (F_V'/F_M') (C) and non-photochemical quenching (NPQ) (D) for C and S treatments as a function of discrete time periods (indicated by numbers on horizontal axis). A bar represents the mean (± SE) of the data per period and treatment. Significant differences within a period are indicated by '*' ($P < 0.05$). Driving forces temperature and VPD can be found in Table 5.1 (chamber 1).

Next to the electron transport chain, also the Calvin cycle can suffer from Cd damage. In literature, the quantum efficiency of CO_2 assimilation, Φ_{CO2}, has been used in this context (Baker, 2008; Baker & Oxborough, 2004). However, the ratio of Φ_{CO2} over Φ_{PSII} seems more interesting because it represents the number of moles of CO_2 assimilated compared to the amount of energy (photons) used in the electron transport chain. The latter would be total absorbed energy in Φ_{CO2} which also contains energy for fluorescence and NPQ. Therefore, Figure 5.5 displays both, but only to explain the ratio. For Φ_{CO2}, the rise during spring followed by a decline during summer parallels for both treatments with the time pattern of A_{net} which is rather obvious upon consulting the Φ_{CO2} formula (section 2.2.2). In addition, the lower values for S were already observed in A_{net}. A bar chart of the ratio of Φ_{CO2} over Φ_{PSII} (Figure 5.5.B) shows the same time trend as Φ_{CO2} because Φ_{PSII} was rather constant. A higher value for S in the spring phenological is followed by lower values during the summer stage.

With the aim of explaining this trend, the specificity factor for rubisco, S_R, was calculated for both treatments and all periods according to equations 5.1, 5.2 and 5.3 (Valentini *et al*., 1995) and presented in Figure 5.5.C.

$$S_R = \frac{Jc/Jo}{c/o} \tag{5.1}$$

$$Jc = \frac{1}{3}\cdot(J_t + 8\cdot(A_{net} + R_d)) \tag{5.2}$$

$$Jo = \frac{2}{3}\cdot(J_t - 4\cdot(A_{net} + R_d)) \tag{5.3}$$

In these equations, Jc and Jo are the electron flows for carboxylation and oxygenation respectively; c is the intercellular CO_2 concentration (C_i, measured with LI-COR, section 4.4.1), o the intercellular O_2 fraction calculated with C_i (Ainsworth & Rogers, 2007) and J_t the total electron flow which was set equal to ETR (section 2.2.2).

Figure 5.5.C indicates a similar time pattern for C and S as the ratio Φ_{CO2}/Φ_{PSII}. The higher values for S during the spring phenological stage and the lower values during summer will be discussed in section 6.3.3. In Table 5.7, the percentage increase or decrease for the S treatment compared to C per period is shown for mean chlorophyll *a* fluorescence parameters per period and treatment.

It should be noted that throughout this master thesis, no significant correlations could be found between the Cd concentrations and photosynthetic or chlorophyll *a* fluorescence parameters because all Cd concentrations were very high.

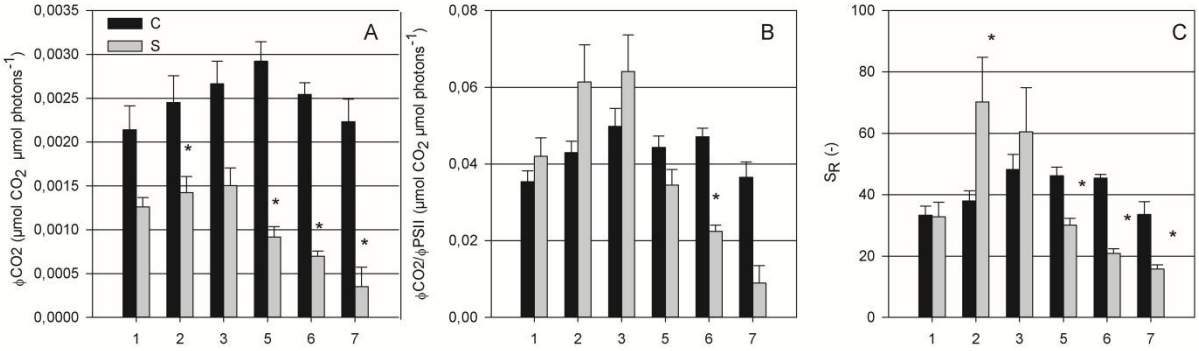

Figure 5.5: Quantum efficiency of CO_2 assimilation (Φ_{CO2}) (A), the ratio of Φ_{CO2} over Φ_{PSII} (Φ_{CO2}/Φ_{PSII}) (B) and specificity factor for rubisco (S_R) (C) for C and S treatments as a function of discrete time periods (indicated by numbers on horizontal axis). A bar represents the mean (± SE) of the data per period and treatment. Significant differences within a period are indicated by '*' ($P < 0.05$). Driving forces temperature and VPD can be found in Table 5.1 (chamber 1).

Table 5.7: Relative difference (%) (increase, +; decrease, -) of S compared to C for mean chlorophyll *a* fluorescence parameters per period and treatment, reported in Figures 5.4 and 5.5.

	Φ_{PSII}	F_V'/F_M'	q_p	NPQ	Φ_{CO2}	Φ_{CO2}/Φ_{PSII}	S_R
Period 1	-46.3	-43.0	-3.3	+39.4	-41.1	+18.6	-1.3
Period 2	-51.5	-30.9	-24.9	+25.3	-41.8	+42.8	+85.0
Period 3	-55.6	-32.5	-33.0	+12.5	-43.5	+28.6	+25.5
Period 5	-57.1	-46.8	-18.7	+111.0	-68.6	-22.1	-34.8
Period 6	-40.7	-39.5	-1.6	+55.8	-72.5	-52.4	-53.9
Period 7	-35.8	-47.7	+2.9	-23.8	-84.2	-75.5	-53.0

5.4 EFFECTS OF HEAT STRESS DURING SPRING OR SUMMER PHENOLOGICAL STAGE ON *Populus canadensis* 'Robusta'

Heat stress was applied during the spring phenological stage (period 2) and during the summer phenological stage (period 6) on control plants (no added Cd^{2+}) resulting in the treatments C.Sp and C.Sum, respectively. Those will be compared with the C treatment and each other. Heat periods are marked grey in all tables and graphs.

5.4.1 Net photosynthesis, dark respiration and stomatal conductance

In Figure 5.6, the effect of heat stress on photosynthesis can unmistakably be observed: A_{net} declines during heat and R_d rises. According to Table 5.8, the significant drop of A_{net} for C.Sp in period 2 cannot completely be elucidated by the R_d rise, pointing out that heat stress induces reduced A_{gross}. A similar result is obtained for C.Sum, although the significant R_d rise is less high, compatible with the lower values in general. Upon recovery, C.Sp shows a stimulation of A_{net} and A_{gross} (Table 5.8 and 5.9) (period 3) compared to the preheat period (period 1), in contrast to C.Sum. The time trend in A_{net} and R_d for C is already mentioned in section 5.3.1. Furthermore, a higher A_{net} starting value of C.Sp than C can be due to natural variation between plants. Table 5.10 presents fresh and dry weights and leaf areas for C.Sp and C.Sum.

In order to explain the heat-induced drop in A_{net}, the potential limitation to the supply of CO_2 is examined by means of g_s (Figure 5.6.C and F). During the spring heat wave, a significant decrease in g_s can be observed, although during summer this decrease is less pronounced (but still significant) because of the overall higher g_s values (Table 5.9). In correlation with a stimulated A_{net}, recovery period 3 shows an enhanced g_s which was not detected in recovery period 7. The time trend for C has also been explained in section 5.3.1.

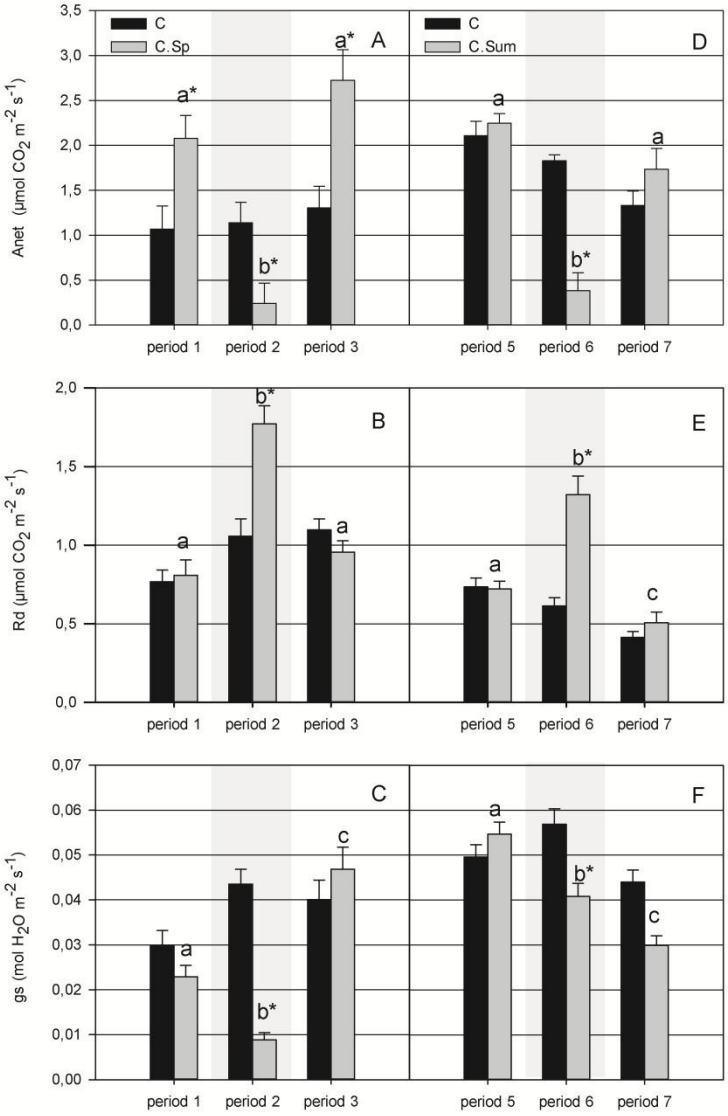

Figure 5.6: Net photosynthesis (A_{net}), dark respiration (R_d) and stomatal conductance (g_s) for C and C.Sp (A, B, C) and for C and C.Sum (D, E, F) treatments as a function of discrete time periods. A bar represents the mean (± SE) of the data per period and treatment. Significant differences ($P < 0.05$) within a treatment over periods are indicated by letters whereas a significant difference compared to C within a period is marked by '*'. Spring and summer growth stages have to be considered separately. Driving forces temperature and VPD can be found in Table 5.1 (chamber 1 for C and C.Sum period 5; chamber 2 for C.Sp and C.Sum periods 6 and 7).

Table 5.8: Mean A_{net}, R_d and A_{gross} values (µmol CO_2 m^{-2} s^{-1}) for C.Sp and C.Sum per period and treatment. A_{net} and R_d values are similar to those displayed in Figure 5.6.

C.Sp	A_{net}	R_d	A_{gross}
Period 1	2.08	0.81	2.89
Period 2	0.24	1.77	2.01
Period 3	2.72	0.96	3.68

C.Sum	A_{net}	R_d	A_{gross}
Period 5	2.22	0.73	2.95
Period 6	0.38	1.32	1.65
Period 7	1.74	0.51	2.24

Table 5.9: Relative difference (%) (increase, +; decrease, -) of C.Sp and C.Sum compared to C.Sp in period 1 and C.Sum in period 5 for mean A_{net}, R_d, A_{gross}, g_s and E per period and treatment, reported in Figures 5.6 and 5.7, except for A_{gross}.

C.Sp	A_{net}	R_d	A_{gross}	g_s	*E*
Period 2	-88.3	+119.0	-30.2	-61.2	+142.9
Period 3	+31.2	+18.2	+27.6	+104.3	+43.4

C.Sum	A_{net}	R_d	A_{gross}	g_s	*E*
Period 6	-82.8	+81.5	-44.0	-25.6	+116.6
Period 7	-22.0	-30.3	-24.0	-45.5	-32.4

Table 5.10: Mean values (± SE) of fresh weight (FW, g), dry weight (DW, g), leaf area (cm^2) and relative water content ($\%H_2O$,%) for all harvested leaves of C.Sp and C.Sum per period.

C.Sp	*FW*	*DW*	*leaf area*	*$\%H_2O$*
period 1	-	-	-	-
period 2	0.610 ± 0.071	0.142 ± 0.018	45.40 ± 4.17	76.8 ± 0.3
period 3	0.912 ± 0.163	0.236 ± 0.052	62.49 ± 11.75	75.4 ± 3.0

C.Sum	*FW*	*DW*	*leaf area*	*$\%H_2O$*
period 5	0.260 ± 0.003	0.077 ± 0.018	20.86 ± 2.40	70.7 ± 6.6
period 6	0.808 ± 0.446	0.239 ± 0.118	46.16 ± 15.16	69.1 ± 2.4
period 7	1.264 ± 0.262	0.434 ± 0.109	-	68.3 ± 3.6

5.4.2 Water relations

Due to the heat, plants closed stomata to prevent dehydration (Figure 5.6.C and F). To gain an idea if this was fruitful, mean water contents in terms of percentage of harvested leaves for C, C.Sp and C.Sum treatments were compared (Table 5.10). For C.Sp, these percentages were slightly higher than for C.Sum.

The transpiration rates shown in Figure 5.7 are rather constant for C, C.Sp and C.Sum except for periods 2 and 6, in which heat significantly intensifies transpiration and during recovery period 3. Note globally the slightly higher values during the summer phenological stage in correlation with g_s.

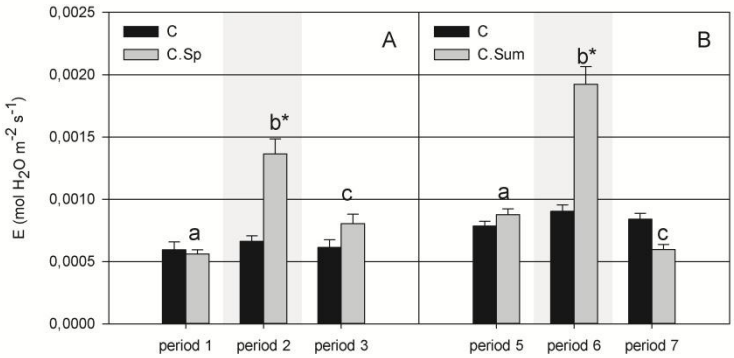

Figure 5.7: Transpiration (E) for C and C.Sp (A) and for C and C.Sum (B) treatments as a function of discrete time periods. A bar represents the mean (± SE) of the data per period and treatment. Significant differences ($P < 0.05$) within a treatment over periods are indicated by letters whereas a significant difference compared to C

within a period is marked by '*'. Spring and summer growth stages have to be considered separately. Driving forces temperature and VPD can be found in Table 5.1 (chamber 1 for C and C.Sum period 5; chamber 2 for C.Sp and C.Sum periods 6 and 7).

5.4.3 Chlorophyll content and chlorophyll *a* fluorescence parameters

In literature, heat was not reported to reduce chlorophyll content and indeed no alterations in leaf greenness were observed (data not shown). A parameter that however was described to undergo changes of which may explain limitations to A_{net} through the electron transport chain is Φ_{PSII}. Surprisingly, an increase during heat periods 2 and 6 and even in recovery period 3 was noticed compared to constant values for C (Figure 5.8.A and E). Correspondingly to A_{net}, Φ_{PSII} of C.Sp starts higher than C (period 1) probably due to natural variation.
The parameters q_p and F_V'/F_M', shown in Figure 5.8, have rather opposite patterns except for C, which showed values nearly constant in time. Upon heat stress, C.Sp and C.Sum attain significantly elevated levels for q_p which drop slightly during recovery. During period 1, the q_p value for C.Sp rises above C addressing the cause for the same trend in Φ_{PSII}. For F_V'/F_M', a decline in heat periods 2 and 6 occurs with a subsequent recovery to initial levels except for C.Sum. In contrast to the Cd effect, F_V/F_M values are not affected by heat stress (data not shown). From Figure 5.8, it can be seen that q_p has a dominating role in determining the pattern of Φ_{PSII}.
The last parameter in association with the electron transport chain (Figure 5.8.D and H), NPQ, shows almost a similar pattern as q_p: a rise during periods 2 and 6 with a minor wane in period 3 and even a increase in period 7. It should be noted that NPQ levels for C are lower during the summer phenological stage. In addition, Table 5.11 presents relative differences of C.Sp and C.Sum to C.Sp in period 1 and C.Sum in period 5 for chlorophyll *a* fluorescence parameters.

Concerning a limiting effect of the Calvin cycle, the parameters Φ_{CO2}, Φ_{CO2}/Φ_{PSII} and S_R for C, C.Sp and C.Sum can be found in Figure 5.9. The time trend in Φ_{CO2} for C is already mentioned in section 5.3.3. Furthermore, the decrease in Φ_{CO2} during heat periods for both C.Sp and C.Sum is comparable with A_{net}, only less pronounced. Compared to the summer phenological stage, Φ_{CO2} values during spring seem less affected by heat and more stimulated afterwards. These findings can now be used to explain patterns in Φ_{CO2}/Φ_{PSII}. For C, spring increasing and summer decreasing time trends can be explained by Φ_{CO2} because Φ_{PSII} is rather constant (section 5.3.3). Although for C.Sp and C.Sum Φ_{CO2}/Φ_{PSII} exposes an analogous trend as Φ_{CO2}, a more prominent drop during heat periods can be observed accompanied by a larger boost in period 7 than the one noticed in Φ_{CO2}. A last parameter, S_R, shows similar trends as Φ_{CO2}/Φ_{PSII} apart from C.Sp in period 1 which is quite larger than C, probably due to natural variation.

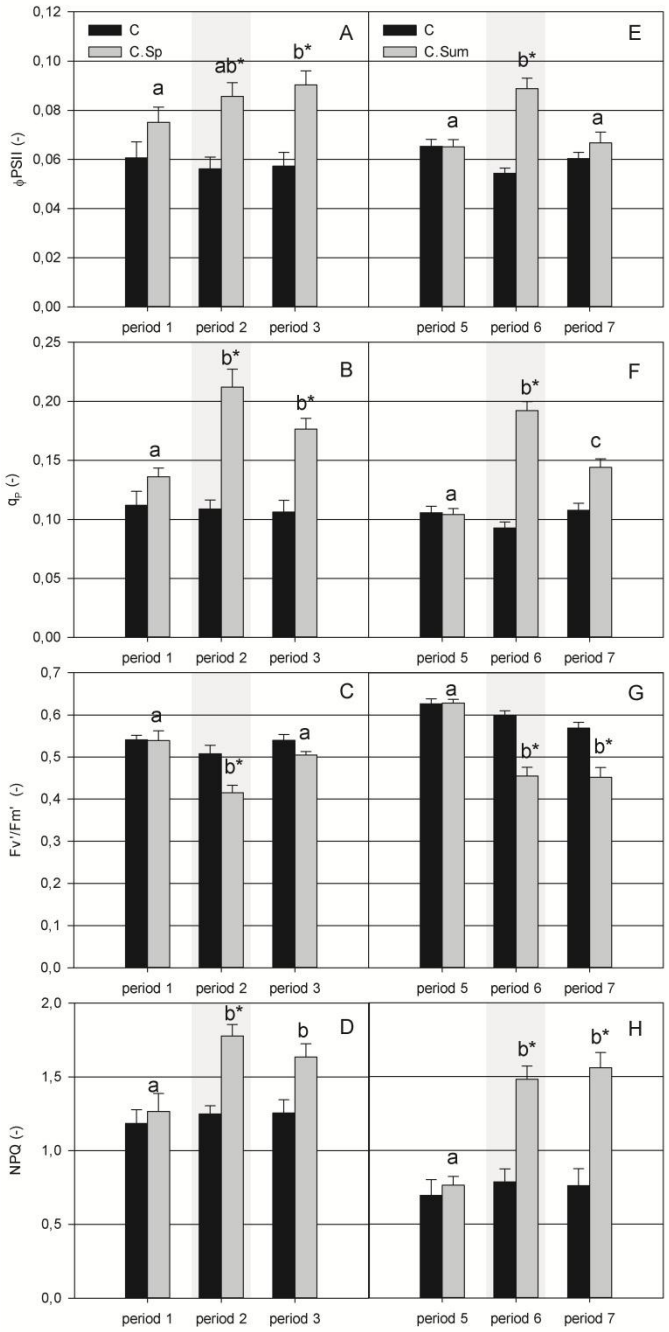

Figure 5.8: PSII operating efficiency (Φ_{PSII}), fraction of open PSII reaction centres (q_p), maximum PSII efficiency in light-adapted leaves (F_V'/F_M') and non-photochemical quenching (NPQ) for C and C.Sp (A, B, C, D) and for C and C.Sum (E, F, G, H) treatments as a function of discrete time periods. A bar represents the mean (± SE) of the data per period and treatment. Significant differences ($P < 0.05$) within a treatment over periods are indicated by letters whereas a significant difference compared to C within a period is marked by '*'. Spring and summer growth stages have to be considered separately. Driving forces temperature and VPD can be found in Table 5.1 (chamber 1 for C and C.Sum period 5; chamber 2 for C.Sp and C.Sum periods 6 and 7).

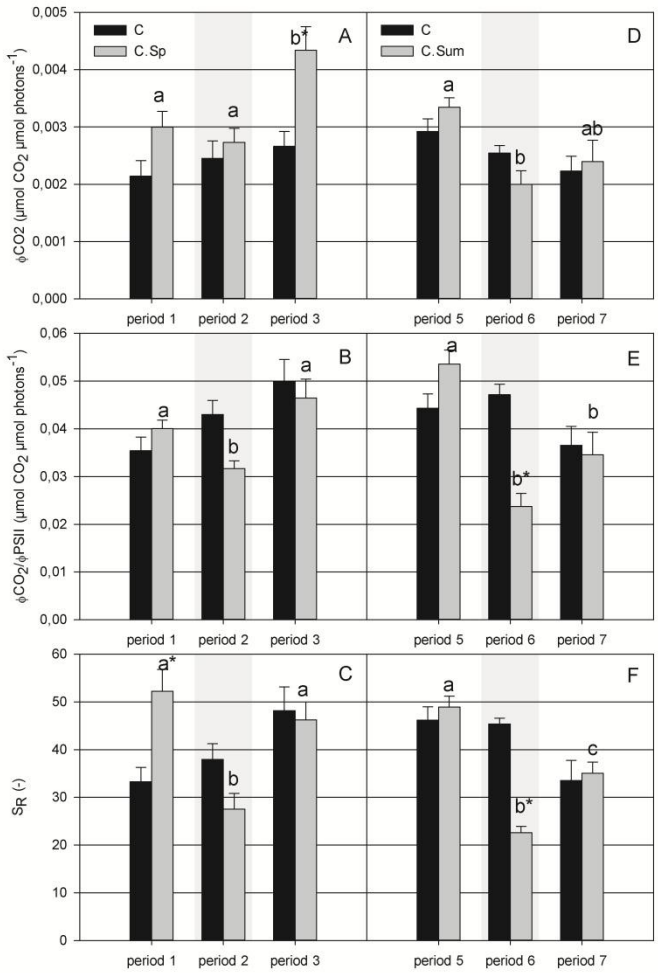

Figure 5.9: Quantum efficiency of CO_2 assimilation (Φ_{CO2}), the ratio of Φ_{CO2} over Φ_{PSII} (Φ_{CO2}/Φ_{PSII}) and specificity factor for rubisco (S_R) for C and C.Sp (A, B, C) and for C and C.Sum (D, E, F) treatments as a function of discrete time periods. A bar represents the mean (± SE) of the data per period and treatment. Significant differences ($P < 0.05$) within a treatment over periods are indicated by letters whereas a significant difference compared to C within a period is marked by '*'. Spring and summer growth stages have to be considered separately. Driving forces temperature and VPD can be found in Table 5.1 (chamber 1 for C and C.Sum period 5; chamber 2 for C.Sp and C.Sum periods 6 and 7).

Table 5.11: Relative difference (%) (increase, +; decrease, -) of C.Sp and C.Sum compared to C.Sp in period 1 and C.Sum in period 5 for mean chlorophyll *a* fluorescence parameters per period and treatment, reported in Figures 5.8 and 5.9.

C.Sp	Φ_{PSII}	F_V'/F_M'	q_p	*NPQ*	Φ_{CO2}	Φ_{CO2}/Φ_{PSII}	S_R
Period 2	+13.9	-23.1	+55.8	+40.3	-8.9	-20.8	-47.3
Period 3	+20.2	-6.4	+29.6	+29.0	+44.7	+16.1	-11.5

C.Sum	Φ_{PSII}	F_V'/F_M'	q_p	*NPQ*	Φ_{CO2}	Φ_{CO2}/Φ_{PSII}	S_R
Period 6	+36.5	-27.5	+84.5	+94.1	-40.2	-55.7	-53.8
Period 7	+2.6	-28.0	+38.3	+104.4	-28.3	-35.5	-28.4

5.5 COMBINED EFFECTS OF CADMIUM AND HEAT STRESS DURING SPRING OR SUMMER PHENOLOGICAL STAGE ON *Populus canadensis* 'Robusta'

In this section, the effects of a simultaneous application of both stressors cadmium and heat will be investigated. Therefore, plants with added Cd^{2+} were exposed to a heat wave during the spring or summer phenological stage leading to the treatments S.Sp and S.Sum respectively. The former will be compared to C, S and C.Sp for the spring periods whereas the latter to C, S and C.Sum for the summer periods. An evaluation of both treatments against each other will also be conducted. Heat periods are marked grey in all tables and graphs.

5.5.1 Net photosynthesis, dark respiration and stomatal conductance

In Figure 5.10.A and D, an analogous response of S.Sp and S.Sum to heat as C.Sp and C.Sum respectively can be detected, although overall values will be lower due to Cd exposure. In heat periods 2 and 6, A_{net} significantly declines to negative values for S.Sp and S.Sum, which indicate more dark respiration than A_{gross}, leading to biomass respiration. This is confirmed in Table 5.12 which displays the values of A_{net} and R_d presented in Figure 5.10 and calculated A_{gross}. In contrast to the previously mentioned decrease in both A_{net} and A_{gross} upon exposure to cadmium or heat, for S.Sp, the decrease in A_{net} during the heat period is more than covered by a significantly boosted R_d (Figure 5.10.B) resulting in a stimulation of A_{gross}. This is a rather stunning result which does not occur during the summer phenological stage, although here the decline in A_{gross} is far less than upon exposure to a single stressor (Cd or heat) (Tables 5.12, 5.13, 5.8 and 5.5). Upon recovery, A_{net} becomes positive and rises even higher than preheat levels during the spring stage parallel with C.Sp (Figure 5.10.A and D). R_d values drop significantly but remain higher compared to periods 1 and 5 also in parallel with C.Sp and C.Sum (Figure 5.10.B and E). This results in an enhanced stimulation of the calculated A_{gross} during recovery period 3, however less than for C.Sp, and a stabilization to the preheat level in period 7 whereas C.Sum cannot reach its preheat level (Table 5.8). It should be noted that, globally, A_{net} values during the summer stage are higher (and thus less negative) due to lower R_d values, except for period 7. Table 5.13 shows relative differences of S.Sp and S.Sum compared to S.Sp in period 1 and S.Sum in period 5 for A_{net}, A_{gross}, R_d, g_s and E. Table 5.14 presents leaf areas, fresh and dry weights for S.Sp and S.Sum.

Now the interesting survey of finding the causes can start with g_s (Figure 5.10.C and F). Although the starting value for S.Sp is already lower than S due to natural variation between plants, g_s for S.Sp declines upon exposure to heat and increases significantly during recovery period 3. A similar trend is followed by C.Sp. During the summer stage (Figure 5.10.F), heat does not cause any change in g_s, although a decline can be observed upon recovery similarly to S. Generally, the lower g_s values during spring compared to summer should be noticed.

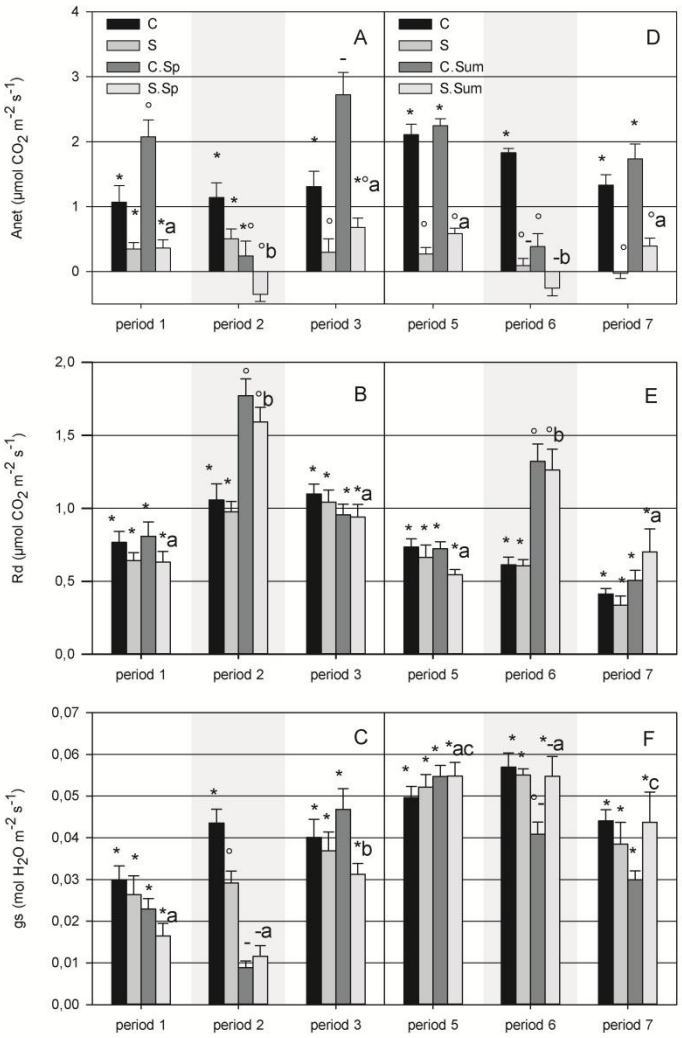

Figure 5.10: Net photosynthesis (A_{net}), dark respiration (R_d) and stomatal conductance (g_s) for C, S, C.Sp and S.Sp (A, B, C) and for C, S, C.Sum and S.Sum (D, E, F) treatments as a function of discrete time periods. A bar represents the mean (± SE) of the data per period and treatment. Significant differences ($P < 0.05$) within treatment S.Sp or S.Sum over periods are indicated by letters whereas significant differences within a period are marked by symbols. Spring and summer growth stages have to be considered separately. Driving forces temperature and VPD can be found in Table 5.1 (chamber 1 for C, S, C.Sum and S.Sum period 5; chamber 2 for C.Sp, S.Sp, C.Sum and S.Sum periods 6 and 7).

Table 5.12: Mean A_{net}, R_d and A_{gross} values (µmol CO_2 m^{-2} s^{-1}) for S.Sp and S.Sum per period and treatment. A_{net} and R_d values are similar to those displayed in Figure 5.10.

S.Sp	*A_{net}*	*R_d*	*A_{gross}*
Period 1	0.36	0.63	0.99
Period 2	-0.37	1.58	1.21
Period 3	0.68	0.94	1.62

S.Sum	*A_{net}*	*R_d*	*A_{gross}*
Period 5	0.57	0.54	1.11
Period 6	-0.26	1.26	1.00
Period 7	0.40	0.71	1.11

Table 5.13: Relative difference (%) (increase, +; decrease, -) of S.Sp and S.Sum compared to S.Sp in period 1 and S.Sum in period 5 for mean A_{net}, R_d, A_{gross}, g_s and E per period and treatment, reported in Figures 5.10 and 5.11, except for A_{gross}.

S.Sp	A_{net}	R_d	A_{gross}	g_s	*E*
Period 2	-201.9	+151.0	+22.5	-26.3	+208.5
Period 3	+88.5	+49.0	+63.4	+89.4	+43.6

S.Sum	A_{net}	R_d	A_{gross}	g_s	*E*
Period 6	-145.2	+135.0	-13.5	-1.6	+181.6
Period 7	-30.5	+31.7	-0.3	-21.7	-8.1

Table 5.14: Mean values (± SE) fresh weight (FW, g), dry weight (DW, g), leaf area (cm^2) and relative water content (%H_2O,%) for all harvested leaves of S.Sp and S.Sum per period.

S.Sp	*FW*	*DW*	*leaf area*	*%H_2O*
period 1	0.8816 ± 0.144	0.1922 ± 0.022	61.14 ± 9.41	78.0 ± 1.0
period 2	0.646 ± 0.103	0.146 ± 0.035	48.26 ± 8.87	78.3 ± 2.6
period 3	0.720 ± 0.057	0.176 ± 0.010	54.96 ± 3.56	75.5 ± 0.7

S.Sum	*FW*	*DW*	*leaf area*	*%H_2O*
period 5	0.368 ± 0.143	0.119 ± 0.030	30.22 ± 8.16	59.4 ± 6.5
period 6	0.281 ± 0.035	0.120 ± 0.012	23.00 ± 1.48	56.7 ± 4.4
period 7	0.306 ± 0.005	0.093 ± 0.018	-	69.7 ± 5.7

5.5.2 Water relations

Relative mean water content for harvested leaves of S.Sp and S.Sum can be found in Table 5.14 and compared to those for other treatments (Table 5.10 and 5.6). Transpiration rates for S.Sp and S.Sum rise significantly higher upon heat followed by a significant decline, in parallel with C.Sp and C.Sum (Figure 5.11). In general, the summer stage shows augmented transpiration rates, especially during period 6, in correlation with higher g_s values.

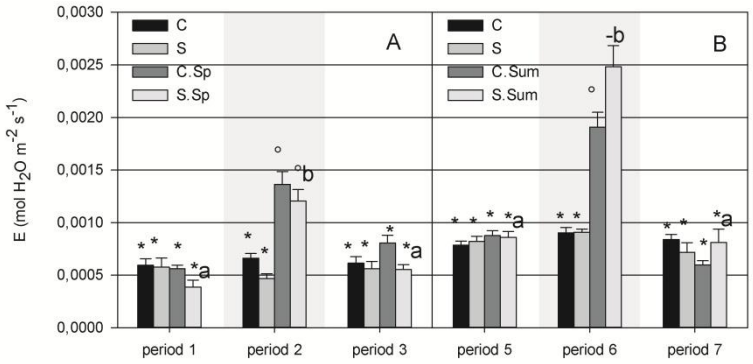

Figure 5.11: Transpiration (E) for C, S, C.Sp and S.Sp (A) and for C, S, C.Sum and S.Sum (B) treatments as a function of discrete time periods. A bar represents the mean (± SE) of the data per period and treatment. Significant differences ($P < 0.05$) within treatment S.Sp or S.Sum over periods are indicated by letters whereas significant differences within a period are marked by symbols. Spring and summer growth stages have to be considered separately. Driving forces temperature and VPD can be found in Table 5.1 (chamber 1 for for C, S, C.Sum and S.Sum period 5; chamber 2 for C.Sp, S.Sp, C.Sum and S.Sum periods 6 and 7).

5.5.3 Chlorophyll content and chlorophyll *a* fluorescence parameters

In accordance with the S treatment, chlorophyll contents in S.Sp and S.Sum are reduced compared to C, as indicated by the leaf greenness in Figure 5.12. However, values for S.Sp and S.Sum tend to rise significantly upon heat exposure. A visual impression is given and will be discussed in section 6.4.3.

In order to find out if a cause for A_{gross} stimulation lies within the electron transport chain, Figure 5.13 represents Φ_{PSII}, q_p, F_V'/F_M' and NPQ. The low Φ_{PSII} values for S.Sp and S.Sum in periods 1 and 5 due to Cd exposure, rise significantly to control levels during heat, parallel with the less pronounced trend in C.Sp and C.Sum. Upon recovery, Φ_{PSII} values for S.Sp and S.Sum decline below C, however, they stay well above S values apart from period 7. In contrast to previously reported parameters, Φ_{PSII} levels in spring and summer stages are comparable in order of magnitude.

Whereas Cd stress had a minor influence on q_p (Figure 5.4.B), the combination of heat and Cd stress induces even a higher rise than C.Sp and C.Sum (Figure 5.13.B and F). However, during recovery, S.Sp and S.Sum are lower than C.Sp and C.Sum respectively but still higher than C and S treatments. For F_V'/F_M' (Figure 5.13.C and G), both Cd and heat resulted in declines (sections 5.3.3 and 5.4.3), thus, S.Sp and S.Sum seem to experience the cumulated effect of both stressors followed by a slight but significant recovery to S levels. Because only Cd caused the related parameter F_V/F_M to decline, values for S.Sp and S.Sum show no particular changes (data not shown).

NPQ values for S.Sp show a larger increase in period 2 than C.Sp due to the synergy of Cd and heat effects (Figure 5.13.D and H). In period 6, the combined effect has rather less impact as the rise upon heat is lower compared to C.Sum. The significant decline in periods 3 and 7 is also specific for the combination of both stressors. Consistent with the finding in section 5.4.3, NPQ follows a similar pattern as q_p, except for periods 1, 3 and 5. Table 5.15 presents relative differences in chlorophyll *a* fluorescence parameters of S.Sp to S.Sp in period 1 and for S.Sum to S.Sum in period 5.

In Figure 5.14.A and D, Φ_{CO2} for S.Sp and S.Sum exhibit a little heat-induced rise respectively decline, which continues in recovery periods. For Φ_{CO2}/Φ_{PSII}, a more significant trend is presented in Figure 5.14.B and E largely explained by the pattern in Φ_{PSII}: a decrease during heat and a rise during recovery (except for period 7). It should be noted that due to the large difference between S and S.Sum in period 5 – although plants were grown in the exact same conditions, the heat-induced significant decrease of S.Sum results in similar values as S which is not the case in period 2. Lastly, Figure 5.14.C and F displays for S_R a pattern likewise to Φ_{CO2}/Φ_{PSII} for S.Sp and S.Sum.

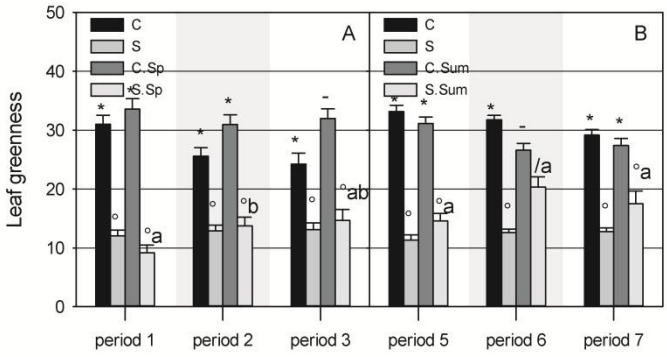

Figure 5.12: Bar chart: Leaf greenness for C, S, C.Sp and S.Sp (A) and for C, S, C.Sum and S.Sum (B) treatments as a function of discrete time periods. A bar represents the mean (± SE) of the data per period and treatment. Significant differences ($P < 0.05$) within treatment S.Sp or S.Sum over periods are indicated by letters whereas significant differences within a period are marked by symbols. Spring and summer growth stages have to be considered separately. Driving forces temperature and VPD can be found in Table 5.1 (chamber 1 for for C, S, C.Sum and S.Sum period 5; chamber 2 for C.Sp, S.Sp, C.Sum and S.Sum periods 6 and 7). Picture: S.Sum plant (October 24, 2011). Note the greener leaves with a reddish tint.

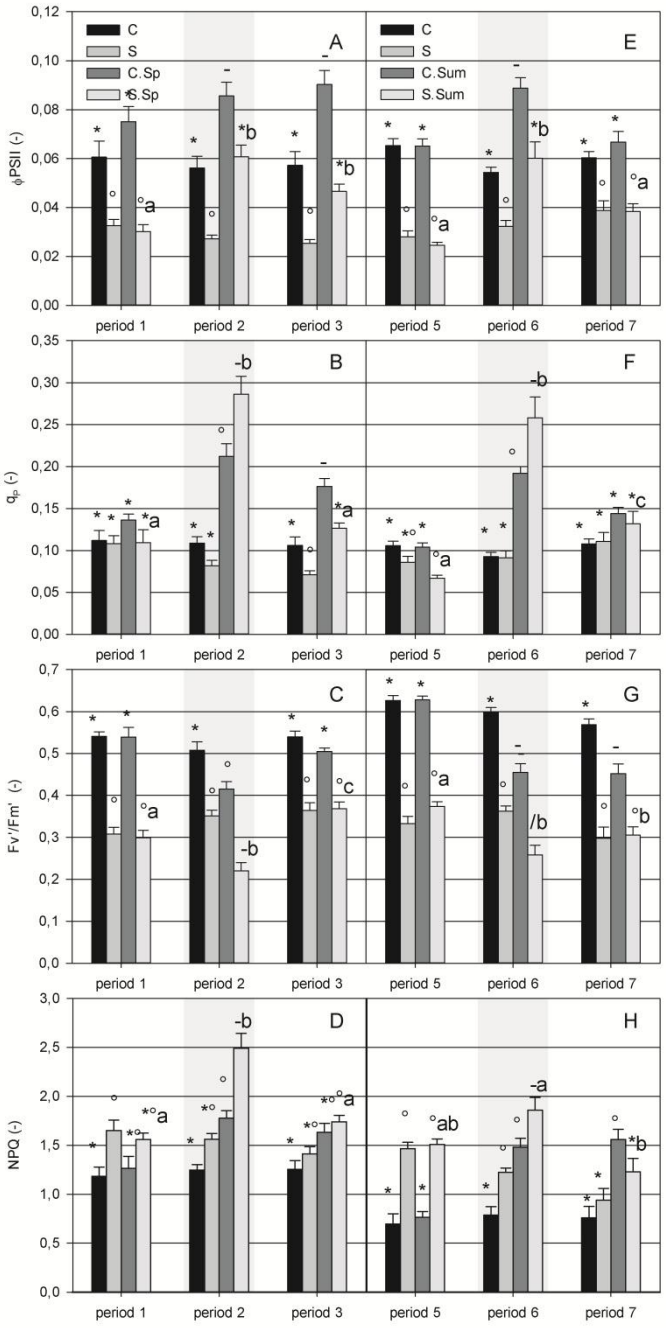

Figure 5.13: PSII operating efficiency (Φ_{PSII}), fraction of open PSII reaction centres (q_p), maximum PSII efficiency in light-adapted leaves (F_V'/F_M') and non-photochemical quenching (NPQ) for C, S, C.Sp and S.Sp (A, B, C, D) and for C, S, C.Sum and S.Sum (E, F, G, H) treatments as a function of discrete time periods. A bar represents the mean (± SE) of the data per period and treatment. Significant differences ($P < 0.05$) within treatment S.Sp or S.Sum over periods are indicated by letters whereas significant differences within a period are marked by symbols. Spring and summer growth stages have to be considered separately. Driving forces temperature and VPD can be found in Table 5.1 (chamber 1 for for C, S, C.Sum and S.Sum period 5; chamber 2 for C.Sp, S.Sp, C.Sum and S.Sum periods 6 and 7).

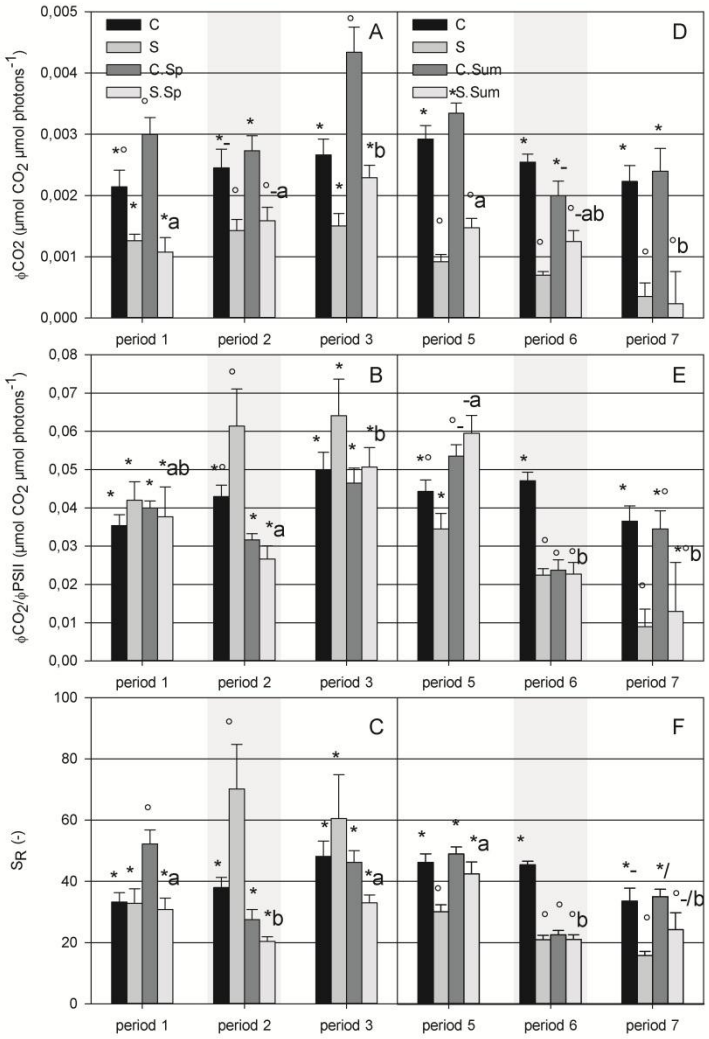

Figure 5.14: Quantum efficiency of CO_2 assimilation (Φ_{CO2}), the ratio of Φ_{CO2} over Φ_{PSII} (Φ_{CO2}/ Φ_{PSII}) and specificity factor for rubisco (S_R) for C, S, C.Sp and S.Sp (A, B, C) and for C, S, C.Sum and S.Sum (D, E, F) treatments as a function of discrete time periods. A bar represents the mean (± SE) of the data per period and treatment. Significant differences ($P < 0.05$) within treatment S.Sp or S.Sum over periods are indicated by letters whereas significant differences within a period are marked by symbols. Spring and summer growth stages have to be considered separately. Driving forces temperature and VPD can be found in Table 5.1 (chamber 1 for for C, S, C.Sum and S.Sum period 5; chamber 2 for C.Sp, S.Sp, C.Sum and S.Sum periods 6 and 7).

Table 5.15: Relative difference (%) (increase, +; decrease, -) of S.Sp and S.Sum compared to S.Sp in period 1 and S.Sum in period 5 for mean chlorophyll *a* fluorescence parameters per period and treatment, reported in Figures 5.13 and 5.14.

S.Sp	Φ_{PSII}	F_V'/F_M'	q_p	*NPQ*	Φ_{CO2}	Φ_{CO2}/Φ_{PSII}	S_R
Period 2	+101.6	-26.3	+162.1	+59.7	+47.4	-29.4	-33.8
Period 3	+54.5	+23.3	+15.8	+11.7	+112.7	+34.5	+7.0

S.Sum	Φ_{PSII}	F_V'/F_M'	q_p	*NPQ*	Φ_{CO2}	Φ_{CO2}/Φ_{PSII}	S_R
Period 6	+144.5	-30.9	+285.7	+23.2	-15.3	-61.8	-50.4
Period 7	+56.0	-18.3	+97.1	-18.5	-53.2	-63.9	-42.9

CHAPTER 6: DISCUSSION

6.1 POTTING COMPOST CHARACTERIZATION AND CADMIUM CONCENTRATIONS IN POTTING COMPOST, POTTING COMPOST SOLUTION AND LEAVES

Probably, the reason for the lower reported IC concentrations in potting compost with added Cd^{2+} (Table 5.2) is the precipitation of $CdCO_3$ and $(Ca\text{-}Cd)CO_3$, because potting compost contains $CaCO_3$ (Martin & Kaplan, 1996). Although the observed pH results in negatively charged organic matter (Tack, 2010), which binds Cd^{2+} in chelates and on particles thereby avoiding Cd to precipitate, Cd concentrations in the potting compost are that high (Table 5.4) that precipitation is inevitable. In fact, because Cd^{2+} was added as $CdSO_4$ and anoxic conditions may have occurred as plants of S, S.Sp and S.Sum treatments did not absorb as much water due to degraded root biomass (visually observed at the end of the experiments) (Tack, 2010), Cd may also have precipitated as CdS which was observed later on in the experiments as a yellowish powder in pot plates (Martin & Kaplan, 1996).

Because heat stimulates organic matter decay, higher NPOC concentrations during heat periods are obvious (Table 5.3). This implies that more Cd may become available for plant uptake (Tack, 2010). However, only a minor rise in potting compost solution Cd concentrations could be observed for S.Sp in period 2 and S.Sum in period 6 (Table 5.4). In addition, S.Sum leaf Cd concentrations did not rise in period 6 although transpiration rates are higher compared to S.Sp in period 2 (Figure 5.11.A and B) and thus Cd uptake should be increased. However, this can be explained by the fact that younger leaves accumulate more Cd (Küpper *et al*., 2007), general different Cd accumulation rates among leaves and the difficulty to sample one leaf twice. Furthermore, leaf Cd concentrations lack a rising trend in time because of the same reason.

According to Schulze et al. (2005), the high Cd leaf concentrations can protect the plants from the effects of the viral infection. This could also be visually observed since plants growing in the potting compost with added Cd^{2+} showed minor symptoms of the infection.

The high Cd concentrations in potting compost for treatments S, S.Sp and S.Sum (Table 5.4) indicate a large pool of immobile Cd bound to organic matter. Comparing those to Cd concentrations in potting compost solutions, smaller amounts of Cd are bioavailable. Apart from the small rise during heat waves and the last two periods which tend to have higher concentrations (probably due to the decay of abscised leaves), a declining trend can be seen in function of time for this bioavailable Cd. This can be due to aging, but cannot be confirmed because no potting compost was analysed for Cd at the end of the experiments. However, leaching and precipitation may have contributed to this decline in bioavailable Cd too.

Potting compost and leaf Cd concentrations observed correspond to values in similar studies (Brooks, 1998; Robinson *et al*., 2000; Tack, 2010). Unterbrunner et al. (2007), for example, reported

total soil Cd concentrations ranging from 0.8 to 678 mg kg^{-1} DW and leaf concentrations up to 45 mg kg^{-1} DW for poplar species. Upon exposure to 360 mg kg^{-1} soil DW for 61 days, Durand et al. (2009) observed a leaf Cd concentration of 84 mg kg^{-1} DW in *Populus tremula* x *Populus alba* and a soil solution concentration of 2.3 mg l^{-1}.

6.2 EFFECTS OF CADMIUM STRESS ON *Populus canadensis* 'Robusta'

6.2.1 Net photosynthesis, dark respiration and stomatal conductance

In Figure 5.1.A and B, the rising trend in A_{net} and R_d during the spring phenological stage indicates growth because of the higher need for energy with a maximum in A_{net} during period 5 for C and period 2 for S. Because for S the maximum in A_{net} appears sooner than for C and because the further decrease in A_{net} for S cannot be explained by R_d, A_{gross} must decrease from period 2. It can be stated that Cd exposure of poplar plants leads to an earlier decline in A_{gross} than if plants are not exposed to Cd^{2+}.
Another effect is the lower overall A_{net} (reduction of 56 to 102%, Table 5.5) due to a diminished A_{gross} since R_d for S is rather similar to C. In Table 5.6, a decreased mean leaf area, fresh and dry weight are reported as a consequence of this reduction in A_{net} (Hasan *et al*., 2009). Apart from many other studies (section 2.3.5), also Pietrini et al. (2010) found reductions in A_{net} of around 80% in a *Populus canadensis* clone with leaf Cd concentrations of 173.3 mg kg^{-1} DW after an exposure period of three weeks to 5.6 mg Cd^{2+} l^{-1}. The slightly reduced R_d in S plants is contradictory to the increase reported in literature (Lee et al., 1976; Vassilev *et al*., 1998). As Cd is shown to provoke oxidative stress (Cheng, 2003; Hall, 2002; Prasad, 1995; Verbruggen *et al*., 2009), reducing power (ATP and NADPH) is needed for repair mechanisms and thus, augmented R_d would be expected to occur (Kieffer *et al*., 2009b; Greger & Ogren, 1991; Schulze *et al*., 2005). In these studies, plants of a few weeks old were exposed to Cd while in this research, cuttings were directly planted in Cd containing potting compost. As such, the cuttings were already exposed prior to leaf development, whereas in other studies, leaves were fully grown when Cd exposure started. Perhaps this could be the reason for the found discrepancy with literature, possibly influenced by acclimation to Cd.

As mentioned in section 5.3.1, g_s is an important element that could cause the reduction in A_{net}. However, Figure 5.1.C presents no significant differences between C and S except for period 2. In addition, g_s is maximally 33.1% lower for the S treatment compared to C (period 2) (Table 5.5) and A_{net} values are minimally 55.9% lower (period 2), thus, stomata will not be the major limitation to A_{net} by reducing CO_2 supply. This was also found by Dai et al. (2012) upon exposure of 12-weeks old *Populus* x *canescens* to 7.9 mg Cd^{2+} l^{-1} for 28 days. Other studies found stomatal closure to be caused by Cd (Burzyński & Kłobus, 2004; Prasad, 1995). Furthermore, a rising trend for C and S should be pointed out in Figure 5.1.C, probably due to an augmented leaf activity.

6.2.2 Water relations

Because the mean relative water contents for C and S are rather equal (Table 5.6), water does not limit A_{net} although less water could probably be absorbed due to a diminished root biomass (visually observed) (Hermle *et al*., 2007; Lux *et al*., 2011).
The time trend for E (Figure 5.2) parallels with g_s because the two determining factors for E are g_s and VPD of which the latter is rather constant. No significant decrease of E occured in correlation with the lack of a decrease in g_s, whereas Gaudet et al. (2011) described a 50 and 75% drop for two 3-weeks old genotypes of *Populus nigra* with mean leaf Cd concentrations of 22.5 and 33.9 mg kg^{-1} DW, respectively. According to Schulze et al. (2005), the inability for sufficient water uptake leads to stomatal closure which decreases E. Apparently, the poplar plants in this study had no difficulty to sufficiently absorb water (Table 5.6). Perhaps the same explanation as for R_d could be suggested here. This would imply that only a drop in E and g_s can be observed due to lower water uptake if healthy plants, which have an increased leaf area and thus a higher need for water (Table 5.6), are exposed to Cd.

6.2.3 Chlorophyll content and chlorophyll *a* fluorescence parameters

In Figure 5.3, Cd clearly results in lower chlorophyll contents of leaves. Several other studies also observed leaf chlorosis (section 2.3.5). This alteration in LHCII which contains about 70% of all chlorophyll (Krupa, 1999) can be explicated by a blockage of chlorophyll synthesis (Cheng, 2003), iron-deficiency (Sárvári *et al.,* 2011) or the substitution of magnesium by Cd leading to unsTable forms of chlorophyll (Küpper *et al.,* 2007). Other visual symptoms such as leaf roll, pinpoint necrosis and faster abscission were also confirmed by literature (Milone *et al*., 2003; Pietrini *et al*., 2010; Schulze *et al*., 2005) with younger leaves exhibiting the symptoms more explicitly (Kieffer *et al*., 2009b; Sárvári *et al*., 2011).

As found by numerous studies, Φ_{PSII} declines significantly upon Cd stress (Figure 5.4.A) (Pietrini *et al.,* 2010; Sárvári *et al*., 2011; Solti *et al*., 2009). Because Φ_{PSII} is determined as the relative amount of active PSII RCs or the amount of energy used in photosynthesis over the total amount of absorbed energy (section 2.2.2), this decline cannot be elucidated by an increase in total absorbed energy. Indeed, this would be rather doubtful given the lower chlorophyll content (Kieffer, 2009a). Thus, less energy enters the electron transport chain, probably due to damage to the stress-sensitive PSII or otherwise to another link in the chain, resulting in lower electron transport rates (formula 2.8, section 2.2.2). This was proven by the significantly lower relative amount of available PSII RCs or the maximum energy fraction for photosynthesis, F_V'/F_M', for S (Figure 5.4.C) (Sárvárí *et al.,* 2011) which is associated with damage to these RCs (Haldimann & Feller, 2004). Furthermore, F_V/F_M reaches healthy levels for C (0.75 - 0.85) but decreased levels for S (Björkman & Demmig, 1987). According to Roháček (2002), this also indicates damage to PSII RCs, caused by damage to the thylakoid

membranes. The latter can be quantified by an increase in F_0' and F_0 for S because this indicates that energy cannot pass PSII (data not shown) (Haldimann & Feller, 2004; Hüve *et al.,* 2012). Thylakoid damage is plausible because many studies reported Cd-induced oxidative stress and lipid peroxidation (Hall, 2002; Hasan *et a*l., 2009; Verbruggen *et al*., 2009). In Figure 6.1, oxidative stress leads to photoinhibition, even at the applied low light intensities, which is probably also the cause here because of the decline in F_V'/F_M' (Nishiyama *et al*., 2006).

In addition to enhanced energy dissipation as fluorescence (F_0 and F_0'), excess energy in S plants is emitted as thermal deactivation (NPQ) of which the high values are shown in Figure 5.4.D. The gradual decline over time is not obvious to explain, but because Figure 5.4.A reports a modest incline in Φ_{PSII} for S during the last periods, probably more PSII RCs become active. The fraction of open RCs (Figure 5.4.B) wanes during the spring phenological stage because of this lessening of NPQ. According to Haldimann and Feller (2004), NPQ protects PSII by keeping RCs open, even at low A_{net}. The further decline of NPQ together with a rise in q_P points out that more energy flows through the electron transport chain, but as was seen before, no increase in A_{net} (Figure 5.1.A) occurs. Therefore, there must be other sinks for electrons.

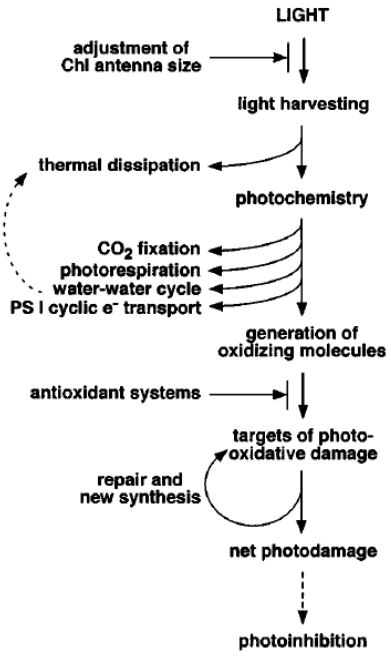

Figure 6.1: Schematic overview of photoprotective processes occurring within chloroplasts (from Niyogi, 1999).

The ratio of Φ_{CO2} over Φ_{PSII} (Figure 5.5.B) indicates higher Calvin cycle efficiencies for S during the first periods because of more A_{gross} (Table 5.5) and a hardly noticeable decline in the amount of active PSII RCs (Figure 5.4.A). During the summer stage, the loss of this efficiency can be better explained by S_R because both parameters are used as a measure for photorespiration (Baker & Oxborough, 2004). Thus, whereas during the spring stage a more decreased electron flow for oxygenation occurred compared to the C treatment, during summer the loss in Calvin cycle efficiency can be clarified by an increase in Jo. Rubisco oxygenase activity (photorespiration) is

therefore an alternative sink for electrons to protect PSII (Haldimann & Feller, 2004). Furthermore, the rise and decline in Calvin cycle efficiencies for both C and S appear to be related to the phenological stage and parameters such as R_d and A_{net}.
It should be noted that the specificity factor for rubisco, S_R, is merely an approximating approach due to the fact that J_t is set equal to ETR which is only the linear electron flow lacking cyclic electron flow.

To conclude, the electron transport chain suffers from Cd stress because oxidative thylakoid damage affected PSII RCs. However, during the summer phenological stage, the Calvin cycle progressively loses its higher efficiency due to photorespiration to protect PSII, resulting in the decline of A_{net}.

6.3 EFFECTS OF HEAT STRESS DURING SPRING OR SUMMER PHENOLOGICAL STAGE ON *Populus canadensis* 'Robusta'

6.3.1 Net photosynthesis, dark respiration and stomatal conductance

Poplar plants grown at 23°C experience negative effects of a heat period (7 days at > 40°C) because their optimum temperature is lower (Sage & Kubien, 2007), namely a 88.3% drop in A_{net} during the spring phenological stage and 82.8% during summer (Table 5.9). These values can partly be explained by a temperature driven rise in R_d to obtain energy for, amongst others, repair mechanisms, but the decline of A_{gross} (Table 5.8 and 5.9) suggests another target of heat stress. The less low A_{net} value for C.Sum due to the lower R_d rise is misleading because A_{gross} shows more heat impact (Table 5.8 and 5.9, Figure 5.6.A, B, D, E). At the end of the growth season, both R_d and A_{gross} rates slow down probably because less energy is needed due to leaf inactivation upon aging, and thus clarifying the greater A_{gross} decline (Hermle *et al*., 2007).
Haldimann and Feller (2004) found a comparable 90% decrease for A_{net} if oaks (*Quercus pubescens* L.) grown at 25°C were exposed to 45°C. Several other studies confirmed this A_{net} decrease and R_d rise upon heat (section 2.4.3), amongst others Bassman and Zwier (1991) who examined several *Populus* clones and Hozain et al. (2009) who reported a 40% reduction of A_{net} at 40°C for *Populus balsamifera*.
In a similar way, the recovery of A_{net} cannot only be addressed to a decline in R_d because A_{gross} rises (Figure 5.6.A, B, D, E, Table 5.8). Moreover, during the spring recovery period, A_{gross} is stimulated indicated by an enormous rise of A_{net} (Figure 5.6.A, Table 5.8 and 5.9). Unfortunately, none of these trends can specifically be seen in leaf weights or surfaces (Table 5.10). Also, in literature, only studies were found that reported difficulty to obtain preheat photosynthesis levels (Haldimann & Feller, 2004). For example, Niinemets et al. (1999) found that after exposure of *Populus tremula* to temperatures above 35°C, preheat photosynthetic capacities were no longer reached at 25°C, probably due to damage to the photosynthetic apparatus. Perhaps, a further examination of the data can explain this discrepancy with literature.

In Figures 5.6.C and F, a first potential cause for the decline in A_{net} during heat is shown, namely reduced g_s limiting the supply of CO_2. However, stomatal conductance lowers only by 25.6% during the summer stage compared to 61.2% during the spring stage, which is in contrast to the rather equal relative A_{net} decline for both growth stages (Table 5.9). In a similar way, g_s cannot explicate the recovery of photosynthesis because it rises in period 3 due to enhanced leaf activity but declines further in period 7 (Table 5.9). According to Silim et al. (2010), a 37°C heat treatment of *Populus balsamifera* (grown at 27/16°C) resulted in a g_s decrease of about 0.35 mol H_2O m^{-2} s^{-1} while R_d tripled and A_{net} decreased about 40%. Figure 5.6.C and F shows a g_s decline for both growth stages of 0.014 mol H_2O m^{-2} s^{-1}, probably confirming the absence of any effect of stomatal conductance to photosynthesis. Also Law and Crafts-Brandner (1999) reported A_{net} to decline, but not due to a decreased g_s.

6.3.2 Water relations

The relative water contents for C.Sp and C.Sum, presented in Table 5.10, point out that no water deficiency occurred. This will be due to stomatal closure which may also be the reason why C.Sp contains relatively more water in period 2 compared to C.Sum in period 6. In fact, the latter had larger stomatal conductance and transpiration rates, probably reducing the relative water content (Figure 5.7.B).

Because VPDs for both period 2 and 6 are similar but higher compared to other periods, transpiration will intensify (Table 5.1). Moreover, period 6 holds an increased E value in correlation with the overall higher g_s during the summer stage (Figures 5.6.C and F and 5.7). The same explanation for period 3 is valuable. The augmented transpiration rates can be interpreted as transpirational cooling, which continues as long as water is available (which was the case in this study) (Salvucci & Crafts-Brandner, 2004).

6.3.3 Chlorophyll content and chlorophyll *a* fluorescence parameters

In contrast to literature (Berry & Björkman, 1980; Schrader *et al*., 2004; Silim *et al*., 2010), the increased Φ_{PSII} and thus electron transport rate reported in Figure 5.8.A and E, denotes that heat activates PSII RCs because chlorophyll contents are similar to C (data not shown). A larger fraction of the total absorbed energy thus enters the electron transport chain, although the maximum fraction of energy for photosynthesis (or the amount of available PSII RCs) decreases in the light (F_V'/F_M') but does not change in the dark (F_V/F_M) during heat. A potential cause for this light-dependent decrease could be light-induced oxidative stress resulting in reversible damage and a reversible form of photoinhibition of PSII (Baker, 2008; Murata *et a*l., 2007; Niyogi *et al*., 1999; Schulze *et al*., 2005; Yamashita *et al.,* 2008). The fact that photodamage and heat damage follow this same pathway,

underwrites the hypothesis that heat alone does not cause damage (unchanged F_V/F_M) but a combination of both does (decrease in F_V'/F_M') (Yamashita *et al.,* 2008). Haldimann and Feller (2004) confirmed this by stating that F_V'/F_M' reductions are linked to damage to PSII RCs. Because no rise in F_0' or F_0 was noticed (data not shown), this damage was not caused by thylakoid damage (Salvucci & Crafts-Brandner, 2004). The decreased F_V'/F_M' values are accompanied by NPQ rise which is shown in Figure 5.8.D and H (Baker, 2008). Another cause for high NPQ is an increased q_p.
Augmented q_p values dominantly cause Φ_{PSII} to incline during heat periods compensating for the lower F_V'/F_M' (Figure 5.8.A, B, E and F). Due to risen NPQ levels, PSII RCs are kept open resulting in the high q_p values (Haldimann & Feller, 2004). Thereby, during the summer stage, the higher relative NPQ rise is mainly due to the larger relative increase in q_p than to the decrease in F_V'/F_M' (Table 5.11). This means that during heat stress the larger fraction of open RCs stimulates electron transport efficiency, Φ_{PSII}.
It should be noted that the higher values of Φ_{PSII} for C.Sp in period 1, which are also reflected in A_{net} and Φ_{CO2}, will probably be due to a faster growth.

Upon recovery, Φ_{PSII} also shows augmented values, at least during the spring phenological stage. This could be part of the reason for the stimulated A_{net} value which was mentioned before. The combination of almost completely recovered F_V'/F_M' values with still a high fraction of open RCs, maintained by a high NPQ level indicating irreversible damage, elucidates the high Φ_{PSII} values (Figures 5.8.A, B, C and D period 3). During the summer stage, NPQ remains high mainly because F_V'/F_M' values are equally low as during period 6. This also indicates a permanent form of damage to PSII, probably because of leaf inactivation at the end of summer.

The previous finding that A_{net} declined upon heat stress (which could not completely be explained by a rise in R_d, section 6.3.1) is still not clarified, in fact, a stimulation of the electron transport chain was found upon heat stress. The only cause that is left is an affected Calvin cycle. A decline during heat periods can already be observed in Φ_{CO2} (Figure 5.9.A and D) but gets more meaning in the ratio of Φ_{CO2} to Φ_{PSII}. Although a larger amount of energy can be used in photosynthesis (Φ_{PSII}), a defect Calvin cycle fixes less CO_2 resulting in a heat-induced decrease in Φ_{CO2}/Φ_{PSII}. S_R clarifies this with an augmented part of the electron flow to rubisco oxygenase (photorespiration). According to Haldimann & Feller (2004), this alternative sink for electrons protects PSII against photoinhibition which is not achieved if looking to F_V'/F_M'.
During recovery periods, a rise in Φ_{CO2}/Φ_{PSII} and thus S_R indicates not per se lower Jo but more important higher Jc flows than C. A heat period seems to stimulate the carboxylation function of the Calvin cycle upon recovery which is another possible explanation for the significant augmentation of A_{net} in period 3.

In conclusion, a heat period reduces A_{net} mainly by an enhanced R_d, but also by Calvin cycle inhibition (photorespiration) and damage to the electron transport chain (PSII RCs). Upon recovery, some PSII

RCs may be repaired as seen in a minor drop of NPQ. The Calvin cycle is stimulated during spring recovery but not during summer because leaves become inactive. Probably, heat shock proteins have functioned in conserving and protecting the enzymes of both the electron transport chain and the Calvin cycle and play an important role in recovery because of their long life times (Efeoğlu, 2009; Heckathorn, 1999).

One aspect that cannot be known from the data is the effect of heat on rubisco activase, because its heat-induced inactivation is often reported as a major limitation to photosynthesis (Portis, 2003; Salvucci & Crafts-Brandner, 2004).

6.4 COMBINED EFFECTS OF CADMIUM AND HEAT STRESS DURING SPRING OR SUMMER PHENOLOGICAL STAGE ON *Populus canadensis* 'Robusta'

6.4.1 Net photosynthesis, dark respiration and stomatal conductance

Formerly, it was observed that Cd brings about very low A_{net} values with a minor reduction of R_d, whereas heat triggered dark respiration which was a major cause for a limited A_{net}. In Figure 5.10.A and D, the combination of both stressors leads to negative A_{net} during heat, but also to a rise (spring) or almost steady-state (summer) of A_{gross} (Table 5.12). For R_d, no synergistic effect occurred (Table 5.13, 5.10 and 5.5). Furthermore, earlier, it was seen that Cd initiated A_{net} and A_{gross} to decline from period 2 and heat recovery periods showed a rise in both with even stimulation during period 3. For S.Sp and S.Sum during recovery periods, the same trend as for C.Sp and C.Sum was seen with lower overall values due to Cd, so, no synergism between both stressors arose which confirms the different targets found in sections 6.2 and 6.3. Thus, the only 'new' thing is the A_{gross} rise or steady-state during heat periods. This finding is in accordance with the results from Hermle et al. (2007), who studied the effect of Cd (10 mg kg^{-1} topsoil) on *Populus tremula* and found a stabilization of A_{net}, g_s and E upon heat together with a rise in R_d, thus, a rise in A_{gross}.
It should be noted that the negative values for A_{net} during heat in both growth stages are also visible in a decline in fresh and dry weights of the harvested leaves (Table 5.14).

In Figure 5.10.C and F, stomatal conductance of S.Sp and S.Sum declines during the spring heat wave but not during summer, parallel with the larger response of stomata to heat in C.Sp than in C.Sum. A similar discourse as in section 6.3.1 leads to the conclusion that g_s cannot be a stimulus for A_{gross} by enhanced CO_2 supply because A_{gross} rises in period 2 whereas g_s declines (Table 5.12).

6.4.2 Water relations

Water is not reported as the major boosting factor of A_{gross} because relative water contents are comparable with C.Sp and C.Sum, which showed an A_{gross} decrease during heat (Table 5.14 and 5.10). Also, S.Sum holds for periods 5 and 7 an equal A_{gross} whereas its water content differs about 10% (Table 5.14 and 5.12). Stomatal closure may be responsible for the augmented relative water contents for S.Sp. In contrast, the higher g_s and E for S.Sum in periods 5 and 6 may result in lower water contents (Figure 5.10.C and F, Figure 5.11.B, Table 5.14).

Heat induces transpiration rates to increase because VPD rises (Figure 5.11, Table 5.1). During the summer stage, E reaches higher values for both C.Sum and S.Sum comparable to the larger g_s (Figure 5.10.F). Also, the difference in E between both treatments can be seen in g_s. Because during the spring growth stage A_{gross} is stimulated but E is globally lower compared to the summer stage, transpirational cooling will not be a driving force for augmented photosynthesis (Salvucci & Crafts-Brandner, 2004).

6.4.3 Chlorophyll content and chlorophyll *a* fluorescence parameters

The bar chart in Figure 5.12 shows augmented chlorophyll contents upon heat which would imply a rise in total absorbed energy. However, because Φ_{PSII} is the ratio of energy for photosynthesis to total absorbed energy, this parameter should decrease which is not the case (Figure 5.13.A and E). On the contrary, in terms of percentage it rises even further than C.Sp and C.Sum (Table 5.13), so, no chlorophyll-induced decrease in Φ_{PSII} is marked by the heat-induced rise in Φ_{PSII}. This is in agreement with visual observations (Figure 5.12 right) showing hardly greener leaves, although a reddish tint can explicate higher greenness levels measured because of the working principle of SPAD. The heat-stimulated Φ_{PSII} values are lower than for C.Sp and C.Sum due to Cd, however, because S.Sp and S.Sum reached C levels during heat, it can be stated that the combination of Cd and heat is equally 'good' as no stress at all (treatment C) and more energy will enter the electron transport chain. However, care must be taken with such conclusions (see below). Despite the Cd-induced damage to the electron transport chain (section 6.2.3), heat will still stimulate the chain which continues in recovery (section 6.3.3).

In order to find out how this can work, F_V'/F_M' and q_p must be studied. The former (Figure 5.13.C and G) starts at lower levels due to Cd-induced damage to PSII RCs, confirmed by low F_V/F_M (data not shown) (Roháček, 2002). Also F_0 and F_0' are increased indicating thylakoid injury (data not shown) (Haldimann & Feller, 2004; Hüve *et al.*, 2012). During heat periods, a further decline in F_V'/F_M' happens whereas F_V/F_M stays constant. This means that an additional light-induced destruction of PSII occurs in heat, which was described in section 6.3.3. Remarkably, upon heat a decline of F_0' takes place pointing out that heat may lessen thylakoid damage which can be seen by a smaller

decline in F_V'/F_M' compared to C.Sp and C.Sum (Figure 5.13.C and G). A potential cause can lie in HSP production. According to Schulze et al. (2005), HSP production is a general stress reaction. Cd stress causes HSPs, which are reported to repair membranes (Lux *et al.,* 2011), to become more abundant (Heckathorn *et al*., 2004; Vierling, 1991). Heat also induced HSP production leading to better protected membranes because the heat-induced HSPs will also contribute to membrane repair (Wang *et al*., 2004). Because no further increase of F_0 or F_0' during heat occurs, heat damage to PSII RCs is not due to thylakoid injury.
Not the reduced maximum absorbed energy, F_V'/F_M', but the compensating increase of q_p gives rise to higher Φ_{PSII} during heat periods (Figure 5.13.B and F). NPQ keeps PSII RCs open to protect them (Figure 5.13.D and H) (Haldimann & Feller, 2004). Thus, although there are less RCs available during heat (F_V'/F_M' decrease), the electron transport efficiency (Φ_{PSII}) rises even more than for C.Sp or C.Sum due to a larger fraction of open RCs (q_p) which in turn is possible by the high NPQ (synergistic effect of Cd and heat). During recovery, NPQ values drop to almost S levels indicating that the heat damage to PSII RCs is quit reversible in contrast to C.Sp and C.Sum (section 6.3.3). The slightly augmented q_p in recovery are the reason that NPQ does not reach S levels. Furthermore, the Φ_{PSII} decline is not clarified by the heat-stimulated F_V'/F_M', but by the lower q_p accompanied by lower NPQ.

It could be stated that due to increased electron transport chain efficiency, A_{gross} will rise. However, firstly, this is not in accordance with section 6.4.3 and secondly, it can also not explain the different A_{gross} reaction between growth stages. When looking towards the Calvin cycle, this may be cleared out. Figure 5.14.B and E show that heat affects Calvin cycle efficiencies (Φ_{CO2}/Φ_{PSII}). For S.Sp, the decline in Φ_{CO2}/Φ_{PSII} is smaller compared to S.Sum because more CO_2 is fixed although for both more energy for photosynthesis is available. For both recovery periods, less energy is available (decline in Φ_{PSII}) but in period 3 more CO_2 assimilation happens. Both in the spring and summer growth stage, not only Jo but surprisingly also Jc are stimulated during heat (in contrast to section 6.3.3), but where Jc doubles, Jo triples (data not shown). This means that the Calvin cycle, which has stimulated turn-over rates due to heat, will not only show an increased photorespiration (Jo), but will also have an augmented CO_2 fixation rate (Jc). Therefore, S_R values are among the lowest for S.Sp and S.Sum during heat (Figure 5.14.C and F). The combination of a stimulated electron transport chain (Φ_{PSII}) and Calvin cycle (Jc) during heat form an explanation for the rise in A_{gross}. Because leaves are more mature and slightly higher photorespiration occurred during the summer growth stage, A_{gross} was less stimulated compared to the spring stage. Both Jc and Jo decrease during recovery, although for period 3 Jc remains rather high explaining the higher A_{net} and A_{gross} rise.

To conclude, a rise (spring) or almost no decline (summer) in A_{gross} is mainly due to a heat-induced stimulation of the Calvin cycle. This could be possible because also the electron transport chain was stimulated during both heat and recovery despite of the Cd-induced thylakoid damage to PSII RCs and the reversible heat-induced PSII RCs injury (photoinhibition).

In section 6.3.3, it was found that a heat period stimulated the Calvin cycle during the recovery period. However, if Cd and heat are applied together, the Calvin cycle is stimulated during both heat and recovery. As mentioned above, probably the Cd-induced HSPs could protect rubisco immediately at the start of the heat shock inducing the stimulation of the Calvin cycle (Heckathorn *et al*., 2004).

CHAPTER 7: GENERAL CONCLUSIONS AND SUGGESTIONS

7.1 OUTCOME OF HYPOTHESES

The executed research pointed out some interesting findings about the effect of Cd, heat and a combination of both on *Populus canadensis* 'Robusta' and enables a discussion of the hypotheses made in Chapter 3.

Upon exposure of poplar plants to a bioavailable Cd^{2+} concentration of about 0.5 mg l^{-1}, photosynthesis rates generally reached lower values than plants without added Cd^{2+} which resulted in lower biomass production. In contrast to literature, no enhanced dark respiration occurred due to acclimation to Cd, probably because plants were exposed prior to leaf development. For the same reason, no significant decrease of stomatal conductance or transpiration could be observed. The low photosynthesis rates could be explained by reduced chlorophyll contents of LHCII and damage to PSII RCs, which was indicated by a decrease of Φ_{PSII} and F_V'/F_M'. A thorough examination of other fluorescence parameters pointed out that oxidative stress and lipid peroxidation of the thylakoid membranes could be the reason for this PSII injury, which might even lead to photoinhibition. Also the Calvin cycle caused diminished photosynthesis during the summer growth stage because of photorespiration in order to protect PSII. During the spring stage, however, a tendency towards inclined photosynthesis occurred because Calvin cycle efficiencies were higher than plants without added Cd^{2+}, despite the lower energy input from the electron transport chain. This increase in photosynthesis lasted, however, shorter than for not exposed plants. Hypothesis 1.a can thus be confirmed but hypothesis 1.b, which states that the spring growth stage is more influenced, is weakened.

Heat stress (7 days at 40°C) caused photosynthesis to decline, especially during the summer growth stage. A rise in dark respiration and transpiration occurred, which declined after heat stress to control levels. Furthermore, no water deficiency could be observed, probably due to stomatal closure during heat periods. In contrast to literature, a rise in Φ_{PSII} indicated that more electrons flowed through the electron transport chain and thus more energy could be produced. This was possible because augmented non-photochemical quenching kept PSII RCs open to protect them from further damage, even during recovery periods, indicating irreversible damage. A light-induced injury of PSII could be observed in a decrease of F_V'/F_M', but this was not caused by thylakoid damage and was reversible upon recovery in the spring growth stage. As a consequence, a stimulation of the electron transport chain in spring recovery resulted in higher photosynthesis rates. This was not the case during the summer stage recovery because of leaf inactivation, which is normal at the end of the growth stage. During heat periods, this stimulated electron flow and thus excess energy was consumed by photorespiration in the Calvin cycle, explaining the reduced photosynthesis rates.

Remarkably, carboxylation activity of rubisco was increased during the spring recovery period possibly by heat-induced HSPs, also explaining the higher photosynthesis. In order to obtain information about rubisco activase, protein research should be conducted, but this was out of the scope of this master thesis. Upon these findings, hypothesis 2.a can thus not completely be confirmed. For hypothesis 2.b, it was found that the opposite was true.

The influence of a heat period on Cd-exposed plants leads to a rise (during the spring growth stage) or almost steady-state (during the summer growth stage) of gross photosynthesis, accompanied by a boosted dark respiration, so, net, the plants respired biomass. A further rise of A_{gross} and decline of R_d during recovery periods were observed. Stomatal conductance declined during heat and transpiration rose in order to cool down the plant. Furthermore, the electron transport chain was even more stimulated upon heat exposure than plants without added Cd^{2+} due to a larger fraction open RCs, despite the Cd-induced thylakoid injury and the extra but reversible heat- and light-induced damage to PSII RCs. It was found that heat lessened thylakoid damage, probably due to the extra HSP production. Upon recovery, the electron transport chain is still rather stimulated except for the summer growth stage due to leaf inactivity. The extra energy produced was consumed by an accelerated Calvin cycle by photorespiration, but surprisingly also by an augmented rubisco carboxylase activity explicating the rise (spring) or steady-state (summer) in A_{gross}. Probably, HSPs present due to Cd stress could immediately protect rubisco upon heat stress. Also during the spring recovery period, carboxylation stayed high resulting in a stimulation of A_{gross}. Because leaves are more mature and higher photorespiration occurred during the summer growth stage, A_{gross} was less stimulated compared to the spring stage. From all these findings, hypothesis 3 can be confirmed.

7.2 APPLICATION OF *Populus canadensis* 'Robusta' IN PHYTOREMEDIATION

According to the characteristics which Brooks et al. (1998) stated to be important for potential phytoremediation plants, *Populus canadensis* would be a good vegetation type for phytoremediation of Cd polluted soils. It is a fast growing tree with large biomass production, easy to harvest and with a leaf Cd accumulation parallel to hyperaccumulators (> 100 mg kg^{-1} DW). A disadvantage can be the impact of these toxic Cd concentrations on photosynthesis, reducing plant growth. Typically, plants are harvested every year (Brooks *et al*., 1998) with the remaining biomass sprouting the next year. In this study, poplar plants were exposed to Cd for 155 days which approximates the duration of the growth season and therefore, could be representative for a phytoremediation cycle. However, because of their reduced growth upon Cd exposure, they would probably not have sprouted in a next growth season if they were kept for another year. However, if it is considered economically feasible to harvest and replace poplar plants frequently, perhaps twice in one year, this will probably not be a limitation.

7.3 SUGGESTIONS FOR FUTURE RESEARCH

In order to observe clear trends between measured parameters and Cd concentrations, it could be interesting to apply a range of (lower) Cd concentrations in the potting compost, instead of one high Cd concentration. This would also be more comparable with contaminated soils in the field where Cd concentrations show more variation on one site (Robinson *et al*., 2000). Also, a repetition of the experiments in the field could be useful in order to conclude if poplar would be suitable for phytoremediation.

Because in polluted sites also other heavy metals can occur, perhaps a mixture of metals could be applied.

Furthermore, a protein study can gain supplementary information about HSP concentrations and the reaction of rubisco activase to Cd, heat or a combination of both.

As a last point, next to temperature inclines, global change is also accompanied by elevated CO_2 concentrations and drought stress. A combination of these stressors could gain important information in a changing world.

LIST OF REFERENCES

Ainsworth, E.A. & Rogers, A. (2007). The response of photosynthesis and stomatal conductance to rising CO2: mechanisms and environmental interactions. Plant, Cell and Environment, 30, 258-270.

Alcamo, J., Moreno, J.M., Nováky, B., Bindi, M., Corobov, R., Devoy, R.J.N., Giannakopoulos, C., Martin, E., Olesen, J.E. & Shvidenko, A. (2007). Europe. In: Parry, M.L., Canziani, O.F., Palutikof, J.P., van der Linden, P.J. & Hanson, C.E. (eds) Climate Change 2007: Impacts, Adaptation and Vulnerability. Contribution of Working Group II to the Fourth Assessment Report of the Intergovernmental Panel on Climate Change. Cambridge University Press, Cambridge, UK, 541-580.

Allakhverdiev, S.I., Kreslavski, V.D., Klimov, V.V., Los, D.A., Carpentier, R. & Mohanty, P. (2008). Heat stress: an overview of molecular responses in photosynthesis. Photosynthesis Research, 98, 541-550.

Asada, K. (2006). Production and Scavenging of Reactive Oxygen Species in Chloroplasts and Their Functions. Plant Physiology, 141, 391-396.

ATSDR, U.S. Department of Health and Human Services, Public Health Service, Agency for Toxic Substances and Disease Registry (2008). Draft toxicological profile for cadmium. http://www.atsdr.cdc.gov/toxprofiles/tp5.pdf (consulted 5 April 2012), 512p.

Baker, N.R. (2008). Chlorophyll Fluorescence: A Probe of Photosynthesis In Vivo. Annual Review of Plant Biology, 59, 89-113.

Baker, N.R. & Oxborough, K. (2004). Chlorophyll Fluorescence as a Probe of Photosynthetic Productivity. In: Papageorgiou, G.C. & Govindjee (eds) Chlorophyll a Fluorescence: A Signature of Photosynthesis. The Netherlands, 65-82.

Barceló, J., Cabot, C. & Poschenrieder, CH. (1986). Cadmium-Induced Decrease of Water Stress Resistance in Bush Bean Plants (*Phaseolus vulgaris* L. cv. Contender) II. Effects of Cd on Endogenous Abscisic Acid Levels. Journal of Plant Physiology, 125, 27-34.

Bassman, J.H. & Zwier, J.C. (1991). Gas exchange characteristics of *Populus trichocarpa, Populus deltoides* and *Populus trichocarpa x P. deltoids* clones. Tree Physiology, 8, 145-159.

Bernacchi, C.J., Portis, A.R., Nakano, H., von Caemmerer, S. & Long, S.P. (2002). Temperature Response of Mesophyll Conductance. Implications for the Determination of Rubisco Enzyme Kinetics and for Limitations to Photosynthesis in Vivo. Plant Physiology, 130, 1992-1998.

Berry, J. & Björkman, O. (1980). Photosynthetic response and adaptation to temperature in higher plants. Annual Review of Plant Physiology, 31, 491-543.

Bierkens, J., De Raeymaecker, B., Cornelis, C., Schoeters, G., Hooghe, R., Verbeiren, S., Ruttens, A., Vangronsveld, J., Smolders, E., Schoeters, I., Van Geert, K., Van Gestel, G., Geysen, D., Dedecker, D. & Van De Wiele, K. (2010). Voorstel voor herziening bodemsaneringsnormen voor cadmium. OVAM, België, Mechelen, 78p.

Blaudez, D., Botton, B. & Chalot, M. (2000). Cadmiup uptake and subcellular compartmentation in the ectomycorrhizal fungus *Paxillus involutus*. Microbiology, 146, 1109-1117.

Bolhàr-Nordenkampf, H.R. & Öquist, G. (1993). Chlorophyll fluorescence as a tool in photosynthesis research. In: Hall, D.O., Scurlock, J.M.O., Bolhàr-Nordenkampf, H.R., Leegood, R.C., & Long, S.P. (eds) Photosynthesis and Production in a Changing Environment: a field and laboratory manual. U.K., London, 193 – 206.

Bradl, H.B. (2004). Adsoprtion of heavy metal ions on soils and soils constituents. Journal of Colloid and Interface Science, 277, 1-18.

Brooks, A. & Farquhar, G.D. (1985). Effect of temperature on the CO_2/O_2 specificity of ribulose-1,5-bisphospate carboxylase/oxygenase and the rate of respiration in the light. Planta, 165, 397-406.

Brooks, R.R., Chambers, M.F., Nicks, L.J. & Robinson, B.H. (1998). Phytomining. TRENDS in Plant Science, 3, 359-362.

Bukhov, N.G., Wiese, C., Neimanis, S. & Heber, U. (1999). Heat sensitivity of chloroplasts and leaves: Leakage of protons from thylakoids and reversible activation of cyclic electron transport. Photosynthesis Research, 59, 81-93.

Burzyński, M. & Kłobus, G. (2004). Changes of photosynthetic parameters in cucumber leaves under Cu, Cd, and Pb stress. Photosynthetica, 42, 505-510.

Cheng, S. (2003). Effects of Heavy Metals on Plants and Resistance Mechanisms. Environmental Science & Pollution Research, 10, 256-264.

Clemens, S., Palmgren, M.G. & Krämer, U. (2002). A long way ahead: understanding and engineering plant metal accumulation. TRENDS in Plant Science, 7, 309-315.

Cottenie, A. & Verloo, M. (1984). Analytical diagnosis of soil pollution with heavy-metals. Fresenius' Zeitschrift für Analytische Chemie, 317, 389-393.

Curie, C., Cassin, G., Couch, D., Divol, F., Higuch, K., Le Jean, M., Misson, J., Schikora, A., Czernic, P. & Mari, S. (2009). Metal movement within the plant: contribution of nicotianamine and yellow stripe 1-like transporters. Annuals of Botany, 103, 1-11.

Dai, H., Wei, Y., Zhang, Y., Gao, P., Chen, J., Jia, G., Yang, T., Feng, S., Wang, C., Wang, Y., Sa, W. & Wei, A. (2012). Influence of photosynthesis and chlorophyll synthesis on Cd accumulation in Populus x canescens. Journal of Food Agriculture & Environment, 10, 1020-1023.

DalCorso, G., Farinati, S., Maistri, S. & Furini, A. (2008). How Plants Cope with Cadmium: Staking All on Metabolism and Gene Expression. Journal of Integrative Plant Biology, 50, 1268-1280.

De Boeck, H.J., Dreesen, F.E., Janssens, I.A. & Nijs, I. (2010). Climatic characteristics of heat waves and their simulation in plant experiments. Global Change Biology, 16, 1992-2000.

Dokmeci, A.H., Ongen, A. & Dagdeviren, S. (2009). Environmental toxicity of cadmium and health effect. Journal of Environmental Protection and Ecology, 10, 84-93.

Du Laing, G., Vanthuyne, D.R.J., Vandecasteele, B., Tack, F.M.G. & Verloo, M.G. (2007). Influence of hydrological regime on pore water metal concentrations in a contaminated sediment-derived soil. Environmental Pollution, 147, 615-625.

Durand, T.C., Sergeant, K., Planchon, S., Carpin, S., Label, P., Morabito, D., Hausman, J. & Renaut, J. (2010). Acute metal stress in *Populus tremula x P. alba* (717-1B4 genotype): Leaf and cambial proteome changes induced by cadmium^{2+}. Proteomics, 10, 349-368.

Efeoğlu, B. (2009). Heat Shock Proteins and Heat Shock Response in Plants. Gazi University Journal of Science, 22, 67-75.

Ernst, W.H.O. (1980). Biochemical aspects of cadmium in plants. In: Nriagu, J.O. (ed) Cadmium in the Environment. Part I: Ecological Cycling. John Wiley and Sons, New York, 639-653.

Evans, L.J. (1989). Chemistry of metal retention by soils – several processes are explained. Environmental Science & Technology, 23, 1046-1056.

Fagioni, M., D'Amici, G.M., Timperio, A.M. & Zolla, L. (2009). Proteomic Analysis of Multiprotein Complexes in the Thylakoid Membrane upon Cadmium Treatment. Journal of Proteome Research, 8, 310-326.

Feller, U., Crafts-Brandner, S.J. & Salvucci, M.E. (1998). Moderately High Temperatures Inhibit Ribulose-1,5-Bisphosphate Carboxylase/Oxygenase (Rubisco) Activase-Mediated Activation of Rubisco. Plant Physiology, 116, 539-546.

Forstner, U. (1993). Metal speciation – Generall concepts and applications. International Journal of Environmental Analytical Chemistry, 51, 5-23.

Franco, E., Alessandrelli, S., Masojídek, J., Margonelli, A. & Giardi, M.T. (1999). Modulation of D1 protein turnover under cadmium and heat stresses monitored by [^{35}S]methionine incorporation. Plant Science, 144, 53-61.

Gaudet, M., Pietrini, F., Beritognolo, I., Iori, V., Zacchini, M., Massacci, A., Mugnozza, G.S. & Sabatti, M. (2011). Intraspecific variation of physiological and molecular response to cadmium stress in *Populus nigra* L. Tree Physiology, 31, 1309-1318.

Genty, B., Briantais, J-M. & Baker, N.R. (1989). The relationship between the quantum yield of photosynthetic electron transport and quenching of chlorophyll fluorescence. Biochimica et Biophysica Acta, 990, 87-92.

Goormachtigh, S. (2012). Hittestress, zware metalen en hun effect op *Populus canadensis* 'Robusta'. Masterthesis, Gent, België, Faculteit Bio-ingenieurswetenschappen.

Govindjee (1995). 63 years since Kautsky – Chlorophyll-a fluorescence. Australian Journal of Plant Physiology, 22, 131-160.

Greger, M. & Ogren, E. (1991). Direct and indirect effects of Cd^{2+} on photosynthesis in sugar-beet (*Beta vulgaris*). Physiologia Plantarum, 83, 129-135.

Gu, J.G., Qi, L., Jiang, W. & Liu, D. (2007). Cadmium accumulation and its effects on growth and gas exchange in four Populus cultivars. Acta Biologica Cracoviensia series Botanica, 49, 7-14.

Habashi, F. (1997). Handbook of Extractive Metallurgy. Wiley-VCH, Weinheim, 869-890.

Haldimann, P. & Feller, U. (2004). Inhibition of photosynthesis by high temperature in oak (Quercus pubescens L.) leaves grown under natural conditions closely correlates with a reversible heat-dependent reduction of the activation state of ribulose-1,5-bisphospate carboxylase/oxygenase. Plant, Cell and Environment, 27, 1169-1183.

Hall, J.L. (2002). Cellular mechanisms for heavy metal detoxification and tolerance. Journal of Experimental Botany, 53, 1-11.

Hanssens, J. (2010). Invloed van bodemvervuiling (metaaltoxiciteit) op de ecofysiologie van populier tijdens gesimuleerde hittegolven. Masterthesis, Gent, België, Faculteit Bio-ingenieurswetenschappen, 81p.

Hasan, S.A., Fariduddin, Q., Ali, B., Hayat, S. & Ahmad, A. (2009). Cadmium: Toxicity and tolerance in plants. Journal of Environmental Biology, 30, 165-174.

Havaux, M. (1993). Rapid photosynthetic adaptation to heat-stress triggered in potato leaves by moderately elevated-temperatures. Plant, Cell and Environment, 16, 461-467.

Havaux, M. (1996). Short-term responses of photosystem I to heat stress - Induction of a PSII-independent electron transport through PSI fed by stromal components. Photosynthesis Research, 47, 85-97.

Heber, U. (2002). Irrungen, Wirrungen? The Mehler reaction in relation to cyclic electron transport in C3 plants. Photosynthesis Research, 73, 223-231.

Heckathorn, S.A., Downs, C.A. & Coleman, J.S. (1999). Small heat shock proteins protect electron transport in chloroplasts and mitochondria during stress. American Zoologist, 39, 865-876.

Hermle, S. Vollenweider, P., Günthardt-Goerg, M.S., McQuattie, C.J. & Matyssek, R. (2007). Leaf responsiveness of *Populus tremula* and *Salix viminalis* to soil contaminated with heavy metals and acidic rainwater. Tree Physiology, 27, 1517-1531.

Heyno, E., Klose, C. & Krieger-Liszkay, A. (2008). Origin of cadmium-induced reactive oxygen species production: mitochondrial electron transfer versus plasma membrane NADPH oxidase. New Phytologist, 179, 687-699.

Hozain, M.I., Salvucci, M.E., Fokar, M. & Holaday, A.S. (2009). The differential response of photosynthesis to high temperature for a boreal and temperate *Populus* species relates to differences in Rubisco activation and Rubisco activase properties. Tree Physiology, 30, 32-44.

Hüve, K, Bichele, I., Ivanova, H., Keerberg, O., Pärnik, T., Rasulov, B. Tobias, M. & Niinemets, Ü. (2012). Temperature responses of dark respiration in relation to leaf sugar concentration. Physiologia Plantarum, 144, 320-334.

IPCC (2007). IPCC, 2007: Summary for Policymakers. In: Solomon, S., Qin, D., Manning, M., Chen, Z., Marquis, M., Averyt, K.B., Tignor, M. & Miller, H.L. (eds) Climate Change 2007: The Physical Science Basis. Contribution of Working Group I to the Fourth Assessment Report of the Intergovernmental Panel on Climate Change. Cambridge University Press, Cambridge, United Kingdom and New York, NY, USA, 18p.

Kautsky, H. & Hirsch, A. (1931). Neue Versuche zur Kohlensäureassimilation. Naturwissenschaften, 19, 964.

Kautsky, H., Appel, W. & Amann, H. (1960). Chlorophyllfluorescenz und Kohlensäureassimilation. Biochemische Zeitschrift, 322, 277-292.

Kieffer, P., Planchon, S., Oufir, M., Ziebel, J., Dommes, J., Hoffmann, L., Hausman, J. & Renaut, J. (2009a). Combining Proteomics and Metabolite Analyses To Unravel Cadmium Stress-Response in Poplar Leaves. Journal of Proteome Research, 8, 400-417.

Kieffer, P., Schröder, P., Dommes, J., Hoffmann, L., Renaut, J. & Hausman, J. (2009b). Proteomic and enzymatic response of poplar to cadmium stress. Journal of Proteomics, 72, 379-396.

Kim, K. & Portis, A.R. (2004). Oxygen-dependent H_2O_2 production by Rubisco. Febs Letters, 571, 124-128.

Kirkham, M.B. (2006). Cadmium in plants on polluted soils: Effects of soil factors, hyperaccumulation, and amendments. Geoderma, 137, 19-32.

Krupa, Z., Öquist, G. & Huner, N.P.A. (1993). The effects of cadmium on photosynthesis of Phaseolus vulgaris – a fluorescence analysis. Physiologia Plantarum, 88, 626-630.

Krupa, Z. (1999). Cadmium against Higher Plant Photosynthesis – a Variety of Effects and Where Do They Possibly Come From? Zeitschrift für Naturforschung, 54c, 723-729.

Küpper, H., Parameswaran, A., Leitenmaier, B., Trtílek, M. & Šetlík, I. (2007). Cadmium-induced inhibition of photosynthesis and long-term acclimation to cadmium stress in hyperaccumulator Thlaspi caerulescens. New Phytologist, 175, 655-674.

Larbi, A., Morales, F., Abadia, A., Gogorcena, Y., Lucena, J.J. & Abadia, J. (2002). Effects of Cd and Pb in sugar beet plants grown in nutrient solution: induced Fe deficiency and growth inhibition. Functional plant biology, 29, 1453-1464.

Larcher, W. (2003). Physiological Plant Ecology. Germany, Berlin Heidelberg New York, Springer, 519p.

Latowski, D., Kruk, J. & Strzałka, K. (2005). Inhibition of zeaxanthin epoxidase activity by cadmium ions in higher plants. Journal of Inorganic Biochemistry, 99, 2081-2087.

Law, R.D. & Crafts-Brandner, S.J. (1999). Inhibition and Acclimation of Photosynthesis to Heat Stress Is Closely Correlated with Activation of Ribulose-1,5-Bisphosphate Carboxylase/Oxygenase. Plant Physiology, 120, 173-181.

Lee, K.C., Cunningham, B.A., Paulsen, G.M., Liang, G.H. & Moore, R.B. (1976). Effects of Cadmium on Respiration Rate and Activities of Several Enzymes in Soybean Seedlings. Physiologia Plantarum, 36, 4-6.

Le Quéré, C., Raupach, M.R., Canadell, J.G., Marland, G., Bopp, L., Ciais, P., Conway, T.J., Doney, S.C., Feely, R.A., Foster, P., Friedlingstein, P., Gurney, K., Houghton, R.A., House, J.I., Huntingford, C., Levy, P.E., Lomas, M.R., Majkut, J., Metzl, N., Ometto, J.P., Peters, G.P., Prentice, C., Randerson, J.T., Running, S.W., Sarmiento, J.L., Schuster, U., Sitch, S., Takahashi, T., Viovy, N., van der Werf, G.R. & Woodward, F.I. (2009). Trends in the sources and sinks of carbon dioxide. Nature Geoscience, 2, 831-836.

LI-COR (2008). Using the LI-6400/LI-6400XT Portable Photosynthesis System. LI-COR Biosciences, Inc., Lincoln, NE, USA, version 6, 1280p. ftp://ftp.licor.com/perm/env/LI-6400/Manual/Using_the_LI-6400XT-v6.1.pdf (consulted 2 December 2011).

LI-COR (2011b). Leaf Chamber Fluorometer 6400-40, for use with the LI-6400 Portable Photosynthesis System. LI-COR Biosciences, Inc., Lincoln, NE, USA, 4p. http://www.licor.com/env/products/photosynthesis/brochures.html (consulted 3 December 2011).

LI-COR (2012). LI-6400XT System. Photosynthesis, Fluorescence, Respiration. LI-COR Biosciences, Inc., Lincoln, NE, USA, 13p. http://www.licor.com/env/pdf/photosynthesis/LI6400XTBrochure.pdf (consulted 4 February 2012).

Los, D.A. & Murata, N. (2004). Membrane fluidity and its roles in the perception of environmental signals. Biochimica et Biophysica Acta, 1666, 142-157.

Lunáčková, L., Šottníková, A., Masarovičová, E., Lux, A., Streško, V. (2003). Comparsion of cadmium effect on willow and poplar in response to different cultivation conditions. Biologia Plantarum, 47, 403-411.

Lux, A., Martinka, M., Vaculík, M. & White, P.J. (2011). Root responses to cadmium in the rhizosphere: a review. Journal of Experimental Botany, 62, 21-37.

Malik, D., Sheoran, I.S. & Singh, R. (1992). Carbon metabolism in leaves of cadmium treated wheat seedlings. Plant Physiology and Biochemistry, 30, 223-229.

Martin, H.W. & Kaplan, D.I. (1996). Temporal changes in cadmium, thallium, and vanadium mobility in soil and phytoavailability under field conditions. Water, Air, and Soil Pollution, 101, 399-410.

Maxwell, K. & Johnson, G.N. (2000). Chlorophyll fluorescence – a practical guide. Journal of Experimental Botany, 51, 345, 659-668.

Milone, M.T., Sgherri, C., Clijsters, H. & Navari-Izzo, F. (2003). Antioxidative responses of wheat treated with realistic concentration of cadmium. Environmental and Experimental Botany, 50, 265-276.

Meehl, G.A. & Tebaldi, C. (2004). More Intense, More Frequent, and Longer Lasting Heat Waves in the 21st Century. Science, 305, 994-997.

Mohanty, P., Vani, B. & Prakash, J.S.S. (2002). Elevated temperature treatment induced alteration in thylakoid membrane organization and energy distribution between the two photosystems in Pisum sativum. Zeitschrift für Naturforschung C-A Journal of Biosciences, 57, 836-842.

Mott, K.A. (1988). Do Stomata Respond to CO2 Concentrations Other than Intercellular? Plant Physiology, 86, 200-203.

Murata, N., Takahashi, S., Nishiyama, Y. & Allakhverdiev, S.I. (2007). Photoinhibition of photosystem II under environmental stress. Biochimica et Biophysica Acta, 1767, 414-421.

Nash, D., Miyao, M. & Murata, N. (1985). Heat inactivation of oxygen evolution in Photosystem II particles and its acceleration by chloride depletion and exogenous manganese. Biochimica et Biophysica Acta, 807, 127-133.

Niinemets, Ü., Oja, V. & Kull, O. (1999). Shape of leaf photosynthetic electron transport versus temperature response curve is not constant along canopy light gradients in temperate deciduous trees. Plant, Cell and Environment, 22, 1497-1513.

Nishiyama, Y., Allakhverdiev, S.I. & Murata, N. (2006). A new paradigm for the action of reactive oxygen species in the photoinhibition of photosystem II. Biochimica et Biophysica Acta, 1757, 742-749.

Niyogi, K.K. (1999). Photoprotection revisited: Geneticc and Molecular Approaches. Annual Review of Plant Physiology and Plant Molecular Biology, 50, 333-359.

Nordberg, G.F. (2004). Cadmium and health in the 21st Century – historical remarks and trends for the future. Biometals, 17, 485-489.

Nordic Council of Ministers (2003). Cadmium Review. www.who.int/ifcs/documents/forums/forum5/nmr_cadmium.pdf (consulted 5 April 2012), 26p.

Nriagu, J.O. & Pacyna, J.M. (1988). Quantitative assessment of worldwide contamination of air, water and soils by trace metals. Nature, 333, 134-139.

Pacyna, E.G., Pacyna, J.M., Fudala, J., Strzelecka-Jastrzab, E., Hlawiczka, S., Panasiuk, D., Nitter, S., Pregger, T., Pfeiffer, H. & Friedrich, R. (2007). Current and future emissions of selected heavy metals to the atmosphere from anthropogenic sources in Europe. Atmospheric Environment, 41, 8557-8566.

Pandey, S., Gupta, K. & Mukherjee, A.K. (2007). Impact of cadmium and lead on *Catharanthus roseus* – A phytoremediation study. Journal of Environmental Biology, 28, 655-662.

Pietrini, F., Zacchini, M., Iori, V., Pietrosanti, L., Ferretti, M. & Massacci, A. (2010). Spatial distribution of cadmium in leaves and its impact on photosynthesis: examples of different strategies in willow and poplar clones. Plant Biology, 10, 355-363.

Pinto, M. (1980). Control of photosynthesis by photosynthate demand – possible mechanisms. Photosynthetica, 14, 611-637.

Portis, A.R.Jr. (2003). Rubisco activase – Rubisco's catalytic chaperone. Photosynthesis Research, 75, 11-27.

Poschenrieder, C., Gunsé, B. & Barceló, J. (1989). Influence of Cadmium on Water Relations, Stomatal Resistance, and Abscisic Acid Content in Expanding Bean Leaves. Plant Physiology, 90, 1365-1371.

Prasad, M.N.V. (1995). Cadmium toxicity and tolerance in vascular plants. Environmental and Experimental Botany, 35, 525-545.

Prasad, M.N.V. & Freitas, H.M. (2003). Metal hyperaccumulation in plants – Biodiversity prospecting for phytoremediation technology. Electronic Journal of Biotechnology, 6, 285-321.

Raven, P.H., Evert, R.F. & Eichhorn, S.E. (2005). Biology of Plants. New York, U.S., W.H. Freeman and Company Publishers, 686p.

Robinson, B.H., Mills, T.M., Petit, D., Fung, L.E., Green, S.R. & Clothier, B.E. (2000). Natural and induced cadmium-accumulation in poplar and willow: Implications for phytoremediation. Plant and Soil, 227, 301-306.

Roháček, K. (2002). Chlorophyll fluorescence parameters: the definitions, photosynthetic meaning, and mutual relationships. Photosynthetica, 40, 13-29.

Roháček, K. & Barták, M. (1999). Technique of the modulated chlorophyll fluorescence: basic concepts, useful parameters, and some applications. Photosynthetica, 37, 339-363.

Sadegh Safarzadeh, M., Bafghi, M.S., Moradkhani, D. & Ojaghi Ilkhchi, M. (2007) A review on hydrometallurgical extraction and recovery of cadmium from various resources. Minerals Engineering 20, 211-220.

Sage, R.F. & Kubien, D.S. (2007). The temperature response of C_3 and C_4 photosynthesis. Plant, Cell and Environment, 30, 1086-1106.

Salvucci, M.E. & Crafts-Brandner, S.J. (2004). Inhibition of photosynthesis by heat stress: the activation state of Rubisco as a limiting factor in photosynthesis. Physiologia Plantarum, 120, 179-186.

Satarug, S., Baker, J.R., Urbenjapol, S., Haswell-Elkins, M., Reilly, P.E.B., Williams, D.J. & Moore, M.R. (2003). A global perspective on cadmium pollution and toxicity in non-occupationally exposed population. Toxicology Letters, 137, 65-83.

Sárvári, É., Solti, Á., Basa, B., Mészáros, I., Lévai, L. & Fodor, F. (2011). Impact of moderate Fe excess under Cd stress on the photosynthetic performance of poplar (*Populus jacquemontiana var. glauca* cv. Kopeczkii). Plant Physiology and Biochemistry, 49, 499-505.

Sauvé, S., Manna, S., Turmel, M-C., Roy, A.G. & Courchesne, F. (2003). Solid-solution partitioning of Cd, Cu, Ni, Pb, and Zn in the organic horizons of a forest soil. Environmental Science & Technology, 37, 5191-5196.

Schär, C., Vidale, P.L., Lüthi, D., Frei, C., Häberli, C., Liniger, M.A. & Appenzeller, C. (2004). The role of increasing temperature variability in European summer heatwaves. Nature, 427, 332-336.

Schmidt, W. (1988). Luminescence of organic molecules – theory and analytical applications in photosynthesis. In: Lichtenthaler, H.K. (ed) Applications of Chlorophyll Fluorescence. Kluwer Academic Publishers, 211-216.

Schrader, S.M., Wise, R.R., Wacholtz, W.F., Ort, D.R. & Sharkey, T.D. (2004). Thylakoid membrane responses to moderately high leaf temperature in Pima cotton. Plant, Cell and Environment, 27, 725-735.

Schreiber, U. & Armond, P.A. (1978). Heat-induced changes of chlorophyll fluorescence in isolated chloroplasts and related heat-damage at the pigment level. Biochimica et Biophysica Acta, 502, 138-151.

Schulze, E., Beck, E. & Müller-Hohenstein, K. (2005). Plant Ecology. Springer, Germany, Berlin, 702p.

Sell, J., Kayser, A., Schulin, R. & Brunner, I. (2005). Contribution of ectomycorrhizal fungi to cadmium uptake of poplars and willows from a heavily polluted soil. Plant and Soil, 277-245-253.

Seregin, I.V. & Ivanov, V.B. (2001). Physiological Aspects of Cadmium and Lead Toxic Effects on Higher Plants. Russian Journal of Plant Physiology, 48, 523-544.

Seuntjens, P., Tirez, K., Šimůnek, J., van Genuchten, M.Th., Cornelis, C. & Geuzens, P. (2001). Aging Effects on Cadmium Transport in Undisturbed Contaminated Sandy Soil Columns. Journal of Environmental Quality, 30, 1040-1050.

Sharkey, T.D. (2005). Effects of moderate heat stress on photosynthesis: importance of thylakoid reactions, rubisco deactivation, reactive oxygen species, and thermotolerance provided by isoprene. Plant, Cell and Environment, 28, 269-277.

Siedlecka, A. & Baszynski, T. (1993). Inhibition of electron flow around photosystem-I in chloroplasts of Cd-treated maize plants is due to Cd-induced iron-deficiency. Physiologia Plantarum, 87, 199-202.

Sigfridsson, K.G.V., Bernát, G., Mamedov, F. & Styring, S. (2004). Molecular interference of Cd^{2+} with Photosystem II. Biochimica et Biophysica Acta, 1659, 19-31.

Silim, S.N., Ryan, N. & Kubien, D.S. (2010). Temperature responses of photosynthesis and respiration in *Populus balsamifera* L.: acclimation versus adaptation. Photosynthesis Research, 104, 19-30.

Silver, S. (1996). Bacterial resistances to toxic metal ions – a review. Gene, 179, 9-19.

Solti, Á., Szűcs, J., Basa, B. & Sárvári, É. (2009). Functional and organisational change of photosystem II in poplar thylakoids under Cd stress (Dissipative PSII centres in Cd treated poplar thylakoids). 8th Alps-Adria Scientific Workshop, Bosnia-Herzegovina, 4p.

Solti, Á., Gáspár, L., Mészáros, I., Szigeti, Z., Lévia, L. & Sárvári, É. (2008a). Impact of Iron Supply on the Kinetics of Recovery of Photosynthesis in Cd-stressed Poplar (*Populus glauca*). Annals of Botany, 102, 771-782.

Solti, Á., Szégi, P., Bása, B., Mészáros, I. & Sárvári, É. (2008b). Alleviation of Cd induced inhibition of photosynthesis under long-term Cd treatment in poplar. Cereal Research Communications, 36, 239-242.

Steppe, K. (2011). Ecofysiologie. Cursus, Gent, Faculteit Bio-ingenieurswetenschappen, Universiteit Gent, Vakgroep toegepaste ecologie en milieubiologie, Laboratorium voor Plantecologie, 182p.

Stitt, M. & Grosse, H. (1988). Interactions between Sucrose Synthesis and CO2 Fixation IV. Temperature-dependent adjustment of the relation between sucrose synthesis and CO2 fixation. Journal of Plant Physiology, 133, 392-400.

Tack, F.M.G. (2010). Trace elements: general soil chemistry, principles and processes. In: Hooda, P. (ed) Trace elements in soils. Wiley-Blackwell, 9-39.

Terry, N. (1980). Limiting factors in photosynthesis. 1. Use of iron stress to control photochemical capacity invivo. Plant Physiology, 65, 114-120.

Trenberth, K.E., Jones, P.D., Ambenje, P., Bojariu, R., Easterling, D., Klein Tank, A., Parker, D., Rahimzadeh, F., Renwick, J.A., Rusticucci, M., Soden, B. & Zhai, P. (2007). Observations: Surface and Atmospheric Climate Change. In: Solomon, S., Qin, D., Manning, M., Chen, Z., Marquis, M., Averyt, K.B., Tignor, M. & Miller, H.L. (eds) Climate Change 2007: The Physical Science Basis. Contribution of Working Group I to the Fourth Assessment Report of the Intergovernmental Panel on Climate. Cambridge University Press, Cambridge, United Kingdom and New York, NY, USA.

Tudoreanu, L. & Philips, C.JC. (2004). Empirical models of cadmium accumulation in maize, rye grass and soya bean plants. Journal of the Science of Food and Agriculture, 84, 845-852.

Unterbrunner, R., Puschenreiter, M., Sommer, P., Wieshammer, G., Tlustoš, P., Zupan, M. & Wenzel, W.W. (2007). Heavy metal accumulation in trees growing on contaminated sites in Central Europe. Environmental Pollution, 148, 107-114.

Uraguchi, S., Mori, S., Kuramata, M., Kawasaki, A., Arao, T. & Ishikawa, S. (2009a). Root-to-shoot Cd translocation via the xylem is the major process determining shoot and grain cadmium accumulation in rice. Journal of Experimental Botany, 60, 2677-2688.

Uraguchi, S., Kiyono, M., Sakamoto, T., Watanabe, I. & Kuno, K. (2009b). Contributions of apoplasmic cadmium accumulation, antioxidative enzymes and induction of phytochelatins in cadmium tolerance of the cadmium-accumulating cultivar of black oat (*Avena strigosa* Schreb.). Planta, 230, 267-276.

Valentini, R., Epron, D., De Angelis, P., Matteucci, G. & Dreyer, E. (1995). *In situ* estimation of net CO_2 assimilation, photosynthetic electron flow and photorespiration in Turkey oak (*Q. cerris* L.) leaves: diurnal cycles under different levels of water supply. Plant, Cell and Environment, 18, 631-640.

Van Kooten, O. & Snel, J.F.H. (1990). The use of chlorophyll fluorescence nomenclature in plant stress physiology. Photosynthesis Research, 25, 147-150.

Vassilev, A., Berova, M. & Zlatev, Z. (1998). Influence of Cd2+ on growth, chlorophyll content, and water relations in young barley plants. Biologia Plantarum, 41, 601-606.

Verbruggen, N., Hermans, C. & Schat, H. (2009). Mechanisms to cope with arsenic or cadmium excess in plants. Current Opinion in Plant Biology, 12, 364-372.

Vierling, E. (1991). The roles of heat shock proteins in plants. Annual Review of Plant Physiology and Plant Molecular Biology, 42, 579-620.

Wahid, A., Gelani, S., Ashraf, M. & Foolad, M.R. (2007). Heat tolerance in plants: An overview. Environmental and Experimental Botany, 61, 199-223.

Walker, D. (1987). Fluorescence. In: Walker, D. (ed) The Use of the Oxygen Electrode and Fluorescence Probes in Simple Measurements of Photosynthesis. Sheffield, U.K., 17-46.

Wang, W., Vinocur, B., Shoseyov, O. & Altman, A. (2004). Role of plant heat-shock proteins and molecular chaperones in the abiotic stress response. Trends in Plant Science, 9, 244-252.

Weis, E. & Berry, J.A. (1988). Plants and high-temperature stress. Symposia of the Society for Experimental Biology, 42, 329-46.

White, P.J. & Brown, P.H. (2010). Plant nutrition for sustainable development and global health. Annals of Botany, 105, 1073-1080.

Yamada, M., Hidaka, T. & Fukamachi, H. (1996). Heat tolerance in leaves of tropical fruit crops as measured by chlorophyll fluorescence. Scientia Horticulturae, 67, 39-48.

Yamane, Y., Shikanai, T., Kashino, Y., Koike, H. & Satoh, K. (2000). Reduction of Q_A in the dark: Another cause of fluorescence F_0 increases by high temperatures in higher plants. Photosynthesis Research, 63, 23-34.

Yamasaki, T., Yamakawa, T., Yamane, Y., Koike, H., Satoh, K. & Katoh, S. (2002). Temperature Acclimation of Photosynthesis and Related Changes in Photosystem II Electron Transport in Winter Wheat. Plant Physiology, 128, 1087-1097.

Yamashita, A., Nijo, N., Pospíšil, P., Morita, N., Takenaka, D., Aminaka, R., Yamamoto, Y. & Yamamoto, Y. (2008). Quality Control of Photosystem II Reactive oxygen species are responsible for the damage to photosystem II under moderate heat stress. The Journal of Biological Chemistry, 283, 28380-28391.

Yamori, W., Noguchi, K., Hanba, Y.T. & Terashima, I. (2006). Effects of internal conductance on the temperature dependence of the photosynthetic rate in spinach leaves from contrasting growth temperatures. Plant and Cell Physiology, 47, 1069-1080.